Award Number: W81XWH-07-1-0523

TITLE: Biochemical characterisation of *TSC1* and *TSC2* variants identified in patients with tuberous sclerosis complex

PRINCIPAL INVESTIGATOR: Mark Nellist

CONTRACTING ORGANIZATION: Erasmus MC
3015 GE Rotterdam, The Netherlands

REPORT DATE: July 2008

TYPE OF REPORT: Annual

PREPARED FOR: U.S. Army Medical Research and Materiel Command
Fort Detrick, Maryland 21702-5012

DISTRIBUTION STATEMENT:

Approved for public release; distribution unlimited

REPORT DOCUMENTATION PAGE

Form Approved
OMB No. 0704-0188

1. REPORT DATE	2. REPORT TYPE Annual	3. DATES COVERED
01-07-2008		1 Jul 2007 – 30 Jun 2008

4. TITLE AND SUBTITLE

Biochemical characterisation of *TSC1* and *TSC2* variants identified in patients with tuberous sclerosis complex

5a. CONTRACT NUMBER

5b. GRANT NUMBER
W81XWH-07-1-0523

5c. PROGRAM ELEMENT NUMBER

6. AUTHOR(S)

Mark Nellist, Marianne Hoogeveen-Westerveld, Dicky Halley

5d. PROJECT NUMBER

5e. TASK NUMBER

5f. WORK UNIT NUMBER

7. PERFORMING ORGANIZATION NAME(S) AND ADDRESS(ES) AND ADDRESS(ES)

Erasmus MC,
3015 GE Rotterdam,
The Netherlands

8. PERFORMING ORGANIZATION REPORT NUMBER

9. SPONSORING / MONITORING AGENCY NAME(S) AND ADDRESS(ES)
U.S. Army Medical Research and Materiel Command,
Fort Detrick,
Maryland 21702-5012

10. SPONSOR/MONITOR'S ACRONYM(S)

11. SPONSOR/MONITOR'S REPORT NUMBER(S)

12. DISTRIBUTION / AVAILABILITY STATEMENT

Approved for public release; distribution unlimited

13. SUPPLEMENTARY NOTES

14. ABSTRACT

The key findings of the project during the research period are as follows:
1. Derivation of 62 unclassified TSC2 variants: 27 classified as pathogenic; 10 classified as neutral; 27 still unclassified/analysis not complete.
2. Derivation of 20 unclassified TSC1 variants: 8 classified as pathogenic; 7 classified as neutral; 5 still unclassified/analysis not complete
3. Demonstration that *TSC1* missense mutations cause TSC.
4. Identification of a region of TSC1 (amino acids 50 - 224) required for maintaining TSC1 at sufficient levels in the cell to form a stable TSC1-TSC2 complex and inhibit mTOR.
5. Identification of amino acid residues involved in (i) TSC1-TSC2 binding, and (ii) rhebGAP activity.
6. Robust assay for detection of pathogenic TSC2 variants.
7. Improvements in assay cost, throughput and reproducibility.

15. SUBJECT TERMS
Tuberous Sclerosis Complex, unclassified variants, TSC1, TSC2

16. SECURITY CLASSIFICATION OF:			17. LIMITATION OF ABSTRACT	18. NUMBER OF PAGES	19a. NAME OF RESPONSIBLE PERSON USAMRMC
a. REPORT U	**b. ABSTRACT** U	**c. THIS PAGE** U	U U	91	**19b. TELEPHONE NUMBER** *(include area code)*

Standard Form 298 (Rev. 8-98)
Prescribed by ANSI Std. Z39.18

Table of Contents

Introduction

   Subject: Tuberous sclerosis complex (TSC) is a genetic disorder affecting approximately 1 in 10 000 individuals (1). TSC is caused by mutations in either the *TSC1* or *TSC2* tumour suppressor genes (2, 3). The *TSC1* and *TSC2* gene products form a protein complex that inhibits the activity of the mammalian target of rapamycin (mTOR). mTOR coordinates nutritional, hormonal and other cues to regulate the cellular growth machinery. Therefore, inactivation of the TSC1-TSC2 complex results in inappropriate mTOR activity and cell growth defects (4).

   Mutation analysis of the *TSC1* and *TSC2* genes is a useful diagnostic tool for helping individuals and families affected by TSC (5). In most cases of TSC, a definite pathogenic *TSC1* or *TSC2* mutation is identified. However, in some cases it is difficult to determine whether sequence changes identified in the *TSC1* or *TSC2* genes are pathogenic, or not. These 'unclassified variants', typically missense changes, small in-frame insertions or deletions, or changes that could affect splicing, present a significant problem for diagnostics and genetic counselling.

   Purpose: The purpose of this research project is to develop and apply assays of TSC1-TSC2 function to determine whether specific unclassified *TSC1* and *TSC2* variants are pathogenic or not. In this way, the individuals carrying these variants, as well as their families, can obtain clearer information about their condition and the associated risks. Furthermore, correlation of the biochemical effects of the different variants with the observed patient phenotypes could provide insight into genotype-phenotype correlations in TSC and, in addition, identification of amino acids and/or regions that are important for different aspects of TSC1-TSC2 function could help define the structural and catalytic domains of the TSC1-TSC2 complex.

   Scope: The specific aims of the project were to:
1. Apply functional assays to determine whether specific *TSC1* and *TSC2* variants are pathogenic mutations.
2. Determine whether specific *TSC1* and *TSC2* mutations are associated with specific TSC phenotypes.
3. To identify amino acid residues that are essential for TSC1 or TSC2 function.
4. To develop a simple, reliable and rapid test for TSC1-TSC2 function.

Body

1. Application of functional assays to determine whether specific TSC1 and TSC2 variants are pathogenic mutations.

Unclassified *TSC1* and *TSC2* variants were selected from our patient cohort (5). We focused on resolving cases where the individuals or families concerned would potentially benefit from the results (6-8). This included individuals who did not necessarily fulfil the diagnostic criteria for TSC. In addition, we selected TSC1 and TSC2 variants that we considered likely to provide insights into TSC1-TSC2 function. For example, amino acid changes in domains that have, as yet, no clearly defined function. Furthermore, we analysed reported missense mutations that we considered might have an effect on RNA splicing. Where no RNA was available, we analysed the predicted missense variant to determine whether the amino acid substitution affected the function of the TSC1-TSC2 complex (7, 9, 10).

To investigate the effects of amino acid substitutions and small in-frame insertions or deletions on TSC1 and TSC2 function, we introduced the corresponding nucleotide changes into existing TSC1 and TSC2 expression constructs by site-directed mutagenesis, and expressed the variants in mammalian cells in culture. To determine the biological activity of the TSC1 and TSC2 variants we used 4 different assays (11):

1. *Coimmunoprecipitation.* To estimate the strength of the physical interaction between different TSC1 and TSC2 variants we transfected human embryonic kidney (HEK) 293T cells with TSC1 and TSC2 expression constructs. After 24 hours, TSC1-TSC2 complexes were immunoprecipitated from the cell lysates, separated by denaturing polyacrylamide gel electrophoresis (SDS-PAGE) and analysed by immunoblotting.

2. *Phosphorylation of ectopically expressed p70 S6 kinase upon coexpression of TSC1 and TSC2.* The TSC1-TSC2 complex inhibits the kinase activity of mTOR, preventing phosphorylation of p70 S6 kinase (S6K), a mTOR substrate. We transfected HEK 293T cells with TSC1, TSC2 and S6K expression constructs. After 24 hours the cell lysates were separated by denaturing polyacrylamide gel electrophoresis (SDS-PAGE) and transferred to nitrocellulose membranes. Phosphorylated S6K was detected using a commercially available antibody specific for S6K phosphorylated at the T389 position. To obtain a semi-quantitative estimate of TSC1-TSC2 levels and S6K phosphorylation, the blots were scanned.

3. *Phosphorylation of ribosomal protein S6 in Tsc1 -/- and Tsc2 -/- mouse embryo fibroblasts upon ectopic expression of TSC1 and TSC2.* *Tsc1 -/-* and *Tsc2 -/-* mouse embryo fibroblasts (MEFs) have constitutive phosphorylation of the ribosomal protein S6, the downstream target of S6K. We transfected *Tsc1 -/-* or *Tsc2 -/-* MEFs with TSC1 and/or TSC2 expression constructs. Twenty-four hours after transfection, S6 phosphorylation in the TSC1/TSC2 expressing cells was determined by fluorescent double-label immunocytochemistry using antibodies specific for S6 phosphorylated at the S235/236 position. To obtain an estimate of TSC1-TSC2 activity, individual MEFs expressing the different variants and showing clear down-regulation of S6 phosphorylation were counted (>50 cells per experiment).

4. *In vitro GTPase activity of rheb in the presence of immunoprecipitated TSC1-TSC2 complexes.* We expressed recombinant glutathione S transferase-tagged rheb in bacteria and loaded the purified GTPase with ^{32}P-GTP. After incubation with

immunoprecipitated TSC1-TSC2 complexes, thin-layer chromatography followed by phosphoimaging was performed to quantify the rhebGTP:rhebGDP ratio and thereby estimate the rate of rheb-GTP hydrolysis.

At the start of the project we had used these assays to analyse approximately 30 TSC2 variants and 5 TSC1 variants (Supporting data, Tables 1 and 2), including a few previously unclassified variants. Some amino acid substitutions destabilised the TSC1-TSC2 complex. Other substitutions had no effect on the formation or stability of the complex, but through direct effects on catalytic activity, still impaired the ability of the complex to inhibit mTOR signalling. Other variants studied had no discernible effect on the activity of the TSC1-TSC2 complex in our assays. We concluded that these variants were neutral variants, and not responsible for the TSC phenotype.

We have now completed analysing the majority of the unclassified missense variants in our own patient cohort and have begun to analyse more unclassified variants from the *TSC1* and *TSC2* LOVD databases (12, 13). In addition, we have received a small number of requests from various groups world-wide to investigate unclassified variants identified in these laboratories. We are currently analysing these variants (Supporting data, Tables 1 and 2). Since the start of the project we have analysed, or are in the process of analysing, 62 TSC2 variants and 20 TSC1 variants. The analysis of 24 TSC2 variants and 8 TSC1 variants have been completed and published (8 - 10), and a manuscript describing another 12 TSC1 variants is in preparation (see Appendix).

Assays to determine the effect of *TSC1* and *TSC2* variants on the structure and function of the TSC1-TSC2 protein complex cannot determine whether *TSC1* and *TSC2* variants affect the splicing of the nascent *TSC1* and *TSC2* mRNAs. To determine whether putative *TSC1* and *TSC2* splice site mutations are pathogenic, we will analyse the transcription and splicing of the *TSC1* and *TSC2* mRNAs in TSC patient fibroblasts using reverse transcriptase-polymerase chain reaction (RT-PCR) in combination with DNA sequencing and pyrosequencing. We are currently waiting for final ethical approval to approach patients for skin biopsies.

We routinely determine the likelihood that a nucleotide change causes a splicing defect using 3 different computer-based algorithms (14 - 16). Using this approach we have identified 8 reported missense changes (3 in *TSC2* and 5 in *TSC1*) that our analysis suggests are more likely to be pathogenic splice site mutations. In these cases, the predicted amino acid substitutions did not affect protein function and it will therefore be essential to establish whether splicing is affected. We will request skin biopsies from the relevant TSC patients and analyse the expression and splicing of the *TSC1* and *TSC2* mRNAs in cultured fibroblasts using a protocol already in routine use in our laboratory. We will isolate RNA from cells that have been pretreated with cycloheximide, to inhibit nonsense-mediated RNA decay, and thereby increase the rate of detection of aberrantly spliced mRNAs. A case-specific RT-PCR will be performed to detect abnormally spliced *TSC1* or *TSC2* mRNA transcripts. When no aberrantly spliced transcripts are detected, single nucleotide polymorphisms from within the *TSC1* and *TSC2* coding regions will be analysed to determine whether there is mRNA expression from both alleles. To obtain a quantitative estimate of the allele-specific expression of *TSC1* and *TSC2* mRNAs, pyrosequencing will be performed across the heterozygous regions. If a new splice

isoform is detected that results in a small in-frame deletion or insertion, we will test the predicted TSC1 or TSC2 variant using our functional assay.

2. Determine whether specific TSC1 and TSC2 mutations are associated with specific TSC phenotypes.

The functional studies have been critical in establishing whether specific changes in the *TSC1* and *TSC2* genes are pathogenic. Interestingly, some of the unclassified variants were identified in individuals and/or families exhibiting only mild or minor symptoms of TSC. Prior to the start of the project we had identified 2 TSC2 missense variants in different families with apparently mild TSC phenotypes (6, 17). For one variant, the functional tests indicated that the amino acid substitution did not inactivate TSC2 completely. Although the activity of the variant was clearly less than the wild-type protein, it was also more active than other TSC2 missense mutants (6). We have since confirmed this, using an improved immunoblotting protocol (Supporting data, Figure 3), and have identified more variants that may also have an intermediate effect on TSC2 function (Supporting data, Figure 4). We are still collecting data to be able to establish whether there are more mildly affected families and/or individuals with similar missense mutations.

3. Identification of amino acid residues/domains that are essential for TSC1 or TSC2 function.

At the start of the project we had identified 3 regions of particular interest:

1. Amino acid substitutions within the N-terminal region (amino acids 1 - 200) of TSC1 that destabilise TSC1.

2. Substitutions to a central region of TSC2 (amino acids 600 - 900) that disrupt TSC1-TSC2 binding

3. Substitutions outside the predicted TSC2 GAP domain that inactivate the complex.

Our analysis of more variants has enabled us to confirm these regions as important for TSC1-TSC2 function, and to further define different structural and catalytic regions in both TSC1 and TSC2. We have compared the results of our functional studies with computer-based predictions of the effects of the different amino acid substitutions.

Amino acid substitution prediction methods use sequence and/or structural information to predict the effects of amino acid changes on protein function (18, 19). In the absence of adequate genetic or functional data, prediction methods have been applied to try and resolve whether specific variants are pathogenic or not (20). The more information there is about a particular protein, the more accurate the prediction is likely to be. We have compared our functional data with predictions using the SIFT algorithm. There was a reasonable correlation between our findings and the predictions of the SIFT algorithm (Supporting data, Tables 1 and 2, and Figures 1 and 2), however there were also cases where there was disagreement. Some predicted tolerated changes were found to affect TSC1-TSC2 function; while no effect on function could be established for some changes that were predicted not to be tolerated. For example, SIFT analysis of TSC2 predicts that the majority of amino acid substitutions between residues 1100 and 1500 are tolerated (Supporting data, Figure 2). In this region we have already identified 3 pathogenic variants (V1199G, P1202H and P1497S) as well as 4 non-pathogenic variants

(P1292A, R1386W, S1410L and G1416D). This indicates that predictive methods are not reliable for molecular genetic diagnostics and that functional tests provide important, extra insight into the effects of different amino acid changes.

Numerous studies using truncated TSC2 proteins, including our own, have indicated that the N-terminal region of TSC2 is important for the interaction with TSC1. Our analysis of TSC2 variants confirms this. So far we have identified 12 residues between amino acids 200 and 800 that are critical for this interaction, and 8 substitutions within this region that do not significantly affect the TSC1-TSC2 interaction in our assays. In addition, 4 amino acid substitutions between amino acids 800 and 1000 prevented formation of the TSC1-TSC2 complex, indicating that the TSC1-binding region of TSC2 extends past residue 800. Furthermore, we have tested 6 substitutions mapping to the N-terminal 200 amino acids. These changes do not have such dramatic effects on TSC1-TSC2 binding, indicating that this region of TSC2 is not so important for the interaction with TSC1. Amino acid substitutions to the C-terminal region of TSC2 (amino acids 1000 - 1807) do not prevent TSC1-TSC2 binding. However, as predicted from homology studies, missense changes to the region with homology to other GAP proteins still result in inactivation of the TSC1-TSC2 complex. We have identified 22 amino acid substitutions between codon 900 and the C-terminal that do not prevent TSC1-TSC2 binding, but result in inactivation of the TSC1-TSC2 complex. In the same region, 9 amino acid changes did not affect TSC1-TSC2 function. These results indicate that the region of TSC2 necessary for GAP activity extends considerably further than the domain defined by homology with rap1GAP (2).

Less is known about the exact role of TSC1 within the TSC1-TSC2 complex (4, 21). SIFT analysis indicates that the N-terminal and C-terminal regions of the protein are not very tolerant of amino acid substitutions, while a large central domain is predicted to be quite tolerant of amino acid substitutions (Supporting data, Figure1). At the start of the project, it was still unclear whether missense mutations in the *TSC1* gene would lead to TSC. We analysed a series of putative pathogenic TSC1 missense variants, and were able to demonstrate for the first time that *TSC1* missense mutations cause TSC (9). We have now extended this analysis to include more putative pathogenic variants, as listed in the LOVD *TSC1* mutation database (12). Our analysis indicates that TSC1 missense mutations are clustered to a region containing the first 300 amino acids of TSC1, and that these substitutions affect the turn-over and stability of TSC1 in the cell (manuscript in preparation; see Appendix). Our analysis has therefore provided useful new information about the structure and function of TSC1.

4. Development of a rapid test for TSC1-TSC2 function.

One of the principle aims of the project was to improve the methodology of the functional analysis of unclassified *TSC1* and *TSC2* variants. At the start of the project our approach was to perform several different assays to analyse TSC1-TSC2 binding and the effect of TSC1-TSC2 on mTOR activity (see Section 1. above *"Application of functional assays to determine whether specific TSC1 and TSC2 variants are pathogenic mutations"*). We focused on these 2 aspects of TSC1-TSC2 function because mutations in either *TSC1* or *TSC2* cause the same disease, indicating that it is inactivation of the complex that is the critical event in TSC pathogenesis and because the rhebGAP activity and inhibition of mTOR signalling is the most clearly defined and intensively studied

function of the complex. Our hypothesis is that an active TSC1-TSC2 complex is essential for preventing the lesions associated with TSC from developing and that the TSC1-TSC2 interaction must be necessary for full rhebGAP activity.

The advantage of performing several independent assays in parallel was that it allowed the effects of different amino acid changes to be characterised with more certainty and indicated not only whether specific changes were disease-causing but also how these changes affected the TSC1-TSC2 complex and, as a consequence, signal transduction through mTOR. Multiple, independent assays were also helpful in confirming whether a variant was pathogenic or not. Discrepancies between the tests would help indicate that there was a potential problem. Fortunately, in general, the correlation between the different assays was good. Variants that did not form a stable TSC1-TSC2 complex were also unable to inhibit mTOR activity. Furthermore, we noticed that the levels of TSC1 detected by immunoblotting were significantly reduced in the presence of TSC2 variants that were unable interact with TSC1. Because this was clearly visible on direct immunoblots, the coimmunoprecipitation assay was made redundant. Furthermore, because some variants were unable to form a complex, we were unable to always assay the rhebGAP activity effectively. We found that the rhebGAP activity of TSC2 alone was significantly reduced compared to the TSC1-TSC2 complex, consistent with other reports (22). For this reason, and because the rhebGAP assay was complicated to set up and difficult to perform, we have focused on the immunoblot assay to assay both the TSC1-TSC2 interaction and effects on mTOR signalling.

For TSC2 variants we performed both single- and co-transfection experiments in *Tsc2* -/- MEFs. Somewhat surprisingly, we noticed that TSC2 variants that were unable to interact with TSC1, and did not inhibit S6K phosphorylation in cotransfected HEK 293T cells, were still able to inhibit S6 phoshorylation in *Tsc2* -/- MEFs. However, we concluded that this was an artefact of the over-expression of TSC2 in the MEFs because in MEFs over-expressing these variants together with TSC1 we did not observe significant inhibition of S6 phosphorylation. Furthermore, counting cells was time-consuming and less objective than the other tests because the experimenter had to decide whether each cell exhibits inihibition of S6 phosphorylation. Therefore, we decided to focus principally on the immunoblot assay, as this was the most reliable and straight-forward approach. It was quicker, easier and cheaper than the other methods and provided information on the stability of the variants being tested as well as on their biochemical activities. We have used this assay to determine whether specific variants in the *TSC1* and *TSC2* genes are pathogenic, causing disease in TSC patients. Furthermore, due to improvements in the protocol, we have been able to increase the numbers of variants that are analysed, and to reduce the cost per analysed variant.

To facilitate the analysis of unclassified *TSC1* and *TSC2* variants we developed a new, robust, reliable and rapid assay of TSC1-TSC2 function. Because the preparation of the TSC1 and TSC2 variant constructs by site-directed mutagenesis is an unavoidable step, we focused on developing improved methods for assaying TSC1-TSC2 activity. First we developed an enzyme-linked immunosorbent assay (ELISA) to detect TSC1-TSC2-dependent changes in the mTOR signal transduction pathway. However, we were unable to obtain satisfactorily reliable data due to high background signals. Therefore we decided to set up an in-cell Western (ICW) assay using secondary antibodies labelled with fluorochromes that are excited by irradiation in the infrared spectrum and

consequently suffer from less background noise than more conventional conjugates (23). ICW assays have the advantage of being reproducible, amenable to automation and simple to perform. For example, they are conveniently carried out in a 96-well microtitre plate format whcih makes handling and analysis straightforward. This approach proved more successful. We demonstrated that TSC1-TSC2 activty could be assayed using an ICW (10). Furthermore, the ICW assay was more reproducible than the existing immunoblotting approach and could, in part, be performed on a robot workstation. Comparison of the ICW results with results of the other assays of TSC1-TSC2 function indicated that the assay provided a good estimate of the ability of TSC2 variants to inhibit mTOR, but did not reveal whether this was because the TSC1-TSC2 interaction was affected. Furthermore, the ICW required large quantities of antibody, making the test relatively expensive. To overcome both these problems we reverted to our original immunoblot assay and concentrated on streamlining and improving the protocol. In particular, we have now switched to a new gel-buffer system that has overcome the previous reliability problems and reduced the time required for the running and blotting of the gels. Our current assay allows us to analyse the TSC1-TSC2 interaction and the activation of mTOR for 24 variants on a single gel.

Despite these improvements, assaying for the activity of TSC1 and TSC2 variants remains expensive and time-consuming. In particular, the construction of the mutants by site-directed mutagenesis remains a significant bottleneck.

Key Research Accomplishments

1. Derived 62 unclassified TSC2 variants: 27 pathogenic; 10 neutral; 27 still unclassified/analysis not complete (Supporting data, Table 2).

2. Derived 20 unclassified TSC1 variants: 8 pathogenic; 7 neutral; 5 unclassified/analysis not complete (Supporting data, Table 1).

3. Identification of *TSC1* missense mutations that cause TSC (9).

4. Identification of a region of TSC1 (amino acids 50 - 224) required for maintaining TSC1 at sufficient levels in the cell to form a stable TSC1-TSC2 complex and inhibit mTOR (manuscript in preparation; Appendix).

5. Identification of amino acid residues involved in (i) TSC1-TSC2 binding, and (ii) rhebGAP activity.

6. Robust assay for detection of pathogenic TSC2 variants (10).

7. Improvements in assay cost, throughput and reproducibility.

Reportable Outcomes

1. Manuscripts:

Nellist M, Sancak O, Goedbloed M, Adriaans, Wessels M, Maat-Kievit A, Baars M, Dommering C, van den Ouweland A and Halley D. "Functional characterisation of the TSC1-TSC2 complex te assess multiple *TSC2* variants identified in single families affected by tuberous sclerosis complex". BMC Med. Genet. (2008) 9:10 doi:10.1186/1471-2350-9-10.

Nellist M, van den Heuvel D, Schluep D, Exalto C, Goedbloed M, Maat-Kievit A, van Essen T, van Spaendonck-Zwarts, Jansen F, Helderman P, Bartalini G, Vierimaa O, Penttinen M, van den Ende J, van den Ouweland A and Halley D. "Missense mutations to the *TSC1* gene cause tuberous sclerosis complex". Eur. J. Hum. Genet. (2008) doi:10.1038/ejhg.2008.170.

Coevoets R, Arican S, Hoogeveen-Westerveld M, Simons E, van den Ouweland A, Halley D and Nellist M. "A reliable cell-based assay for testing unclassified *TSC2* gene variants." Eur. J. Hum. Genet. (2008) doi:10.1038/ejhg.2008.184.

2. Abstracts/Presentations:

Nellist M "Functional analysis of TSC1 and TSC2 variants" 9th International Research Conference on Tuberous Sclerosis Complex, 11 - 13th September 2008, University of Sussex, Brighton, U.K. (oral presentation).

Mozaffari M, Hoogeveen-Westerveld M and Nellist M "Functional analysis of *TSC1* missense mutations identified in individuals with tuberous sclerosis complex" Poster Session, 6th November 2008, LAM/TSC Seminar series, Harvard Medical School, Boston, Massachusetts, U.S.A. (poster presentation).

3. Degrees awarded (supported by this award):

4. Databases:

Data generated by this study has been added to the LOVD *TSC1* and *TSC2* mutation databases (12, 13).

Conclusions

Pathogenic, non-truncating *TSC1* and *TSC2* mutations can be distinguished from non-pathogenic changes by studying the effects of the changes on the TSC1-TSC2 protein complex, or on splicing of the *TSC1* and *TSC2* mRNAs. Functional characterisation of unclassified *TSC1* and *TSC2* variants complements existing diagnostic tests and enables appropriate clinical care and counselling for more TSC patients and their relatives.

Characterisation of multiple TSC1 and TSC2 variants has helped to define structural and catalytic domains in TSC1 and TSC2. Identification of the amino acid residues that are essential for regulating TSC1 and TSC2 turn-over and for maintaining both the interaction between the two proteins and the integrity of the GAP domain should help provide insight into the folding and three-dimensional structure of both proteins, as well as the regulation and mechanism of GAP catalysis. The stability of the different TSC1 and TSC2 variants, the strength of the TSC1-TSC2 interaction and the GAP activity all influence the biological activity of the TSC1 and TSC2 variants *in vivo*.

In addition, the characterisation of the variants has provided insight into genotype-phenotype correlations in TSC. We have obtained ecidence that some non-truncating TSC2 mutations retain some activity and may be associated with a less severe TSC phenotype.

We have assayed 2 aspects of TSC1 and TSC2 function to determine whether specific amino acid changes are pathogenic. In addition to these protein experiments, we will perform RT-PCR to establish whether putative splice site mutations in the *TSC1* and *TSC2* genes affect mRNA transcription, and cause disease. Prior to the start of the project we investigated the effects of 4 unclassified splice site variants by RT-PCR. A *TSC2* c.336+2insGT change reduced expression of the normal *TSC2* mRNA and produced a mutant splice variant derived from a site 90 bp downstream of the normal donor site. A *TSC2* c.2546-27del14 change resulted in expression of a mutant mRNA species containing 104 nucleotides from intron 21. A *TSC2* c.599+4A>G substitution that cosegregated with TSC in a multi-generation family only revealed the normal TSC2 mRNA. No TSC2 mRNA was transcribed from the mutant allele. Likewise, mRNA from a *TSC2* c.4611G>A mutant allele was either unstable or not transcribed. We are currently awaiting ethical approval to be able to continue with these experiments.

In total, we have tested, or are in the process of testing, 91 TSC2 variants and 25 TSC1 variants. So far, we have classified 45 TSC2 variants and 11 TSC1 variants as pathogenic, and 20 TSC2 variants and 9 TSC1 variants as not pathogenic.

Innovations:

The functional characterisation of TSC1 and TSC2 variants has extended the current diagnostic service that can be offered to TSC patients and their families. Further, it has helped identify and characterise the structural and functional domains in TSC1 and TSC2, and provided insight into specific genotype-phenotype correlations in TSC.

Impact:

Test to allow pathogenic and non-pathogenic *TSC1* and *TSC2* variants to be distinguished are of direct importance to the individuals who carry or may inherit these

variants, and the data generated by this study will have a significant impact on individuals and families affected by TSC in whom 'unclassified variants' have been identified.

The results from the study have already enabled families to obtain more certainty about their condition and to be be able to seek appropriate and accurate care and counselling. In addition, comparison of the biochemical effects of different pathogenic variants with the corresponding phenotypes in the affected individuals has provided additional insight into possible genotype-phenotype correlations in TSC. In particular, we have established that specific non-truncating mutations could be associated with a less severe TSC phenotype.

Finally, the identification of amino acids essential for TSC1-TSC2 function has provided more insight into the molecular mechanisms of TSC1-TSC2 function. These data will be useful not only for assessing and testing the accuracy of current predictive methods of amino acid analysis but also in the development of new, improved predictive methods.

References

1.   Gomez M, Sampson J, Whittemore V, eds. *The tuberous sclerosis complex*. Oxford University Press, Oxford, UK, 1999.

2.   The European Chromosome 16 TSC Consortium. Identification and characterisation of the tuberous sclerosis gene on chromosome 16. Cell 75 (1993) 1305-1315.

3.   van Slegtenhorst M, de Hoogt R, Hermans C, Nellist M, Janssen LAJ, Verhoef S, Lindhout D, van den Ouweland AMW, Halley DJJ, Young J, Burley M, Jeremiah S, Woodward K, Nahmias J, Fox M, Ekong R, Wolfe J, Povey S, Osborne J, Snell RG, Cheadle JP, Jones AC, Tachataki M, Ravine D, Sampson JR, Reeve MP, Richardson P, Wilmer F, Munro C, Hawkins TL, Sepp T, Ali, JBM, Ward S, Green AJ, Yates JRW, Short MP, Haines JH, Jozwiak S, Kwiatkowska J, Henske EP and Kwiatkowski DJ. Identification of the tuberous sclerosis gene (*TSC1*) on chromosome 9q34. Science (1997) 277 805-808.

4.   Huang J and Manning BD: The TSC1-TSC2 complex: a molecular switchboard controlling cell growth. Biochem J. (2008) 412 179-190.

5.   Sancak O, Nellist M, Goedbloed M, Elfferich P, Wouters C, Maat-Kievit A, Zonnenberg B, Verhoef S, Halley D and van den Ouweland A. Mutational analysis of the TSC1 and TSC2 genes in a diagnostic setting: Genotype - phenotype correlations and comparison of diagnostic DNA techniques in Tuberous Sclerosis Complex. Eur. J. Hum. Genet. (2005) 13 731-741.

6.   Jansen A, Sancak O, D'Agostino D, Badhwar A, Roberts P, Gobbi G, Wilkinson R, Melanson D, Tampieri D, Koenekoop R, Gans M, Maat-Kievit A, Goedbloed M, van den Ouweland AMW, Nellist M, Pandolfo M, McQueen M, Sims K, Thiele E, Dubeau F, Andermann F, Kwiatkowski DJ, Halley DJJ and Andermann E. Mild form of tuberous sclerosis complex is associated with TSC2 R905Q mutation. Ann. Neurol. (2006) 60 528-539.

7.   Jansen FE, Braams O, Vincken KL, Algra A, Anbeek P, Jennekens-Schinkel A, Halley D, Zonnenberg BA, van den Ouweland A, van Huffelen AC, van Nieuwenhuizen O and Nellist M. (2006) Overlapping neurological and cognitive phenotypes in patients with *TSC1* or *TSC2* mutations. Neurology (2008) 70 908-915.

8.   Nellist M, Sancak O, Goedbloed M, Adriaans, Wessels M, Maat-Kievit A, Baars M, Dommering C, van den Ouweland A and Halley D. Functional characterisation of the TSC1-TSC2 complex te assess multiple *TSC2* variants identified in single families affected by tuberous sclerosis complex. BMC Med. Genet. (2008) 9:10 doi:10.1186/1471-2350-9-10.

9.   Nellist M, van den Heuvel D, Schluep D, Exalto C, Goedbloed M, Maat-Kievit A, van Essen T, van Spaendonck-Zwarts, Jansen F, Helderman P, Bartalini G, Vierimaa O, Penttinen M, van den Ende J, van den Ouweland A and Halley D. Missense mutations to the *TSC1* gene cause tuberous sclerosis complex. Eur. J. Hum. Genet. (2008) doi:10.1038/ejhg.2008.170.

10.   Coevoets R, Arican S, Hoogeveen-Westerveld M, Simons E, van den Ouweland A, Halley D and Nellist M. A reliable cell-based assay for testing unclassified *TSC2* gene variants. Eur. J. Hum. Genet. (2008), doi:10.1038/ejhg.2008.184.

11.   Nellist M, Sancak O, Goedbloed MA, Rohe C, van Netten D, Mayer K, Tucker-Williams A, van den Ouweland AMW and Halley DJJ. Distinct effects of single amino acid changes to tuberin on the function of the tuberin-hamartin complex. Eur. J. Hum. Genet. (2005) 13 59-68.

12.   Tuberous sclerosis database - Leiden Open Variation Database [www.chromium.liacs.nl/lovd/index.php?select_db=TSC1].

13.   Tuberous sclerosis database - Leiden Open Variation Database [www.chromium.liacs.nl/lovd/index.php?select_db=TSC2].

14.   NetGene2 Server [www.cbs.dtu.dk/services/NetGene2].

15.   BDGP: Splice Site Prediction by Neural Network [www.fruitfly.org/seq_tools/splice.html].

16.   Human Splicing Finder [www.umd.be/HSF/HSF.html].

17.   Mayer K, Goedbloed M, van Zijl K, Nellist M and Rott HD. Characterisation of a novel TSC2 missense mutation in the GAP related domain associated with minimal clinical manifestations of tuberous sclerosis. J. Med. Genet. (2004) 41 e64.

18.   Ng PC and Henikoff S. Predicting the effects of amino acid substitutions on protein function. Annu. Rev. Genomics Hum. Genet. (2006) 7 61-80.

19.   Ng PC and Henikoff S. Accounting for human polymorphisms predicted to affect protein function. Genome Res. (2002) 12 436-446.

20.   Mathe E, Olivier M, Kato S, Ishioka C, Hainaut P and Tavtigian SV. Computational approaches for predicting the biological effect of p53 missense mutations: a comparison of three sequence analysis based methods. Nuc. Acids. Res. (2006) 34 1317-1325.

21.   Rosner M, Hanneder M, Siegel N, Valli A, Fuchs C, Hengstschlager M. The tuberous sclerosis gene products hamartin and tuberin are multifunctional proteins with a wide spectrum of interacting partners. Mut. Res. (2008) 658 234-246.

22.   Garami A, Zwartkruis FJ, Nobukuni T, Joaquin M, Roccio M, Stocker H, Kozma SC, Hafen E, Bos JL and Thomas G. Insulin activation of rheb, a mediator of mTOR/S6K/4E-BP signaling, is inhibited by TSC1 and 2. Mol. Cell (2003) 11 1457-1466.

23.   Schutz-Geschwender A, Zhang Y, Holt T, McDermitt D, Olive DM (2004) Quantitative, two-color Western blot detection with infrared fluorescence. http://www.licor.com/bio/PDF/IRquant.pdf (25 Jul.2006).

Supporting Data

Table 1. Functional classification of TSC1 variants. Variants analysed as part of the current project are indicated in bold.

nucleotide change	effect on splicing predicted?	amino acid change	SIFT prediction	effect on TSC2 function?	status	reference
c.149T>C	**no**	**p.L50P**	**not tolerated**	**yes**	**pathogenic**	**see appendix**
c.153A>C	**no**	**p.E51D**	**tolerated**	**no**	**not pathogenic**	**see appendix**
c.182T>C	**no**	**p.L61P**	**not tolerated**	**yes**	**pathogenic**	**see appendix**
c.278T>G	**no**	**p.L93R**	**not tolerated**	**yes**	**pathogenic**	**see appendix**
c.350T>C	no	p.L117P	**not tolerated**	yes	pathogenic	9
c.379_381delTGT	**yes**	**p.128delV**	**-**	**yes**	**pathogenic**	**9**
c.397G>T	**no**	**p.V133F**	**not tolerated**	**yes**	**pathogenic**	**see appendix**
c.539T>C	**no**	**p.L180P**	**not tolerated**	**yes**	**pathogenic**	**9**
c.568C>T	no	p.R190C	not tolerated	no	not pathogenic	see appendix
c.569G>C	**no**	**p.R190P**	**not tolerated**	**yes**	**pathogenic**	**see appendix**
c.572T>A	**no**	**p.L191H**	**not tolerated**	**yes**	**pathogenic**	**9**
c.593_595delACT	no	p.NF198delinsI	-	yes	pathogenic	9
c.671T>G	no	p.M224R	not tolerated	yes	pathogenic	9
c.737G>A	**yes**	**p.R246K**	**not tolerated**	**no**	**pathogenic splice***	**9**
c.913G>A	**yes**	**p.G305R**	**tolerated**	**no**	**pathogenic splice***	**9**
c.913G>T	**yes**	**p.G305W**	**tolerated**	**no**	**pathogenic splice***	**9**
c.1001C>T	**no**	**p.S334L**	**tolerated**	**no**	**not pathogenic**	**see appendix**
c.1433A>G	**yes**	**p.E478G**	**tolerated**	**no**	**not pathogenic**	**see appendix**
		p.479insGN	**-**	**possible**	**analysis not yet completed**	

nucleotide change	effect on splicing predicted?	amino acid change	SIFT prediction	effect on TSC2 function?	status	reference
c.1526G>A	no	p.R509Q	tolerated	no	not pathogenic	9
c.1648C>G	no	p.Q550E	tolerated	no	not pathogenic	see appendix
c.1974C>G	no	p.D658E	tolerated	no	not pathogenic	see appendix
c.1976C>T	no	p.A659V	tolerated	no	not pathogenic	see appendix
c.2420T>C	no	p.I807T	tolerated	no	not pathogenic	see appendix
c.3103G>A	no	p.G1035S	tolerated	no	not pathogenic	9
c.3290G>A	no	p.R1097H	tolerated	no	not pathogenic	9

Table 2. Functional classification of TSC2 variants. Variants analysed as part of the current project are indicated in bold.

nucleotide change	effect on splicing predicted?	amino acid change	SIFT prediction	effect on TSC2 function?	status	reference
c.170G>A	**no**	**p.R57H**	**not tolerated**	**possible**	**analysis not yet completed**	
c.185G>A	**no**	**p.G62E**	**tolerated**	**no**	**not pathogenic**	**10**
c.292C>T	**no**	**p.R98W**	**not tolerated**	**yes (mild)**	**unclassified**	**10**
c.395C>G	**no**	**p.S132C**	**tolerated**	**no**	**not pathogenic**	**8**
c.429C>G	**no**	**p.F143L**	**tolerated**	**yes (mild)**	**unclassified**	**8**
c.586G>A	**no**	**p.A196T**	**tolerated**	**no**	**not pathogenic**	
c.646G>A	**no**	**p.E216K**	**tolerated**	**possible**	**analysis not yet completed**	
c.656T>C	**no**	**p.L219P**	**not tolerated**	**yes**	**pathogenic**	
c.730T>C	**no**	**p.C244R**	**not tolerated**	**yes**	**pathogenic**	**8**
c.825C>A	**no**	**p.N275K**	**tolerated**	**possible**	**analysis not yet completed**	
c.824delACA	**no**	**p.275delN**	**-**	**yes**	**pathogenic**	**10**
c.1001T>C	**no**	**p.V334A**	**not tolerated**	**possible**	**analysis not yet completed**	
c.1001T>G	**no**	**p.V334G**	**not tolerated**	**possible**	**analysis not yet completed**	
c.1019T>C	**no**	**p.L340P**	**not tolerated**	**yes**	**pathogenic**	
c.1100G>A	no	p.R367Q	tolerated	no	not pathogenic	11
c.1118A>C	**yes**	**p.Q373P**	**tolerated**	**no**	**pathogenic splice**	**10**

nucleotide change	effect on splicing predicted?	amino acid change	SIFT prediction	effect on TSC2 function?	status	reference
c.1235A>T	yes	p.E412V	not tolerated	no	not pathogenic	7
		p.412del8	-	**yes**	**pathogenic splice**	
c.1255C>T	**yes**	**p.P419S**	**not tolerated**	**possible**	**analysis not completed yet**	
c.1366G>A	**no**	**p.E456K**	**tolerated**	**no**	**not pathogenic**	
c.1385G>A	**no**	**p.R462H**	**not tolerated**	**possible**	**analysis not completed yet**	
c.1385_1386delinsCT	**no**	**p.R462P**	**not tolerated**	**possible**	**analysis not completed yet**	
c.1397T>C	**no**	**p.L466P**	**tolerated**	**yes**	**pathogenic**	
c.1574A>G	no	p.N525S	tolerated	no	not pathogenic	11
c.1736del78	**no**	**p.580del26**	**-**	**yes**	**pathogenic**	**10**
c.1791insCAC	no	p.597insH	-	yes	pathogenic	
c.1792T>C	**no**	**p.Y598H**	**tolerated**	**yes**	**pathogenic**	**8**
c.1796A>T	no	p.K599M	tolerated	no	not pathogenic	11
c.1820C>A	**no**	**p.A607E**	**tolerated**	**yes**	**pathogenic**	**10**
c.1819G>T	**no**	**p.A607S**	**tolerated**	**no**	**not pathogenic**	
c.1819G>A	no	p.A607T	tolerated	no	not pathogenic	
c.1826_1828dup	no	p.609insS	-	yes	pathogenic	11
c.1832G>A	no	p.R611Q	not tolerated	yes	pathogenic	11
c.1831C>T	no	p.R611W	not tolerated	yes	pathogenic	11
c.1841C>A	no	p.A614D	tolerated	yes	pathogenic	11
c.1844T>C	no	p.F615S	tolerated	yes	pathogenic	11
c.1865G>C	**no**	**p.R622C**	**not tolerated**	**possible**	**analysis not completed yet**	
c.1864C>T	**no**	**p.R622W**	**not tolerated**	**yes**	**pathogenic**	

nucleotide change	effect on splicing predicted?	amino acid change	SIFT prediction	effect on TSC2 function?	status	reference
c.2078T>C	**no**	**p.L693P**	**not tolerated**	**possible**	**analysis not completed yet**	
c.2087G>A	no	p.C696Y	not tolerated	yes	pathogenic	11
c.2306T>A	no	p.V769E	tolerated	yes	pathogenic	11
c.2363T>G	**no**	**p.M788R**	**not tolerated**	**possible**	**analysis not completed yet**	
c.2458_2460del	no	p.820delI	-	yes	pathogenic	8
c.2476C>A	no	p.L826M	not tolerated	no	not pathogenic	11
c.2666C>T	**no**	**p.A889V**	**not tolerated**	**possible**	**analysis not completed yet**	
c.2690T>C	**no**	**p.F897S**	**not tolerated**	**yes**	**pathogenic**	
c.2713C>G	no	p.R905G	not tolerated	yes	pathogenic	6
c.2714G>A	no	p.R905Q	not tolerated	yes (mild)	pathogenic	6, 11
c.2713C>T	no	p.R905W	not tolerated	yes	pathogenic	6
c.2747T>G	no	p.L916R	not tolerated	yes	pathogenic	
c.2853A>T	**no**	**p.R951S**	**tolerated**	**possible**	**analysis not completed yet**	
c.2963G>C	no	p.R988P	tolerated	no	not pathogenic	
c.2978C>T	no	p.T993M	tolerated	no	not pathogenic	8
c.3082G>A	**no**	**p.D1028N**	**not tolerated**	**possible**	**analysis not completed yet**	
c.3095G>C	no	p.R1032P	not tolerated	yes	pathogenic	
c.3106T>C	**no**	**p.S1036P**	**not tolerated**	**possible**	**analysis not completed yet**	
c.3182T>C	**no**	**p.L1061P**	**not tolerated**	**yes**	**pathogenic**	
c.3203C>A	**no**	**p.T1068I**	**not tolerated**	**yes**	**pathogenic**	**10**
c.3224C>T	**no**	**p.T1075I**	**not tolerated**	**no**	**not pathogenic**	**10**

nucleotide change	effect on splicing predicted?	amino acid change	SIFT prediction	effect on TSC2 function?	status	reference
c.3476G>T	no	p.R1159L	tolerated	possible	analysis not completed yet	
c.3476G>A	no	p.R1159Q	tolerated	possible	analysis not completed yet	
c.3475C>T	no	p.R1159W	tolerated	possible	analysis not completed yet	
c.3596T>G	no	p.V1199G	tolerated	yes	pathogenic	10
c.3598C>T	no	p.R1200W	not tolerated	possible	analysis not completed yet	
c.3605C>A	no	p.P1202H	tolerated	yes	pathogenic	11
c.3943C>G	no	p.P1313A (P1292A)	tolerated	no	not pathogenic	10
c.4105C>T	no	p.R1369W (R1346W)	tolerated	possible	analysis not completed yet	
c.4225C>T	no	p.R1409W (R1386W)	tolerated	no	not pathogenic	
c.4298C>T	no	p.S1433L (S1410L)	tolerated	no	not pathogenic	10
c.4316G>A	no	p.G1439D (G1416D)	tolerated	no	not pathogenic	10
c.4490C>G	no	p.P1497R (P1474R)	not tolerated	possible	analysis not completed yet	
c.4489C>T	no	p.P1497S (P1474S)	tolerated	yes	pathogenic	
c.4489C>A	no	p.P1497T (P1474T)	not tolerated	possible	analysis not completed yet	
c.4525_4527del	no	p.1510delF (1487delF)	-	no	not pathogenic	
c.4601T>A	no	p.L1534H (L1511H)	not tolerated	yes	pathogenic	8
c.4604A>C	no	p.D1535A (D1512A)	not tolerated	yes	pathogenic	10
c.4643T>C	no	p.L1548P (L1525P)	not tolerated	yes	pathogenic	
c.4700G>T	no	p.G1567V (G1544V)	not tolerated	yes	pathogenic	10

nucleotide change	effect on splicing predicted?	amino acid change	SIFT prediction	effect on TSC2 function?	status	reference
c.4726del57	**no**	**p.1575del19 (1552del19)**	**-**	**yes**	**pathogenic**	**10**
c.4733T>C	**no**	**p.L1578P (L1555P)**	**not tolerated**	**yes**	**pathogenic**	
c.4735G>A	no	p.G1579S (G1556S)	not tolerated	yes	pathogenic	17
c.4918C>T	**no**	**p.H1640Y (H1617Y)**	**not tolerated**	**yes**	**pathogenic**	**10**
c.4927A>C	**no**	**p.N1643H (N1620H)**	**not tolerated**	**possible**	**analysis not completed yet**	
c.4928A>T	**no**	**p.N1643I (N1620I)**	**not tolerated**	**possible**	**analysis not completed yet**	
c.4929C>G	**no**	**p.N1643K (N1620K)**	**not tolerated**	**possible**	**analysis not completed yet**	
c.4928A>G	no	p.N1643S (N1620S)	not tolerated	yes	pathogenic	
c.4937T>G	**no**	**p.V1646G (V1623G)**	**not tolerated**	**yes**	**pathogenic**	**10**
c.5057A>C	no	p.Q1686P (Q1663P)	tolerated	yes	pathogenic	
c.5138G>A	no	p.R1713H (R1690H)	not tolerated	yes	pathogenic	
c.5228G>A	**no**	**p.R1743Q (R1720Q)**	**not tolerated**	**yes**	**pathogenic**	**10**
c.5227C>T	**no**	**p.R1743W (R1720W)**	**not tolerated**	**yes**	**pathogenic**	**10**
c.5238_5255del18	**no**	**p.1746del6 (1723del6)**	**-**	**possible**	**analysis not completed yet**	
c.5376G>C	**no**	**p.Q1792H (Q1769H)**	**not tolerated**	**possible**	**analysis not completed yet**	
c.5383C>T	no	R1795C (R1772C)	not tolerated	no	not pathogenic	8
c.5386C>A	**no**	**p.L1796I (L1773I)**	**tolerated**	**possible**	**analysis not completed yet**	

Figure 1. Comparison of TSC1 SIFT prediction analysis and data from the LOVD *TSC1* mutation database.

(A) TSC1 SIFT prediction analysis. Graphical representation of the SIFT analysis results for TSC1. Each amino acid is represented by a box. Solid green boxes represent positions that are completely tolerant (all amino acid changes are possible); open green boxes represent positions where one or two amino acid substitutions are not tolerated. Solid red boxes represent completely intolerant positions (no amino acid changes tolerated); open red boxes represent positions where only three or fewer amino acid changes are tolerated. The stop codon is indicated in blue.

(B) TSC1 variants listed in the LOVD *TSC1* mutation database. Graphical representation of variants listed in the LOVD *TSC1* mutation database. Each amino acid is represented by a box. Green indicates a neutral variant; red indicates a pathogenic change; orange indicates an unclassified variant. Variants analysed as part of this project are highlighted in bold. The stop codon is indicated in blue.

Figure 2. Comparison of TSC2 SIFT prediction analysis and data from the LOVD *TSC2* mutation database.

(A) TSC2 SIFT prediction analysis. Graphical representation of the SIFT analysis results for TSC2. Each amino acid is represented by a box. Solid green boxes represent positions that are completely tolerant (all amino acid changes are possible); open green boxes represent positions where one or two amino acid substitutions are not tolerated. Solid red boxes represent completely intolerant positions (no amino acid changes tolerated); open red boxes represent positions where only three or fewer amino acid changes are tolerated. The stop codon is indicated in blue.

(B) TSC2 variants listed in the LOVD *TSC2* mutation database. Graphical representation of variants listed in the LOVD *TSC2* mutation database. Each amino acid is represented by a box. Green indicates a neutral variant; red indicates a pathogenic change; orange indicates an unclassified variant. Variants analysed as part of this project are highlighted in bold. The stop codon is indicated in blue.

Figure 3. TSC1-TSC2 dependent inhibition of signalling through mTOR by TSC2 codon 905 variants.

(A) Immunoblot analysis of HEK 293T cells expressing TSC1, S6K and either wild-type TSC2 or the R905G, R905Q or R905W variants. Cells were transfected with decreasing amounts of the wild-type or variant expression constructs. Wild-type TSC2 (TSC2), the TSC2 variants (R905G, R905Q, R905W), TSC1, T389-phosphorylated S6K (T389) and total S6K (S6K) were detected using specific antibodies.

(B) Mean ratio of T389-phosphorylated S6K (T389) to total S6K (T389/S6K) in the presence of wild-type TSC2 and the different vcodon 905 variants. S6K phosphorylation in the presence of the R905Q variant is reduced compared to the pathogenic R905G and R905W variants, but is increased with respect to active, wild-type TSC2. Standard deviations are indicated.

(C) Inhibition of S6 S235/236 phosphorylation in *Tsc2* -/- MEFs. Wild-type TSC2 (TSC2), the TSC2 R905G, R905Q and R905W variants and the R611Q mutant were over-expressed in *Tsc2* -/- MEFs either with or without coexpressed TSC1. Cells expressing the different TSC2 variants were counted in 3 separate experiments (>50 cells

were counted per experiment) and the number of cells showing a clear reduction in S6 phosphorylation were determined. The mean percentage of cells showing inhibition of S6 phosphorylation is indicated for each variant. The proportion of cells expressing the TSC2 R905Q variant and showing inhibition of S6 phosphorylation is reduced compared to wild-type TSC2 but increased compared to the pathogenic R905G, R905W and R611Q mutants. Standard deviations are indicated.

Figure 4. TSC1-TSC2 dependent inhibition of S6K-T389 phosphorylation by the TSC2 R57H variant.
(A) Immunoblot analysis of HEK 293T cells expressing TSC1, S6K and either wild-type TSC2, the R57H variant or the R611Q mutant. Control cells transfected with either TSC1 and S6K only, S6K only or with vector only (control) are also indicated. The TSC2 variants, TSC1, T389-phosphorylated S6K (T389) and total S6K (S6K) were detected using specific antibodies.
(B) - (E) Quantification of the immunoblot shown in (A), showing approximately equal levels of the different TSC2 variants (B); reduced TSC1 levels in the absence of TSC2 or the presence of the R611Q mutant (C); approximately equal levels of S6K (D); increased ratio of T389-phosphorylated to total S6K in the absence of wild-type TSC2 (E). Note that the mean level of TSC1 in the cells excpressing the R57H variant is reduced with respect to the wild-type TSC2 control, and that the mean T389/S6K ratio is increased with respect to the wild-type TSC2, but decreased compared to the pathogenic R611Q mutant.

Figure 1.

A TSC1 SIFT analysis

- ■ no change tolerated
- □ <3 changes tolerated
- □ <2 changes not tolerated
- ■ no restriction
- ■ stop

B TSC1 variants (LOVD)

- ■ pathogenic change
- □ see Table 2.
- ■ unclassified variant
- ■ neutral variant
- ■ stop codon

27
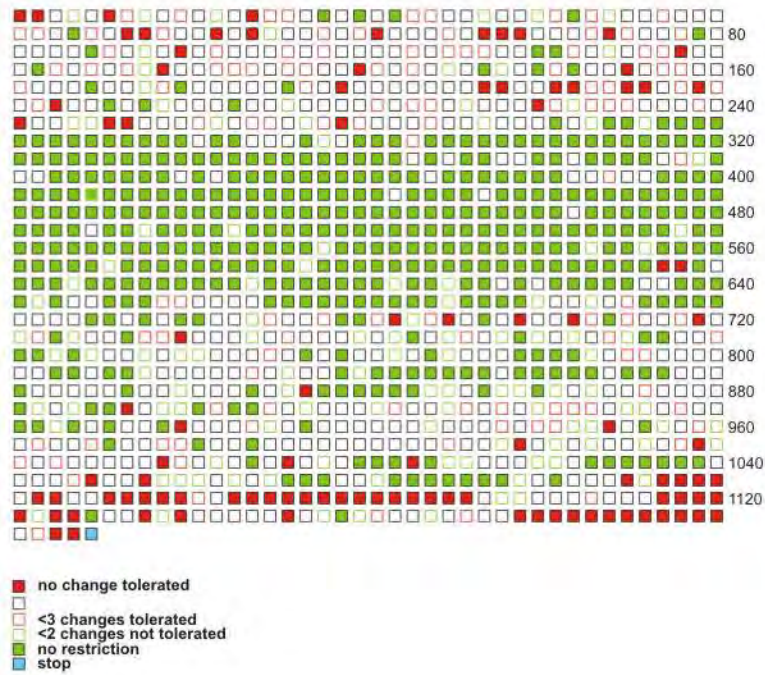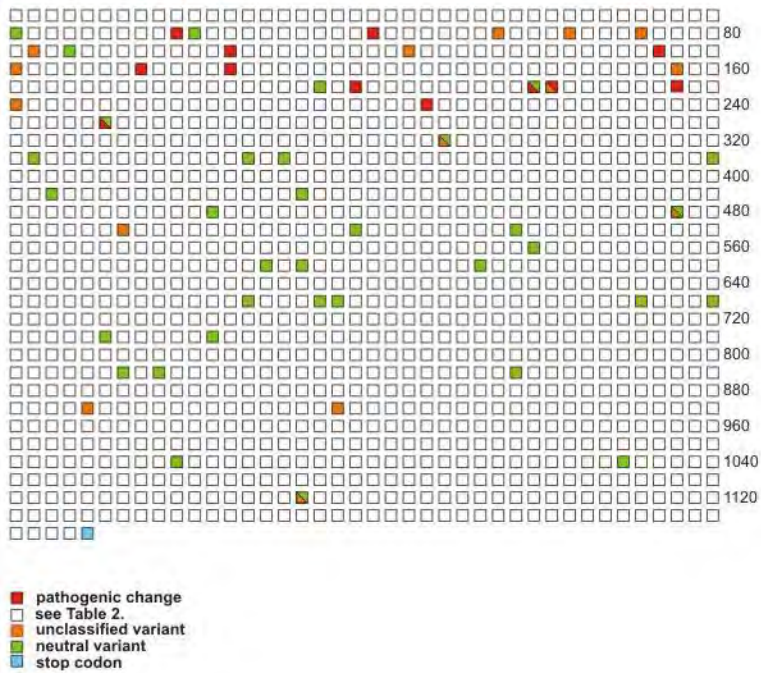
Figure 2.

A   TSC2 SIFT analysis

- ■ no change tolerated
- □
- ■ <3 changes tolerated
- ■ <2 changes not tolerated
- ■ no restriction
- □ stop codon

B   TSC2 variants (LOVD)

- ■ pathogenic change
- □ see Table 1.
- ■ unclassified variant
- ■ neutral variant
- □ stop codon

28
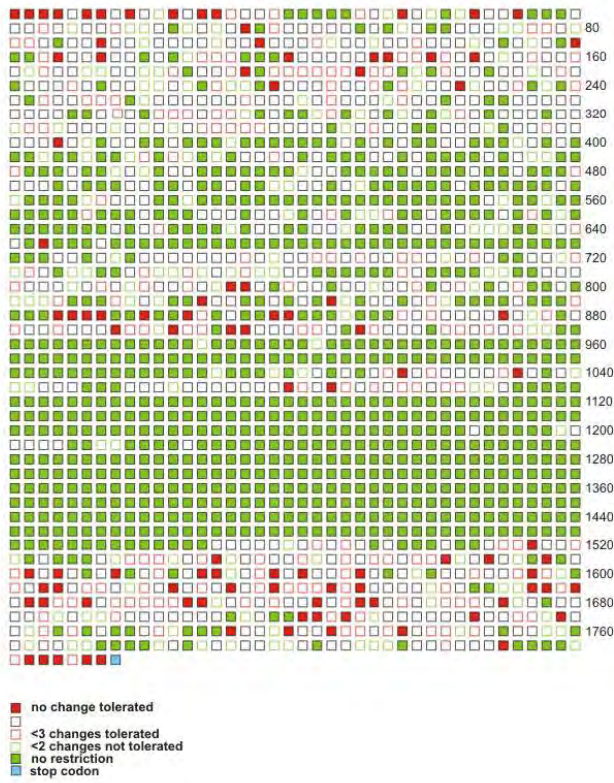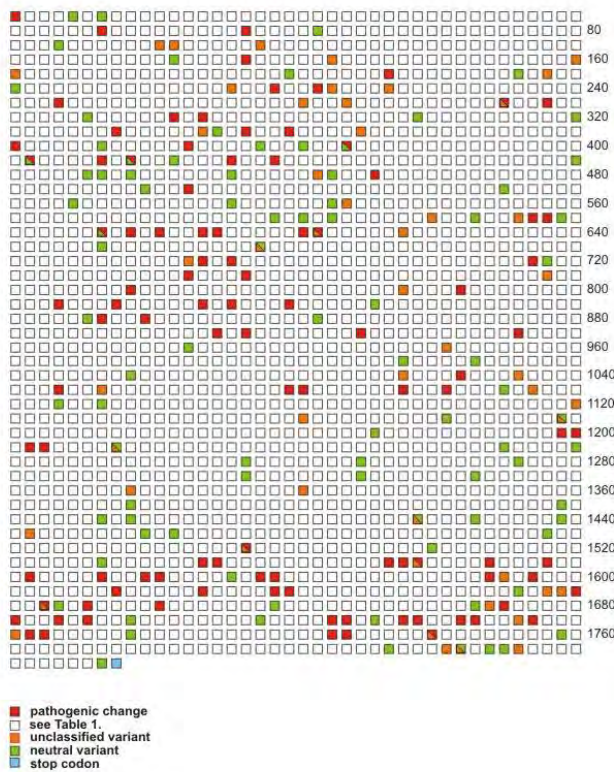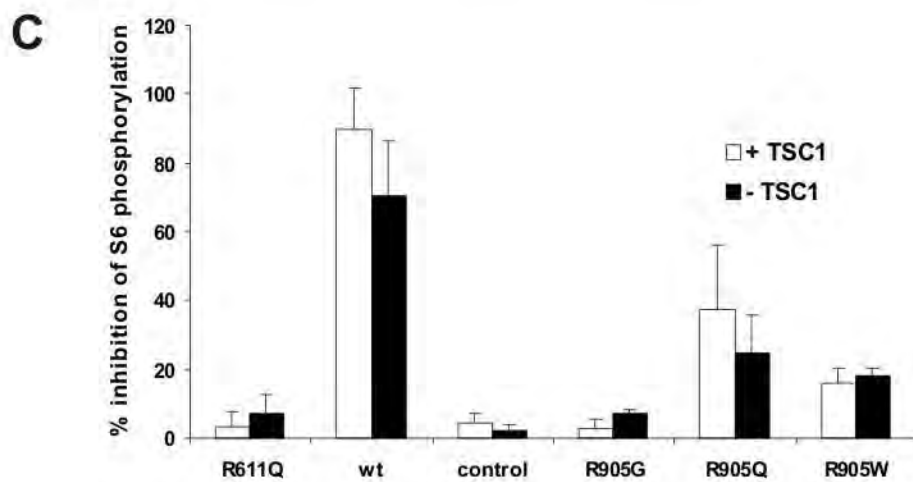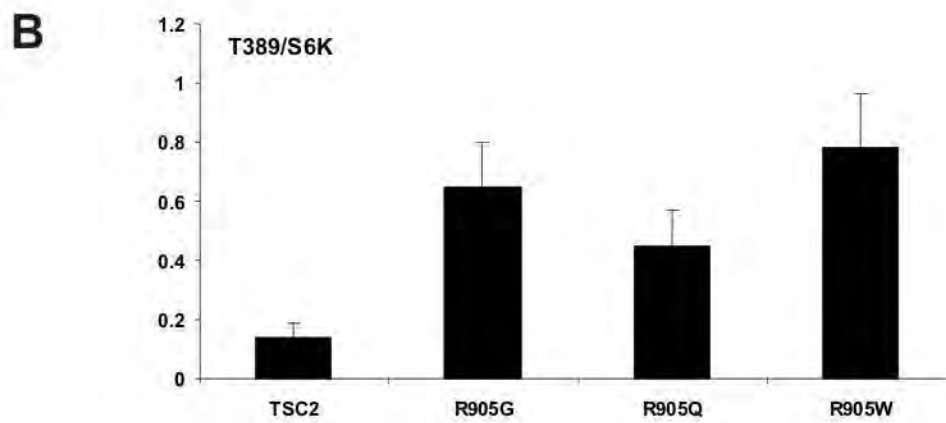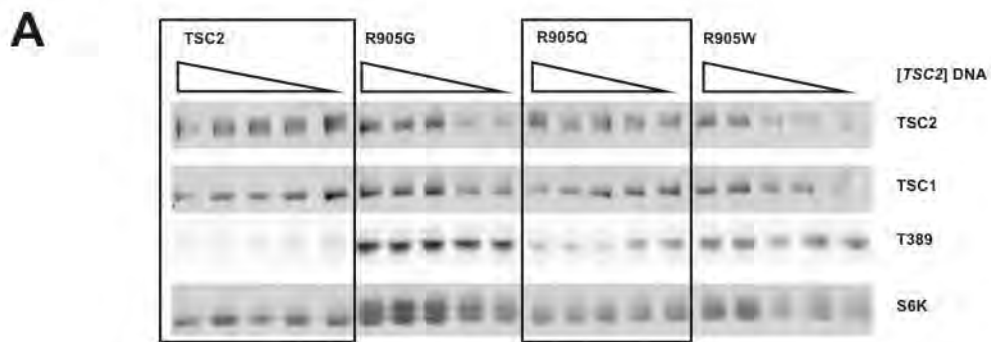
Figure 3.

Figure 4.
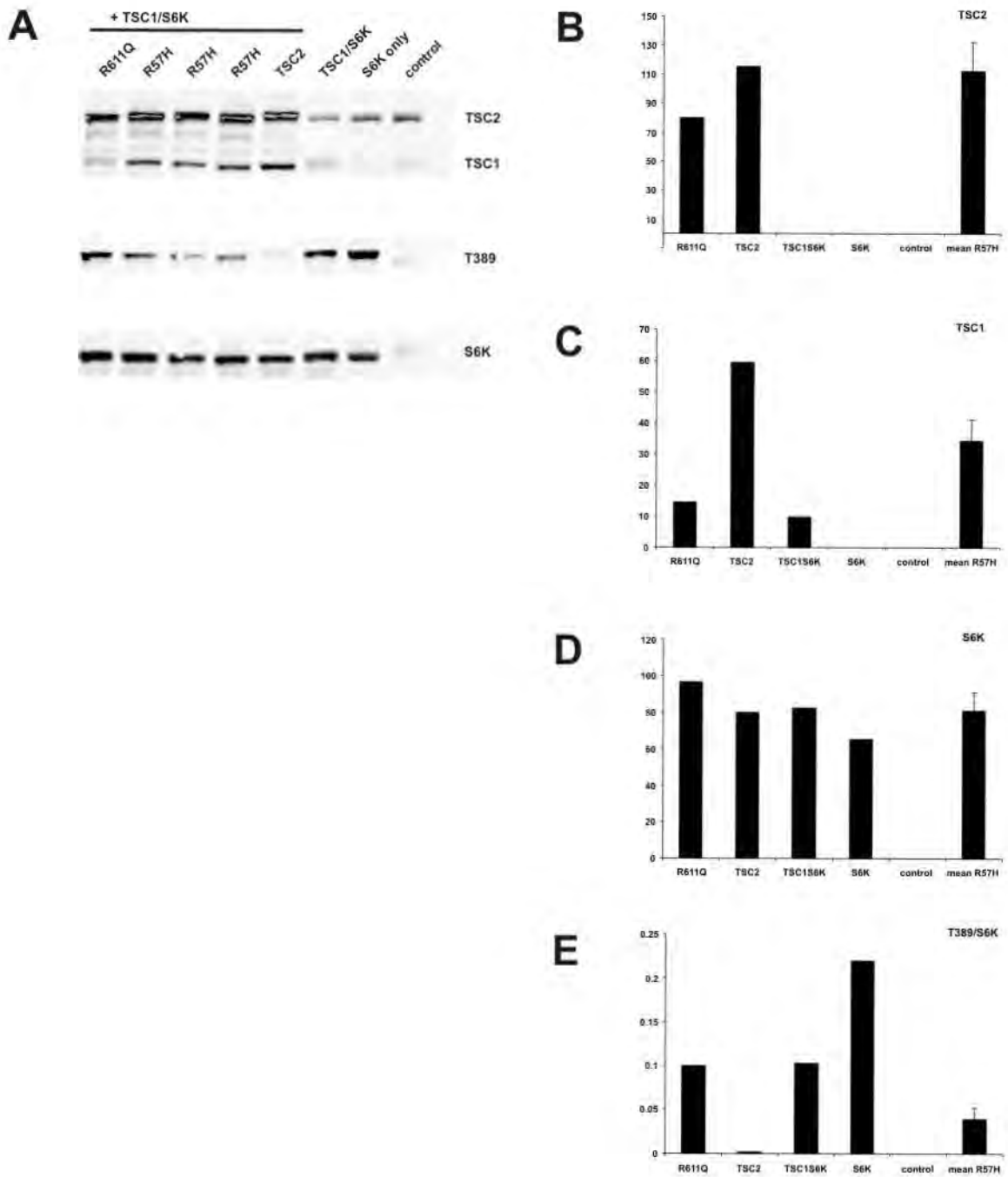
Appendix 2.

Publications and manuscripts in preparation

Nellist M, Sancak O, Goedbloed M, Adriaans, Wessels M, Maat-Kievit A, Baars M, Dommering C, van den Ouweland A and Halley D. "Functional characterisation of the TSC1-TSC2 complex te assess multiple *TSC2* variants identified in single families affected by tuberous sclerosis complex". BMC Med. Genet. (2008) 9:10 doi:10.1186/1471-2350-9-10.

Nellist M, van den Heuvel D, Schluep D, Exalto C, Goedbloed M, Maat-Kievit A, van Essen T, van Spaendonck-Zwarts, Jansen F, Helderman P, Bartalini G, Vierimaa O, Penttinen M, van den Ende J, van den Ouweland A and Halley D. "Missense mutations to the *TSC1* gene cause tuberous sclerosis complex". Eur. J. Hum. Genet. (2008) doi:10.1038/ejhg.2008.170.

Coevoets R, Arican S, Hoogeveen-Westerveld M, Simons E, van den Ouweland A, Halley D and Nellist M. "A reliable cell-based assay for testing unclassified *TSC2* gene variants." Eur. J. Hum. Genet. (2008) doi:10.1038/ejhg.2008.184.

Mozaffari M, Hoogeveen-Westerveld M, Kwiatkowski D, Sampson J, Ekong R, Povey S, van den Ouweland A, Halley D and Nellist M. "Identification of a region required for TSC1 stability by functional analysis of *TSC1* missense mutations identified in individuals with tuberous sclerosis complex." [manuscript in preparation].

BMC Medical Genetics

Functional characterisation of the TSC1–TSC2 complex to assess multiple *TSC2* variants identified in single families affected by tuberous sclerosis complex

Mark Nellist*[1], zgür Sancak[1], Miriam Goedbloed[1], Alwin Adriaans[1], Marja Wessels[1], Anneke Maat-Kievit[1], Marieke Baars[2], Charlotte Dommering[2], Ans van den Ouweland[1] and Dicky Halley[1]

Address: [1]Department of Clinical Genetics, Erasmus Medical Centre, Rotterdam, The Netherlands and [2]Department of Clinical and Human Genetics, Free University Medical Centre, Amsterdam, The Netherlands

Email: Mark Nellist* - m.nellist@erasmusmc.nl; zgür Sancak - Ozgur.Sancak@dsm.com; Miriam Goedbloed - m.goedbloed@erasmusmc.nl; Alwin Adriaans - a.adriaans@erasmusmc.nl; Marja Wessels - m.w.wessels@erasmusmc.nl; Anneke Maat-Kievit - j.a.maat@erasmusmc.nl; Marieke Baars - m.j.baars@amc.uva.nl; Charlotte Dommering - cj.dommering@vumc.nl; Ans van den Ouweland - a.vandenouweland@erasmusmc.nl; Dicky Halley - d.halley@erasmusmc.nl

* Corresponding author

Abstract

Background: Tuberous sclerosis complex (TSC) is an autosomal dominant disorder characterised by seizures, mental retardation and the development of hamartomas in a variety of organs and tissues. The disease is caused by mutations in either the *TSC1* gene on chromosome 9q34, or the *TSC2* gene on chromosome 16p13.3. The *TSC1* and *TSC2* gene products, TSC1 and TSC2, interact to form a protein complex that inhibits signal transduction to the downstream effectors of the mammalian target of rapamycin (mTOR).

Methods: We have used a combination of different assays to characterise the effects of a number of pathogenic TSC2 amino acid substitutions on TSC1–TSC2 complex formation and mTOR signalling.

Results: We used these assays to compare the effects of 9 different TSC2 variants (S132C, F143L, A196T, C244R, Y598H, I820del, T993M, L1511H and R1772C) identified in individuals with symptoms of TSC from 4 different families. In each case we were able to identify the pathogenic mutation.

Conclusion: Functional characterisation of TSC2 variants can help identify pathogenic changes in individuals with TSC, and assist in the diagnosis and genetic counselling of the index cases and/or other family members.

Background

Tuberous sclerosis complex (TSC) is an autosomal dominant disorder characterised by seizures, mental retarda-

tion and the development of hamartomas in a variety of organs and tissues [1]. The disease is caused by mutations in either the *TSC1* gene on chromosome 9q34 [2], or the

TSC2 gene on chromosome 16p13.3 [3]. Loss of heterozygosity studies at the *TSC1* and *TSC2* loci in TSC-associated lesions indicate that *TSC1* and *TSC2* are tumour suppressor genes [1]. Comprehensive screens for mutations at both the *TSC1* and *TSC2* loci have been performed in several large cohorts of TSC patients and a wide variety of different pathogenic mutations have been described [4-10]. In most studies approximately 20% of the identified mutations are either missense changes or small, non-truncating insertions/deletions, predominantly in the *TSC2* gene.

The phenotypic expression of TSC is highly variable and in some cases it can be difficult to establish a definitive clinical diagnosis. Generally the diagnosis is made based on multiple clinical criteria that are categorized into major and minor features [11]. The presence of 2 major features, or one major and 2 minor features, is sufficient for a definite diagnosis. In recent years, mutation analysis has become an additional diagnostic tool in familial as well as sporadic TSC. However, it is sometimes difficult to establish whether an identified nucleotide change, particularly a missense change, is a genuine pathogenic mutation, or a (rare) polymorphism. In familial cases where a missense change cosegregates with TSC, or in cases where key relatives are not available for testing, a distinction cannot be made on genetic grounds alone. Furthermore, many tools for the analysis of amino acid substitutions [12-14], may not predict the effect of a particular substitution reliably.

The *TSC1* and *TSC2* gene products, TSC1 and TSC2, interact to form a protein complex which acts as a GTPase activating protein (GAP) for the rheb GTPase, preventing the rheb-GTP-dependent stimulation of cell growth through the mammalian target of rapamycin (mTOR) [15]. In cells lacking either *TSC1* or *TSC2*, the downstream targets of mTOR, p70 S6 kinase (S6K) and ribosomal protein S6, are constitutively phosphorylated [16,17]. The identification of the role of the TSC1–TSC2 complex in regulating signal transduction through mTOR has made it possible to assess the activity of different TSC1 and TSC2 variants. The effects of amino acid changes on TSC1–TSC2 complex formation, on the activation of rheb GTPase activity by the complex, and on the phosphorylation status of S6K and S6, the downstream effectors of mTOR, can be determined [18,19].

Here, we apply assays of TSC1–TSC2 function to assist in the identification, diagnosis and counselling of 4 families with TSC. In each index case at least 2 changes in the *TSC2* gene were detected. To identify the disease-causing mutation in each family we characterised the effects of the changes on the activity of the TSC1–TSC2 complex. In each case we were able to identify the pathogenic *TSC2*

variant. Our analysis demonstrates that biochemical assays can help resolve otherwise intractable problems in clinical genetic diagnostics.

Methods
Mutation analysis
DNA was extracted from peripheral blood using standard techniques. Mutation analysis was performed using a combination of single-strand conformational polymorphism analysis, denaturing gradient gel electrophoresis, direct sequencing, Southern blotting and fluorescence *in situ* hybridisation, as previously described [8]. In addition, the multiplex ligation-dependent probe amplification assay was performed (MRC Holland, The Netherlands). *TSC2* sequence changes were numbered according to the original cloning paper [3].

To investigate whether the changes had an effect on RNA splicing, 3 different splice-site prediction programs [12-14]. were used. Amino acid substitutions were evaluated using the PAM 250 [15], BLOSUM 62 [16] and Grantham [17] matrices and SCANSITE [23].

Generation of constructs and antisera
Expression constructs encoding the identified variants were derived using the Stratagene QuikChange site-directed mutagenesis kit and in each case verified by sequencing the complete open reading frame. All the other constructs used in this study have been described previously [21,24,25]. Polyclonal rabbit antisera specific for human TSC1 and TSC2 have been described previously [25]. Other antibodies were purchased from Cell Signaling Technology.

Transfections, immunocytochemistry, immunoblotting, immunoprecipitation assays and the *in vitro* assay of rheb GTPase activity were performed as described previously [21].

Results
### *Patient characteristics*
Family 1
(Figure 1A) The index case (II:2) died shortly after birth due to a solitary rhabdomyoma in the right ventricle of the heart. Post-mortem examination did not reveal any other findings indicative of TSC. Both parents underwent a full clinical evaluation. Dermatological, cardiological, ophthalmological, neurological and radiological examinations were negative for signs of TSC except for one nail groove and one hypomelanotic macule in individual I:1. The sibling of the index case (II:1) was healthy, but was not investigated further. At the first trimester of the third pregnancy, mutation analysis of the index case had not been completed and prenatal DNA testing could not be offered. Fetal echocardiography did not reveal any heart
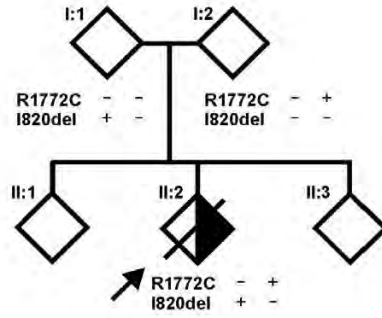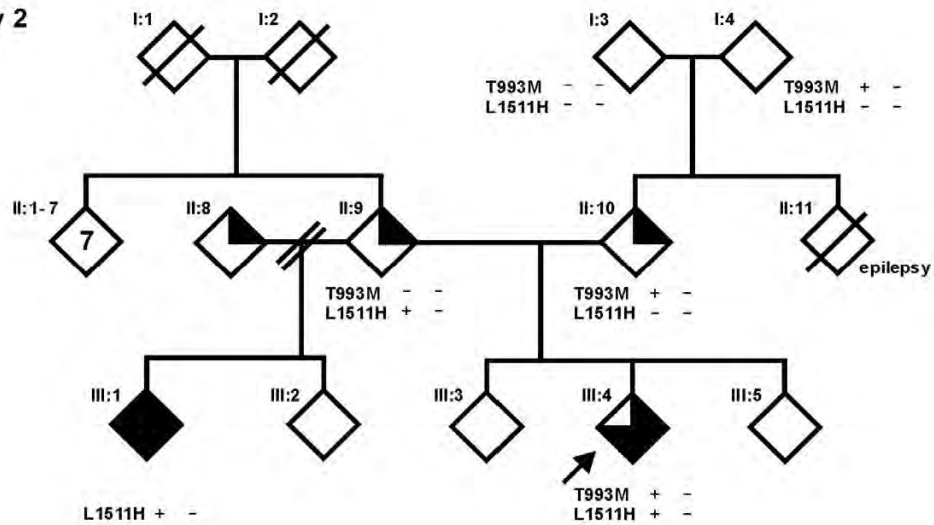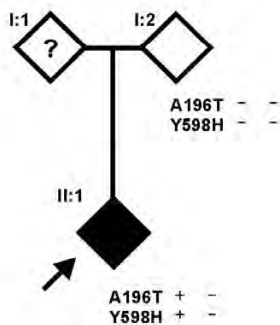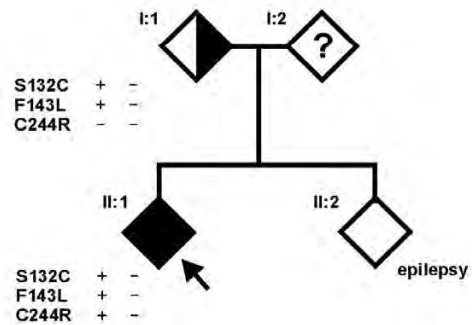
Figure 1
Pedigrees of the investigated families. (A) Family 1, (B) Family 2, (C) Family 3 and (D) Family 4. Arrows indicate the index cases. Clear symbols indicate no signs or symptoms of TSC; 1/4-filled symbols indicate one minor feature of TSC; 1/2-filled symbols indicate possible TSC; 3/4-filled symbols indicate probable TSC, filled symbols indicate definite TSC, and individuals with epilepsy only are indicated. A question mark indicates individuals where no clinical data was available. Genotypes are shown for the individuals where DNA was available for testing.

defects and the pregnancy resulted in the birth of a healthy child (II:3).

Family 2

(Figure 1B) The index case (III:4) had multiple hypomelanotic macules and dental pits, epilepsy and electroencephalographic abnormalities, and was diagnosed with 'probable TSC'. One of the parents of the index case (II:10) had multiple dental pits and a computer tomography scan revealed 2 small calcifications in the nucleus caudatus which were not typical for TSC. Magnetic resonance imaging was performed and showed no additional abnormalities. Individual II:9, the other parent of the index case, had a single 2 centimetre cyst in the left kidney and a single ash leaf-shaped area of hypopigmentation, insufficient for a diagnosis of TSC. Individual II:11, the sibling of II:10, had neurological and ophthalmological problems and died at the age of 13 due to status epilepticus. Individual III:1, the half-sibling of the index case and the child of individual II:9, had a history of possible epilepsy at the age of 3 years and was again diagnosed with epilepsy at 12 years of age. A subsequent full diagnostic work-up identified cortical tubers and 7 hypomelanotic macules, fulfilling the diagnostic criteria for definite TSC. Individual II:8 had multiple dental pits and 10 irregular hypopigmentations, atypical for TSC.

Family 3

(Figure 1C) The index case (II:1) was diagnosed with definite TSC. One parent (I:2) did not show any clinical signs of TSC, and there was no information on the other parent (I:1).

Family 4

(Figure 1D) The index case (II:1) was diagnosed with definite TSC. Individual I:1, the parent of the index case, had angiomyolipoma but no other reported signs of TSC, and individual II:2, the sibling of the index case had epilepsy, but no other signs of TSC.

Mutation analysis
Family 1

The index case (II:2) was heterozygous for 2 changes in the *TSC2* gene: *TSC2* 2476delATC (deletion of isoleucine at codon 820, I820del) and *TSC2* 5332C>T (arginine to cysteine substitution at codon 1772, R1772C). Analysis of the parents indicated that the index case had inherited one change from each parent. No DNA was available from other relatives.

Family 2

The index case (III:4) was heterozygous for 2 missense changes: *TSC2* 2996C>T (threonine to methionine substitution at codon 993, T993M) and *TSC2* 4550T>A (leucine to histidine amino acid substitution at position 1511,

L1511H). Analysis of additional family members (individuals I:3, I:4, II:9, II:10 and III:3) confirmed that one substitution was paternal in origin and the other maternal.

Family 3

The index case (II:1) was heterozygous for 2 missense changes: *TSC2* 604G>A (alanine to threonine substitution at codon 196, A196T) and *TSC2* 1810T>C (tyrosine to histidine substitution at codon 598, Y598H). Neither substitution was detected in parent I:2, and DNA from parent I:1 was not available for testing.

Family 4

The index case (II:1) was heterozygous for 3 missense changes in the *TSC2* gene: *TSC2* 413C>G (serine to cysteine substitution at codon 132, S132C), *TSC2* 447C>G (phenylalanine to leucine substitution at codon 143, F143L) and *TSC2* 748T>C (cysteine to arginine substitution at codon 244, C244R). The S132C and F143L substitutions were inherited from parent I:1. No DNA was available from the other parent.

Comparison of the allele ratios of the index cases and parents did not reveal any evidence for somatic mosaicism in the leukocyte DNA from any of the families studied. None of the changes showed an effect on splicing according to the 3 splice-site prediction programs used.

As shown in Table 1, the identified amino acid changes were compared using the PAM 250 [15], BLOSUM 62 [16] and Grantham matrices [17]. In addition, the degree of conservation of the amino acid residues in different metazoan species was compared, as shown in Table 2.

Functional analysis
Families 1 and 2

The genetic data from families 1 and 2 indicated that in both families the index case had inherited a different, rare *TSC2* variant from each parent. To determine whether the I820del, R1772C, T993M and L1511H variants corresponded to pathogenic mutations, the biochemical activity of each variant was compared to wild-type TSC2 and a known, pathogenic TSC2 missense variant (R611Q) using a variety of functional assays.

To investigate the ability of the TSC2 I820del, R1772C, T993M and L1511H variants to interact with TSC1, coimmunoprecipitation experiments were performed using antibodies specific for TSC1. As shown in Figures 2A and 2B, coimmunoprecipitation of the TSC2 I820del variant was reduced compared to wild-type TSC2, but was not prevented completely (compare the I820del variant to the R611Q variant). The R1772C, T993M and L1511H amino

Table 1: Scores of the BLOSUM 62, PAM 250 and Grantham matrices. BLOSUM 62 scores range between -4 and 11, PAM 250 scores between -8 and 17, and Grantham scores between 5 and 215. For the BLOSUM 62 and PAM 250 matrices, a more negative score corresponds to a less conservative amino acid change. For the Grantham matrix, a higher number reflects a less conservative change.

Amino Acid Substitution	Family	BLOSUM 62	PAM 250	Grantham
TSC2 R1772C	1	-3	-4	180
TSC2 T993M	2	-1	-1	81
TSC2 L1511H	2	-3	-2	99
TSC2 A196T	3	0	1	58
TSC2 Y598H	3	2	0	83
TSC2 S132C	4	-1	0	112
TSC2 F143L	4	0	2	22
TSC2 C244R	4	-3	-4	180

acid substitutions did not reduce TSC1–TSC2 coimmuno-precipitation.

Next, the activation of rheb GTPase activity by the immunoprecipitated variant TSC1–TSC2 complexes was assayed. As shown in Figure 2C, in the presence of the wild-type TSC1–TSC2 complex the ratio of rheb-bound GDP to GTP was 3-fold higher than in the presence of TSC1 alone (control GDP/GTP = 0.4; wild-type GDP/GTP

Table 2: Evolutionary conservation of the variant TSC2 amino acids. Inter-species conservation of the TSC2 S132, F143, A196, C244, Y598 I820, T993, L1511 and R1772 amino acids is shown.

Family 1

	I820	R1772
human	PDII**I**KALP	GQRK**R**LISS
mouse	PDII**I**KALP	GQRK**R**LISS
rat	PDII**I**KALP	GQRK**R**LISS
pufferfish	PDIM**I**KLLP	GQRK**R**LVST
fruitfly	PEAL**M**RKLP	no homology

Family 2

	T993	L1511
human	SRIQ**T**SLTS	SVQL**L**DQIP
mouse	SRIQ**T**SLTS	SVQL**L**DQIP
rat	SRIQ**T**SLTS	SVQL**L**DQIP
pufferfish	RRMH**T**STTT	AVKV**L**DQMP
fruitfly	no homology	AVSL**I**DLVP

Family 3

	A196	Y598
human	DEYI**A**RM V	IQLH**Y**KHSY
mouse	DEYI**A**SM V	IQLH**Y**KHGY
rat	DEYI**A**PM V	IQLH**Y**KHGY
pufferfish	DQNV**A**SM V	LQLH**Y**KNKY
fruitfly	DKDI**L**VGIV	LELH**Y**ERPK

Family 4

	S132	F143	C244
human	KDYP**S** NED	RLEV**F**KALT	IVTL**C**RTIN
mouse	KDYP**S** NED	RLEV**F**KALT	IITL**C**RTIN
rat	KDYP**S** NED	RLEV**F**KALT	IITL**C**RTVN
pufferfish	RDYQPCNED	RLEV**F**KALT	IITL**C**RTVN
fruitfly	IQNHEARED	LLEL**L**DTLT	ITTL**C**RTVN

= 1.4). Coimmunoprecipitation of the TSC2 I820del variant was reduced compared to wild-type TSC2, and consequently the activation of rheb GTPase activity was also reduced (wild-type GDP/GTP = 1.4; I820del GDP/GTP = 0.9).

The immunoprecipitated R1772C and T993M variant complexes increased the GDP/GTP ratio more than 4-fold above the control value, and were therefore both at least as active as wild-type TSC2 (wild-type GDP/GTP = 1.4; R1772C and T993M GDP/GTP = 1.9). In contrast, although TSC1–TSC2 coimmunoprecipitation was unaffected by the L1511H substitution, the activation of rheb GTPase activity was reduced 3-fold compared to wild-type (wild-type GDP/GTP = 1.4; L1511H GDP/GTP = 0.5).

To determine whether the TSC2 I820del, R1772C, T993M and L1511H variants affected mTOR activity, the variants were overexpressed together with TSC1 and S6K in human embryonal kidney 293 cells. Phosphorylation of the exogenous S6K linker domain (T389), as detected by immunoblotting, was used as a read-out for mTOR activity. As shown in Figure 2E and 2F, S6K T389 phosphorylation was increased in the presence of the TSC2 I820del, L1511H and R611Q variants, compared to wild-type TSC2 and the R1772C and T993M variants. To confirm these findings, TSC1 and the TSC2 variants were overexpressed in *Tsc2* -/- mouse embryo fibroblasts (MEFs) [16]. The S235/S236 phosphorylation of S6 in the MEFs expressing the TSC2 variants was determined by double-label immunofluorescent microscopy, as described previously [21]. As shown in Figure 2D, expression of the TSC2 R1772C and T993M variants suppressed S6 phosphorylation in more than 90% of the transfected cells, similar to wild-type TSC2. In contrast, less than 20% of the MEFs expressing the TSC2 I820del, L1511H or R611Q variants showed inhibition of S6 phosphorylation. Therefore, in both assays, the TSC2 I820del and L1511H variants were unable to inhibit mTOR, indicating that both these variants are pathogenic, while the TSC2 R1772C and T993M
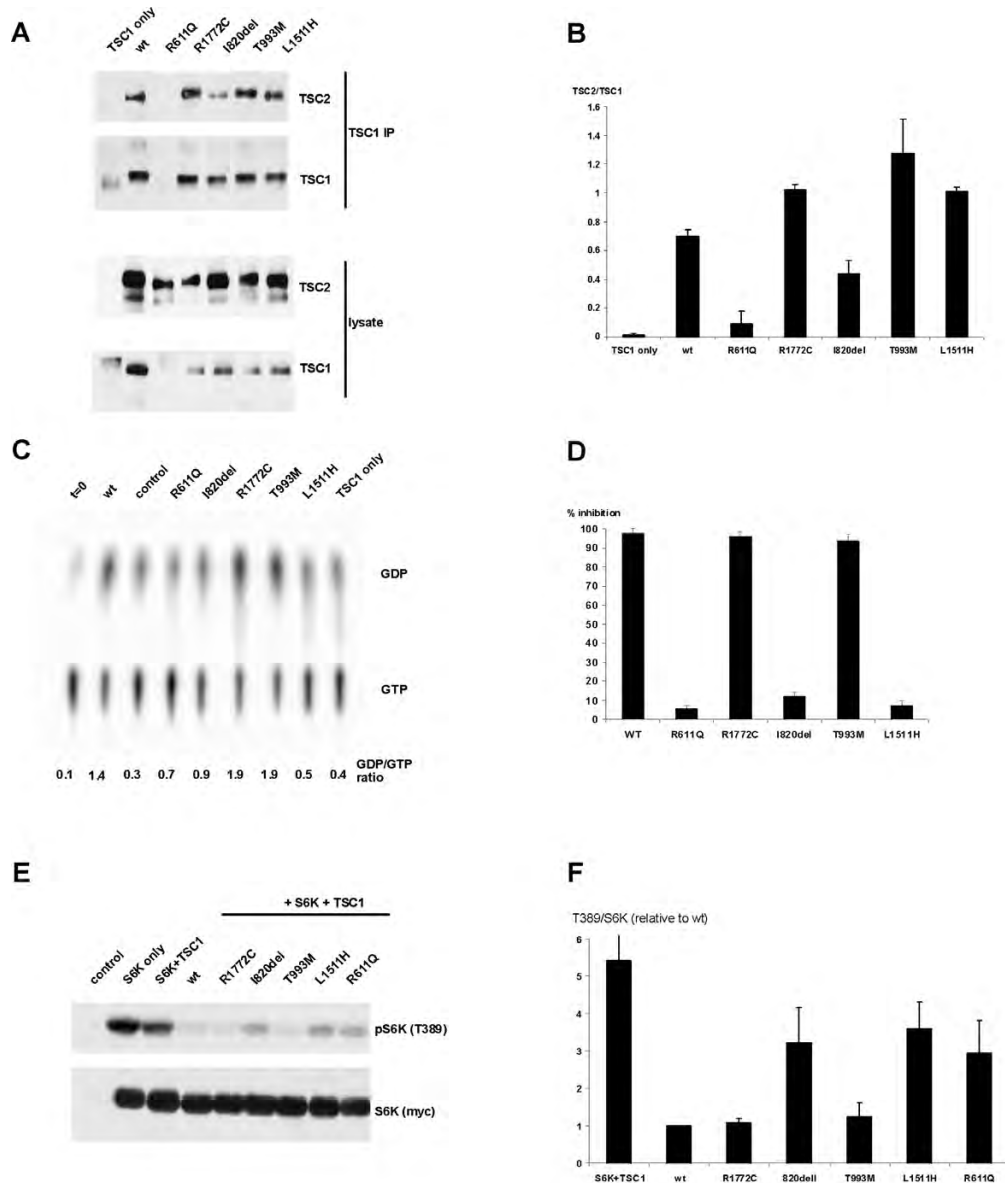
Figure 2
Results of the functional assays on the TSC2 variants identified in family 1 (variants I820del and R1772C) and family 2 (variants T993M and L1511H). (A) Interaction between TSC1 and TSC2 variants. TSC1–TSC2 complexes were immunoprecipitated with antibodies specific for exogenous TSC1 from HEK 293 cells over-expressing TSC1 and wild-type TSC2 (wt) or TSC1 and the TSC2 variants. (B) Interaction between TSC1 and TSC2 variants. Ratio of coimmunoprecipitated TSC2:TSC1, as detected by immunoblotting, was estimated by densitometry scanning (Total Scan). (C) *In vitro* rheb GAP activity of immunoprecipitated TSC1–TSC2 complexes. Rheb-bound GDP/GTP ratios were determined after 90 minutes incubation with the immunoprecipitated wild-type TSC1–TSC2 complex (wt), protein A beads only (control), TSC1 only, or TSC1–TSC2 variant complexes. Rheb-bound GDP/GTP prior to addition of the TSC1–TSC2 complexes is shown (t = 0). (D) Inhibition of S6 phosphorylation in Tsc2 -/- MEFs. Percentage of *Tsc2* -/- MEFs transfected with expression constructs encoding TSC1 and wild-type TSC2, or TSC1 and the TSC2 variants, and showing inhibition of S6 phosphorylation. Data from at least 3 separate experiments are shown. (E) TSC2-dependent inhibition of S6K-T389 phosphorylation. S6K, TSC1 and wild-type TSC2 (wt), or S6K, TSC1 and the TSC2 variants, were coexpressed in HEK 293 cells. Phosphorylation of S6K at the T389 position was determined by immunoblotting. A representative example of at least 3 separate experiments is shown. (E) TSC2-dependent inhibition of S6K-T389 phosphorylation. Ratio of total S6K:T389-phosphorylated S6K, as detected by immunoblotting, was estimated by densitometry scanning (Total Scan). Mean ratios relative to TSC2 wild-type (wt) are shown.

variants were just as active as wild-type TSC2 and are therefore not pathogenic amino acid substitutions.

Families 3 and 4
In families 3 and 4, the clinical and genetic data was incomplete. Multiple *TSC2* variants were identified in the index cases, but it was not clear if they were *de novo*, or had been inherited from an untested parent. It was also unclear whether the changes were confined to the same allele. Therefore, to investigate the effects of the changes on the ability of the TSC1–TSC2 complex to antagonise mTOR signalling, TSC2 variants containing the different combinations of amino acid substitutions were characterised.

As shown in Figure 3A and 3B, S6K T389 phosphorylation was inhibited by expression of the TSC2 S132C, F143L and A196T single variants, and by the S132C/F143L double variant. In contrast, expression of the C244R and Y598H single variants did not inhibit S6K phosphorylation, and expression of TSC1 was reduced in the presence of these variants. Consistent with these observations, the S132C/F143L/C244R triple variant and A196T/Y598H double variant were unable to inhibit S6K phosphorylation and TSC1 expression was reduced in the presence of these variants, compared to in the presence of wild-type TSC2. To provide confirmation for these data, double-label immunofluorescent microscopy was performed to determine whether S6 phosphorylation was down-regulated in *Tsc2* -/- MEFs expressing the different variants. As shown in Figure 3C, expression of the TSC2 C244R, S132C/F143L/C244R, Y598H and A196T/Y598H variants was unable to inhibit S6 phosphorylation in the *Tsc2* -/-MEFs. Therefore, in both assays, the Y598H and C244R variants correspond to the pathogenic mutations in families 3 and 4 respectively.

Discussion
Mutation analysis of the *TSC1* and *TSC2* genes in individuals with TSC, and in those suspected of having the disease, facilitates the diagnosis of TSC, and can help genetic counselling. In most cases, analysis of the patient's DNA results in the identification of a pathogenic mutation. However, in some cases it is impossible to determine from the genetic data alone whether specific, identified changes are pathogenic or not. This can be a particular problem when a change co-segregates with signs of TSC in a single family. To address such cases, we have performed functional analysis of the predicted protein products of the *TSC2* variants identified in 4 families with TSC.

In families 1 and 2 the index case did not fulfil the diagnostic criteria for TSC and had inherited 2 non-truncating *TSC2* nucleotide changes, one from each parent. It was not possible to determine from the clinical and genetic data alone whether the families were affected by TSC and, if that was the case, which nucleotide change was the disease-causing mutation.

In families 3 and 4, in which the index case did fulfil the diagnostic criteria for TSC, it was impossible to determine whether the identified TSC2 variant was pathogenic because essential genetic and/or clinical data was not available. In all the above cases we analysed the effect of the identified changes on the activity of the TSC1–TSC2 complex in order to establish which of the changes were pathogenic mutations.

Families 1 and 2
The *in vitro* GTPase activity of rheb was not stimulated in the presence of the TSC2 I820del and L1511H variants, and neither variant was able to inhibit S6K and S6 phosphorylation as effectively as wild-type TSC2, or the R1772C and T993M variants. In addition, the I820del variant formed a complex with TSC1 less efficiently than wild-type TSC2. The I820del and L1511H changes therefore had similar effects to other pathogenic TSC2 missense mutations, disrupting the function of the TSC1–TSC2 complex *in vitro*. We classified the I820del and L1511H variants as pathogenic mutants. The R1772C and T993M substitutions had no effect on TSC1–TSC2 activity in the assays used and were therefore classified as rare polymorphisms.

In utero cardiac rhabdomyoma was the only sign of TSC in the index patient of family 1 (individual II:2). Rhabdomyoma is the most common foetal and neonatal cardiac tumour and although it can be associated with several different genetic disorders, TSC is implicated in as many as two-thirds of the cases [26]. Confirmation of the inactivating nature of the TSC2 I820del mutation identified in family 1 meant that a diagnosis of TSC could be assigned to individuals I:1 and II:2 with more certainty. Previously, the very mild presentation of the disease in individal I:1 had made diagnosis difficult. Mutation analysis, complemented by functional assays, was required to establish whether this individual carried a pathogenic *TSC2* mutation, and the identification of a mutation in this individual has implications for the family in regard to decisions about having additional children and to the risk of other relatives of the parent. Somatic mosaicism in individual I:1 could not be rigorously excluded, since only leukocyte DNA was available for analysis. Therefore, the recurrence risk for this couple is up to 50%.

Analysis of the TSC2 I820del mutant indicated that the isoleucine residue helps to stabilise TSC1–TSC2 binding. However, since some TSC1–TSC2 binding was detected, and some rheb GAP activity could also be measured, it is possible that the TSC2 I820del variant retains some activ-
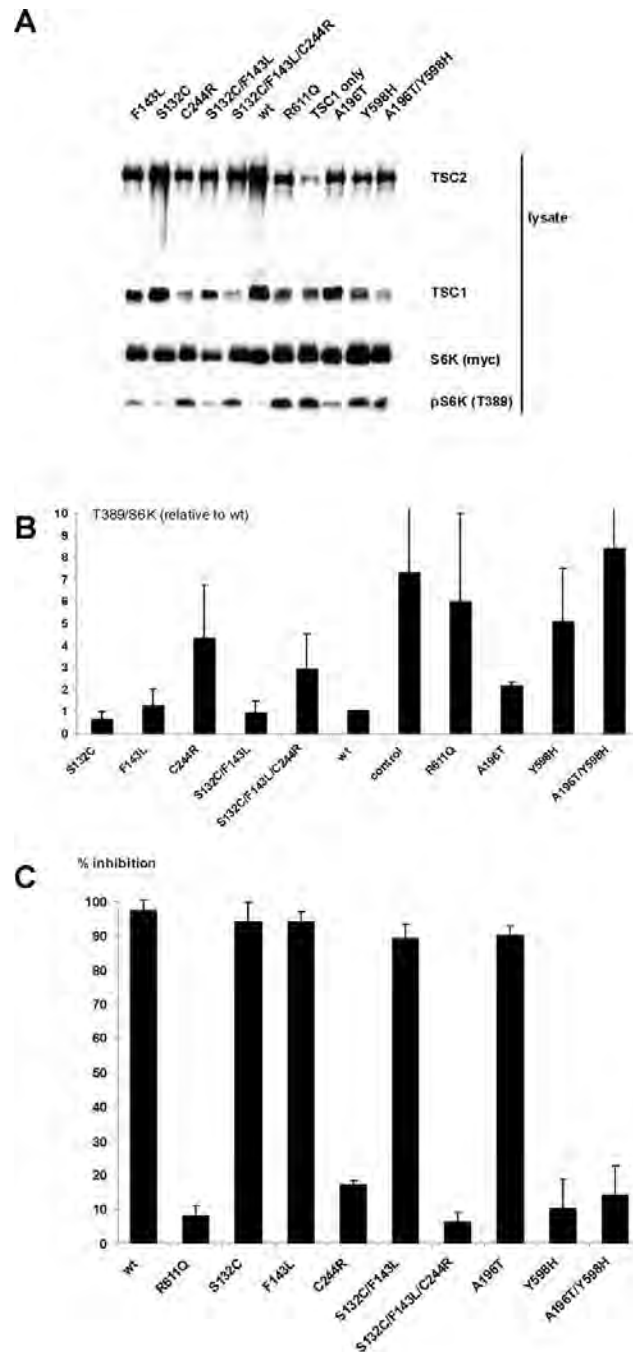
Figure 3
Results of the functional assays on the TSC2 variants identified in family 3 (variants A196T and Y598H) and family 4 (variants S132C, F143L and C244R). (A) TSC2-dependent inhibition of S6K-T389 phosphorylation. S6K, TSC1 and wild-type TSC2 (wt), or S6K, TSC1 and the TSC2 variants, were overexpressed in HEK 293 cells. Phosphorylation of S6K at the T389 position was determined by immunoblotting. A representative example of at least 3 separate experiments is shown. (B) TSC2-dependent inhibition of S6K-T389 phosphorylation. Ratio of total S6K:T389-phosphorylated S6K, as detected by immunoblotting, was estimated by densitometry scanning (Total Scan). Mean ratios relative to TSC2 wild-type (wt) are shown.(C) Inhibition of S6 phosphorylation in *Tsc2* -/- MEFs. Percentage of *Tsc2* -/- MEFs transfected with expression constructs encoding TSC1 and wild-type TSC2, or TSC1 and the TSC2 variants, and showing inhibition of S6 phosphorylation. Data from at least 3 separate experiments are shown.

ity *in vivo*. This provides a possible explanation for the mild symptoms in individual I:1. The second variant identified in family 1, TSC2 R1772C, did not have a deleterious effect on the activity of the TSC1–TSC2 complex. This was somewhat surprising as the R1772 residue is part of the consensus extracellular signal-regulated kinase (ERK) phosphorylation site that has been shown to be involved in regulating the activity of the complex [27,28]. Indeed, SCANSITE [23] indicated that the R1772C substitution destroys the putative ERK phosphorylation site. Furthermore, both the BLOSUM 62 and PAM 250 matrices indicated that the R1772C substitution is likely to have a deleterious effect on TSC2 structure. One possibility is that under certain conditions, the R1772C substitution may have a modifying effect on the TSC1–TSC2 complex, enhancing TSC1–TSC2 activity by preventing the Erk-dependent down-regulation of the complex [28]. This may explain the increased rheb GTPase activity measured in the presence of the TSC2 R1772C variant, compared to wild-type TSC2 (wild-type TSC2 GDP/GTP ratio = 1.4; R1772C GDP/GTP ratio = 1.9; Figure 2B).

Both the 2476delATC (I820del) and 5332C>T (R1772C) variants have been identified in TSC patients by other researchers [29-31]. Strizheva *et al*. [30] suggested that the R1772C substitution could be a pathogenic change while Langkau *et al*. [31] concluded that it was a polymorphism. The status of the I820del change was not certain [29]. Our analysis is consistent with the findings of Langkau *et al*. and, in addition, indicates that the TSC2 I820del variant is pathogenic. Furthermore, this example demonstrates that predictions about the pathogenicity of missense changes based on the results of the BLOSUM 62, PAM 250 and Grantham matrices are not always reliable.

In family 2, mutation analysis resulted in the identification of 2 novel *TSC2* missense changes, 2996C>T (T993M) and 4550T>A (L1511H), in the index case (individual III:4). Individual III:1, the half-sibling of the index case was later diagnosed with TSC on the basis of the accepted clinical criteria and was found to carry the *TSC2* 4550T>A (L1511H) substitution only. No other nucleotide changes were identified in the *TSC1* or *TSC2* genes in either individual. The identification of the TSC2 L1511H change in individual III:1 excluded the T993M change as the common cause of TSC in this family. However, it did not confirm the pathogenicity of the TSC2 L1511H change. The presence of multiple dental pits in both individual II:8 and individual II:10 suggested that the signs of TSC in individuals III:1 and III:4 could be caused by two different mutations, inherited from individuals II:8 and II:12 respectively. However, the functional tests confirmed the pathogenic nature of the TSC2 L1511H substitution, indicating that this was the disease-causing mutation in both cases. The substitution of a basic

histidine residue for a nonpolar leucine residue at position 1511 did not affect the TSC1–TSC2 interaction, but did abrogate the rheb GAP activity of the TSC1–TSC2 complex. Although L1511 is outside the predicted TSC2 GAP domain [3], it is clearly necessary for activity. The substitution of a polar threonine for nonpolar methione at position 993 had no deleterious effect on the TSC1–TSC2 interaction or on the activity of the complex. The T993M substitution occurs at a possible site of protein kinase B (PKB)-dependent phosphorylation [27], and may therefore inhibit PKB-mediated inactivation of the TSC1–TSC2 complex. This may explain why the TSC2 T993M variant, like the R1772C variant, had a higher *in vitro* rheb GAP activity than wild-type TSC2 (wild-type TSC2 GDP/GTP ratio = 1.4; T993M GDP/GTP ratio = 1.9; Figure 2B). The T993M polymorphism may therefore also act as a positive modifier of TSC1–TSC2 activity.

In family 3, 2 missense changes (*TSC2* 604G>A (A196T) and *TSC2* 1810T>C (Y598H)) were identified in the index case (individual II:1). Since there was no genetic or clinical data on one of the parents, it was not possible to determine whether either of the changes was responsible for TSC in this individual. Both variants had been identified previously in other TSC patients [29], however in these patients it was also not clear whether the changes were pathogenic. Functional analysis indicated that the TSC2 Y598H substitution reduced TSC1–TSC2 binding and the TSC1–TSC2 dependent inhibition of mTOR activity. In contrast, the A196T substitution did not affect TSC2 activity. Therefore, the Y598H substitution was responsible for TSC in individual II:1, as well as in other TSC patients [29], and the A196T substitution is a rare polymorphism.

In family 4, 3 missense changes were identified in the *TSC2* gene. The 413C>G (S132C) and 447C>G (F143L) substitutions were inherited from a parent with symptoms suggesting TSC. The third substitution, 748T>C (C244R), was either a *de novo* mutation, or was inherited from the other parent, on whom there was no clinical or genetic data. None of these changes have been described previously [29]. One possibility in this family was that the combination of missense changes was responsible for the TSC phenotype. Therefore we tested all the individual TSC2 single amino acid variants (S132C, F143L and C244R) as well as the TSC2 S132C/F143L double variant and TSC2 S132C/F143L/C244R triple amino acid variant. Neither the S132C nor the F143L changes had a significant effect on TSC1–TSC2 function. In some assays the F143L variant appeared less active than wild-type TSC2, but still had the ability to significantly inhibit mTOR activity. In contrast, the C244R amino acid substitution reduced TSC1–TSC2 binding and was unable to inhibit mTOR activity, either alone or in combination with the S132C and F143L variants. We concluded that the C244R

substitution was the pathogenic mutation in the index case. Individual I:1 tested negative for the *TSC2* 748T>C (C244R) substitution, but was diagnosed with angiomyolipomas. Although insufficient for a definite diagnosis of TSC, the incidence of angiomyolipomas is high in the TSC patient population. One possibility is that this individual is a mosaic for the *TSC2* 748T>C (C244R) susbstitution, and that the angiomyolipoma originates from these mosaic cells. An alternative explanation is that the *TSC2* 447C>G (F143L) substitution does have an effect on TSC2 function, sufficient to allow the formation of angiolipoma. The F143L amino acid substitution may therefore be a negative modifier of TSC1–TSC2 activity, in contrast to the R1772C and T993M substitutions identified in families 1 and 2, that, in some assays, appeared to increase TSC1–TSC2 activity. Although there was no evidence in family 1 or family 2 for the non-pathogenic TSC2 variant acting in trans to neutralise the pathogenic variant, it will be interesting to determine whether there are 'hyperactive' TSC1 and TSC2 variants that can (partially) compensate for the presence of pathogenic TSC1 and TSC2 variants. Improving the sensitivity and reliability of the assays of TSC1–TSC2 activity will allow us to more accurately define the activity of different TSC1 and TSC2 variants.

We did not investigate the other putative functions of TSC2 since, in each family, we were able to differentiate between the TSC2 variants on the basis of their inhibition of mTOR signalling. However, it may also be informative to investigate the effects of pathogenic and non-pathogenic amino acid substitutions on the other proposed functions of TSC2, such as the regulation of p27 [32].

Care must always be taken in the interpretation of nucleotide or amino acid changes identified during molecular genetic investigations. As the examples described here demonstrate, both the affection status of individuals in a family and the nature of the nucleotide changes identified in those individuals are not always clear. To distinguish between pathogenic mutations and harmless polymorphisms, we have analysed the effects of different amino acid changes on the activity of the TSC1–TSC2 complex. In each case we have been able to distinguish pathogenic TSC2 variants from rare polymorphic variants, and thereby identify the mutation in each family. We have shown that functional assays can be a useful tool to complement traditional DNA-based mutation analysis in TSC. Identification of the pathogenic mutations in the TSC families described here enabled not only genetic counselling and prenatal testing for future pregnancies but also improved the diagnosis of affected family members to facilitate their critical clinical care. The use of functional assays to differentiate between polymorphisms and pathogenic mutations, in TSC and other diseases, will facilitate not only the identification of pathogenic mutations but

will also help establish how different amino acid residues contribute to protein function.

Conclusion
Deletion of isoleucine at amino acid residue 820 of TSC2 and the TSC2 L1511H, C244R and Y598H amino acid substitutions are sufficient to cause TSC. The TSC2 R1772C, T993M, S132C, F143L and A196T substitutions are rare polymorphisms that do not inhibit TSC1–TSC2 function, and do not cause TSC.

Abbreviations
DNA, deoxyribonucleic acid; ERK, extracellular regulated kinase; GAP, GTPase activating protein; GDP, guanosine diphosphate; GTP, guanosine triphosphate; HEK 293, human embryonal kidney cells; MEFs, mouse embryo fibroblasts; mTOR, mammalian target of rapamycin; PKB, protein kinase B; rheb, ras homolog expressed in brain; RNA, ribonucleic acid; S6K, p70 S6 kinase; TSC, tuberous sclerosis complex.

Competing interests
The author(s) declare that they have no competing interests.

Authors' contributions
MN, OS, MG and AA performed the practical work; MW, AM-K, MB and CD co-ordinated the clinical investigations of the patients; AvdO and DH led the research. The manuscript was drafted by OS, MN, AvdO and DH, and read and approved by all authors.

Acknowledgements

References
1. Gomez M, Sampson J, Whittemore V, eds: *The tuberous sclerosis complex* Oxford, UK: Oxford University Press; 1999.
2. van Slegtenhorst M, de Hoogt R, Hermans C: **Identification of the tuberous sclerosis gene *TSC1* on chromosome 9q34.** *Science* 1997, **277(5327):**805-808.
3. The European Chromosome 16 Tuberous Sclerosis Consortium: **Identification and characterization of the tuberous sclerosis gene on chromosome 16.** *Cell* 1993, **75(7):**1305-1315.
4. Jones AC, Shyamsundar MM, Thomas MW: **Comprehensive mutation analysis of *TSC1* and *TSC2*, and phenotypic correlations in 150 families with tuberous sclerosis.** *Am J Hum Genet* 1999, **64(5):**1305-1315.
5. van Slegtenhorst M, Verhoef S, Tempelaars A: **Mutational spectrum of the *TSC1* gene in a cohort of 225 tuberous sclerosis complex patients: no evidence for genotype-phenotype correlation.** *J Med Genet* 1999, **36(4):**285-289.

6.   Au KS, Rodriguez JA, Finch JL: **Germ-line mutational analysis of the *TSC2* gene in 90 tuberous sclerosis patients.** *Am J Hum Genet* 1998, **62(2):**286-294.
7.   Dabora SL, Jozwiak S, Franz DN: **Mutational analysis in a cohort of 224 tuberous sclerosis patients indicates increased severity of *TSC2*, compared with *TSC1*, disease in multiple organs.** *Am J Hum Genet* 2001, **68(1):**64-80.
8.   Sancak O, Nellist M, Goedbloed M: **Mutational analysis of the *TSC1* and *TSC2* genes in a diagnostic setting: genotype-phenotype correlations and comparison of diagnostic DNA techniques in tuberous sclerosis complex.** *Eur J Hum Genet* 2005, **13(6):**731-741.
9.   Niida Y, Lawrence-Smith N, Banwell A: **Analysis of both *TSC1* and *TSC2* for germline mutations in 126 unrelated patients with tuberous sclerosis.** *Hum Mutat* 1999, **14(5):**412-422.
10. Au K-S, Williams AT, Roach ES: **Genotype/phenotype correlation in 325 individuals referred for a diagnosis of tuberous sclerosis complex in the United States.** *Genet Med* 2007, **9(2):**88-100.
11. Roach ES, DiMario FJ, Kandt RS: **Tuberous sclerosis consensus conference: recommendations for diagnostic evaluation. National Tuberous Sclerosis Association.** *J Child Neurol* 1999, **14(6):**401-407.
12. **NetGene2 Server**   [http://www.cbs.dtu.dk/services/NetGene2]
13. **SpliceSiteFinder**   [http://www.genet.sickkids.on.ca/~ali/splicesite finder.html]
14. **BDGP: Splice Site Prediction by Neural Network**   [http://www.fruitfly.org/seq_tools/splice.html]
15. Dayhoff MO, Schwartz RM, Orcutt BC: **A model of evolutionary change in proteins.** *"Atlas of Protein Sequence and Structure"* 1978, **5(3):**345-352.
16. Henikoff S, Henikoff J: **Amino acid substitution matrices from protein blocks.** *Proc Natl Acad Sci USA* 1992, **89:**10915-10919.
17. Grantham R: **Amino acid difference formula to help explain protein evolution.** *Science* 1974, **185(4154):**862-864.
18. Li Y, Corradetti MN, Inoki K: **TSC2: filling the GAP in the mTOR signaling pathway.** *Trends Biochem Sci* 2004, **29:**32-38.
19. Zhang H, Cicchetti G, Onda H: **Loss of Tsc1/Tsc2 activates mTOR and disrupts PI3K-Akt signaling through downregulation of PDGFR.** *J Clin Invest* 2003, **112:**1223-1233.
20. Kwiatkowski DJ, Zhang H, Bandura JL: **A mouse model of TSC1 reveals sex-dependent lethality from liver hemangiomas, and up-regulation of p70S6 kinase activity in Tsc1 null cells.** *Hum Mol Genet* 2002, **11(5):**525-534.
21. Nellist M, Sancak O, Goedbloed MA: **Distinct effects of single amino acid changes to tuberin on the function of the tuberin-hamartin complex.** *Eur J Hum Genet* 2005, **13(1):**59-68.
22. Inoki K, Li Y, Zu T: **TSC2 is phosphorylated and inhibited by Akt and suppresses mTOR signalling.** *Nat Cell Biol* 2002, **4(9):**648-657.
23. Obenauer JC, Cantley LC, Yaffe MB: **Scansite 2.0: Proteome-wide prediction of cell signaling interactions using short sequence motifs.** *Nucleic Acids Res* 2003, **31(13):**3635-3641.
24. Nellist M, Verhaaf B, Goedbloed MA: **TSC2 missense mutations inhibit tuberin phosphorylation and prevent formation of the tuberin-hamartin complex.** *Hum Mol Genet* 2001, **10(25):**2889-2898.
25. van Slegtenhorst M, Nellist M, Nagelkerken B: **Interaction between hamartin and tuberin, the *TSC1* and *TSC2* gene products.** *Hum Mol Genet* 1998, **7(6):**1053-1057.
26. Isaacs H Jr: **Fetal and neonatal cardiac tumors.** *Pediatr Cardiol* 2004, **25(3):**252-273.
27. Ballif B, Roux PP, Gerber SA: **Quantitative phosphorylation profiling of the ERK/p90 ribosomal S6 kinase-signaling cassette and its targets, the tuberous sclerosis tumor suppressors.** *PNAS* 2005, **102(3):**667-672.
28. Ma L, Chen Z, Erdjument-Bromage H, Tempst P, Pandolfi PP: **Phosphorylation and functional inactivation of TSC2 by Erk implications for tuberous sclerosis and cancer pathogenesis.** *Cell* 2005, **121(2):**179-193.
29. **Tuberous sclerosis database – Leiden Open Variation Database**   [http://chromium.liacs.nl/LOVD2/TSC/home.php]
30. Strizheva GD, Carsillo T, Kruger WD: **The spectrum of mutations in *TSC1* and *TSC2* in women with tuberous sclerosis and lymphangiomyomatosis.** *Am J Respir Crit Care Med* 2001, **163(1):**253-258.
31. Langkau N, Martin N, Brandt R: ***TSC1* and *TSC2* mutations in tuberous sclerosis, the associated phenotypes and a model to explain observed *TSC1*/*TSC2* frequency ratios.** *Eur J Pediatr* 2002, **161(7):**393-402.
32. Rosner M, Freilinger A, Hanneder M: **p27Kip1 localization depends on the tumor suppressor protein tuberin.** *Hum Mol Genet* 2007, **16(13):**1541-1546.

Pre-publication history

The pre-publication history for this paper can be accessed here:

http://www.biomedcentral.com/1471-2350/9/10/prepub

npg

ARTICLE

Missense mutations to the *TSC1* gene cause tuberous sclerosis complex

Mark Nellist*,[1], Diana van den Heuvel[1], Diane Schluep[1], Carla Exalto[1], Miriam Goedbloed[1], Anneke Maat-Kievit[1], Ton van Essen[2], Karin van Spaendonck-Zwarts[2], Floor Jansen[3], Paula Helderman[4], Gabriella Bartalini[5], Outi Vierimaa[6], Maila Penttinen[7], Jenneke van den Ende[8], Ans van den Ouweland[1] and Dicky Halley[1]

[1]Department of Clinical Genetics, Erasmus Medical Centre, Rotterdam, The Netherlands; [2]Department of Genetics, University Medical Center Groningen, University of Groningen, Groningen, The Netherlands; [3]Department of Child Neurology, Rudolf Magnus Institute for Neuroscience, University Medical Centre Utrecht, Utrecht, The Netherlands; [4]Department of Clinical Genetics, Maastricht University Medical Centre, Maastricht, The Netherlands; [5]Department of Clinical Pediatrics, University of Siena, Siena, Italy; [6]Department of Clinical Genetics, Oulu University Hospital, Oulu, Finland; [7]Clinical Genetics Unit, Department of Pediatrics, Turku University Central Hospital, Turku, Finland; [8]Centre of Medical Genetics, University of Antwerp, Antwerp, Belgium

Tuberous sclerosis complex (TSC) is an autosomal dominant disorder characterised by the development of hamartomas in a variety of organs and tissues. The disease is caused by mutations in either the *TSC1* gene on chromosome 9q34 or the *TSC2* gene on chromosome 16p13.3. The *TSC1* and *TSC2* gene products, TSC1 and TSC2, interact to form a protein complex that inhibits signal transduction to the downstream effectors of the mammalian target of rapamycin (mTOR). Here we investigate the effects of putative *TSC1* missense mutations identified in individuals with signs and/or symptoms of TSC on TSC1–TSC2 complex formation and mTOR signalling. We show that specific amino-acid substitutions close to the N-terminal of TSC1 reduce steady-state levels of TSC1, resulting in the activation of mTOR signalling and leading to the symptoms of TSC.
European Journal of Human Genetics advance online publication, 1 October 2008; doi:10.1038/ejhg.2008.170

Introduction

Tuberous sclerosis complex (TSC) is an autosomal dominant disorder characterised by the development of hamartomas in a variety of organs and tissues, including the brain, skin and kidneys.[1,2]

Mutations in either the *TSC1* gene on chromosome 9q34[3] or the *TSC2* gene on chromosome 16p13.3[4] cause TSC. The *TSC1* and *TSC2* gene products, TSC1 and TSC2, interact to form a protein complex. TSC2 contains a GTPase-activating protein domain and the TSC1–TSC2 complex acts on the rheb GTPase to prevent the rheb-GTP-dependent stimulation of cell growth through the mammalian target of rapamycin (mTOR).[5] In cells lacking either *TSC1* or *TSC2*, the downstream targets of mTOR, including p70 S6 kinase (S6K) and ribosomal protein S6, are constitutively phosphorylated.[6,7] The identification of the role of the TSC1–TSC2 complex in regulating mTOR activity has made it possible to compare TSC1 and TSC2 variants found in the normal population with variants identified in individuals with symptoms of TSC. The effects of amino-acid changes on TSC1–TSC2 complex formation, on the activation of rheb GTPase activity by the complex

*Correspondence: Dr M Nellist, Department of Clinical Genetics, Erasmus Medical Centre, Dr. Molewaterplein 50, 3015 GE Rotterdam, The Netherlands.
Tel: +31 10 7043357; Fax: +31 10 7044736;
E-mail: m.nellist@erasmusmc.nl

and on the phosphorylation status of S6K and S6 can be determined.[8]

Comprehensive screens for mutations at both the TSC1 and TSC2 loci have been performed in several large cohorts of TSC patients, and a wide variety of different pathogenic mutations have been described.[9–15] Although ~20% of the mutations identified in the TSC2 gene are missense changes, missense mutations in the TSC1 gene appear much less frequently. One simple explanation for this observation is that TSC1 missense mutations are rare because the majority of TSC patients have a mutation in the TSC2 gene. According to the TSC1 mutation database,[16] 22 putative missense mutations have been identified in TSC patients. However, only one of these is a confirmed de novo mutation. Here, we investigate the effects of 10 TSC1 missense changes (c.350T>C (p.L117P), c.539T>C (p.L180P), c.572T>A (p.L191H), c.671T>G (p.M224R), c.737G>A (p.R246K), c.913G>A (p.G305R), c.913G>T (p.G305W), c.1526G>A (p.R509Q), c.3103G>A (p.G1035S) and c.3290G>A (p.R1097H)) on TSC1–TSC2 function. We compared these TSC1 variants with wild-type TSC1 and three truncation variants: c.379_381delTGT (p.128delV), c.593_595delACT (p.N198F199delinsI) and c.2075C>T (p.R692X). Our analysis demonstrates that TSC1 missense mutations reduce steady-state levels of TSC1, resulting in increased mTOR activity and leading to the symptoms of TSC.

Materials and methods

Patient characteristics
Samples from patients with either a putative or definite diagnosis of TSC were received for mutation analysis. Details on clinical symptoms were obtained from the treating physicians who were sent a standardised clinical evaluation form (see Supplementary Table 1).

Mutation analysis
DNA was extracted from peripheral blood using standard techniques. Mutation analysis was performed as described earlier,[13] or by direct sequence analysis of all TSC1 and TSC2 coding exons and exon/intron boundaries. In addition, both genes were analysed using the multiplex ligation-dependent probe amplification assay (MRC Holland, Amsterdam, The Netherlands).

To investigate whether the identified changes had an effect on splicing, three different splice-site prediction programs were used,[17–19] as described earlier.[13]

Generation of constructs and antisera
Expression constructs encoding C-terminal YFP- and myc-tagged TSC1 variants were derived using the QuikChange site-directed mutagenesis kit (Stratagene, La Jolla, CA, USA). In each case, the complete open reading frame of the mutated construct was verified by sequence analysis.

The other constructs used in this study have been described earlier.[8,20,21] Polyclonal rabbit antisera specific for human TSC1 and TSC2 have been described earlier.[21] Other antibodies were purchased from Cell Signaling Technology (Danvers, MA, USA).

Functional analysis of TSC1 variants
Expression of TSC1 variants in transfected cells Human embryonal kidney (HEK) 293T cells seeded into 6-cm diameter dishes were transfected with a 1:1 mixture of the TSC1 and TSC2 expression constructs using Lipofectamine Plus (Invitrogen, Carlsbad, CA, USA), following the manufacturer's instructions. Two days after transfection, the cells were lysed in 50 mM Tris-HCl (pH 8.0), 100 mM NaCl, 50 mM NaF, 0.5 mM EDTA and 1% Triton X-100 plus protease inhibitors (Roche, Basel, Switzerland) and separated into supernatant and pellet fractions by centrifugation at 10 000 g for 10 min at 4°C as described earlier.[22] Wild-type TSC1 and the TSC1 variants were immunoprecipitated from the supernatant fractions by incubation with a monoclonal antibody against the C-terminal myc epitope tag for 90 min at 4°C before incubation with Protein G beads (GE Healthcare, Uppsala, Sweden). After gentle agitation for 90 min at 4°C, the beads were washed three times with a >50-fold excess of lysis buffer. The immunoprecipitated proteins were detected by immunoblotting. Blots were developed using enhanced chemiluminescent detection (GE Healthcare).[8]

Immunoblot analysis of S6K T389 phosphorylation in cells overexpressing TSC1 variants HEK 293T cells were transfected with a 4:2:1 mixture of the TSC1, TSC2 and S6K expression constructs. A total of 1.75 μg DNA was diluted in 200 μl Dulbecco's modified Eagle's medium (DMEM) containing 7 μg polyethyleneimine (Polysciences, Warrington, PA, USA). Where necessary, an empty expression vector (pcDNA3; Invitrogen) was added to make up the total amount of DNA. After 15 min at room temperature, the DNA/polyethyleneimine complexes were added to 80% confluent cells in 3.5-cm diameter dishes. After 4 h at 37°C, the transfection mixture was replaced with DMEM containing 10% foetal calf serum. Twenty-four hours after transfection, the cells were harvested and analysed by immunoblotting as before or by near infrared fluorescent detection on an Odyssey™ Infrared Imager (169 μm resolution, medium quality with 0 mm focus offset) (Li-Cor Biosciences, Lincoln, NE, USA). The integrated intensities of the protein bands were determined using the Odyssey software (default settings with background correction; 3-pixel width border average method). The mean ratios of the T389-phosphorylated S6K signal to the total S6K signal (T389/S6K) and the total TSC2 signal to the total TSC1 signal (TSC2/TSC1) were determined relative to wild-type TSC1 from at least three independent experiments (wild-type T389/S6K and TSC2/TSC1 ratios = 1).

Immunofluorescent detection of S235/236 phosphorylation of ribosomal protein S6 in TSC1-deficient cells
$Tsc1-/-$ mouse embryo fibroblasts (MEFs)[7] were transfected with expression constructs encoding wild-type TSC1 or the TSC1 variants, using Lipofectamine Plus (Invitrogen), following the manufacturer's instructions. Twenty-four hours after transfection, S6 (S235/236) phosphorylation in the transfected cells was detected by immunofluorescent microscopy using a rabbit polyclonal antibody specific for S235/236-phosphorylated S6.[23] TSC1 variants were identified either directly (for C-terminal-tagged TSC1-YFP variants) or with a mouse monoclonal antibody against the myc epitope tag (for C-terminal-tagged TSC1-myc variants). If possible, at least 50 cells expressing each TSC1 variant were counted per experiment and the number of cells showing a clear reduction in S6 (S235/236) phosphorylation was noted. The mean proportions of expressing cells with reduced S6 phosphorylation were calculated from at least three independent experiments.

Results
Patient characteristics and mutation analysis
The *TSC1* c.350T>C (p.L117P) change was detected in two generations of a family with TSC (Figure 1a). The index patient (I:1) had epilepsy since the age of 22 years and fulfilled the diagnostic criteria for definite TSC, with facial angiofibroma, ungual fibroma, hypomelanotic macules, a shagreen patch and cerebral white matter migration lines. No mental disability was reported. The youngest child
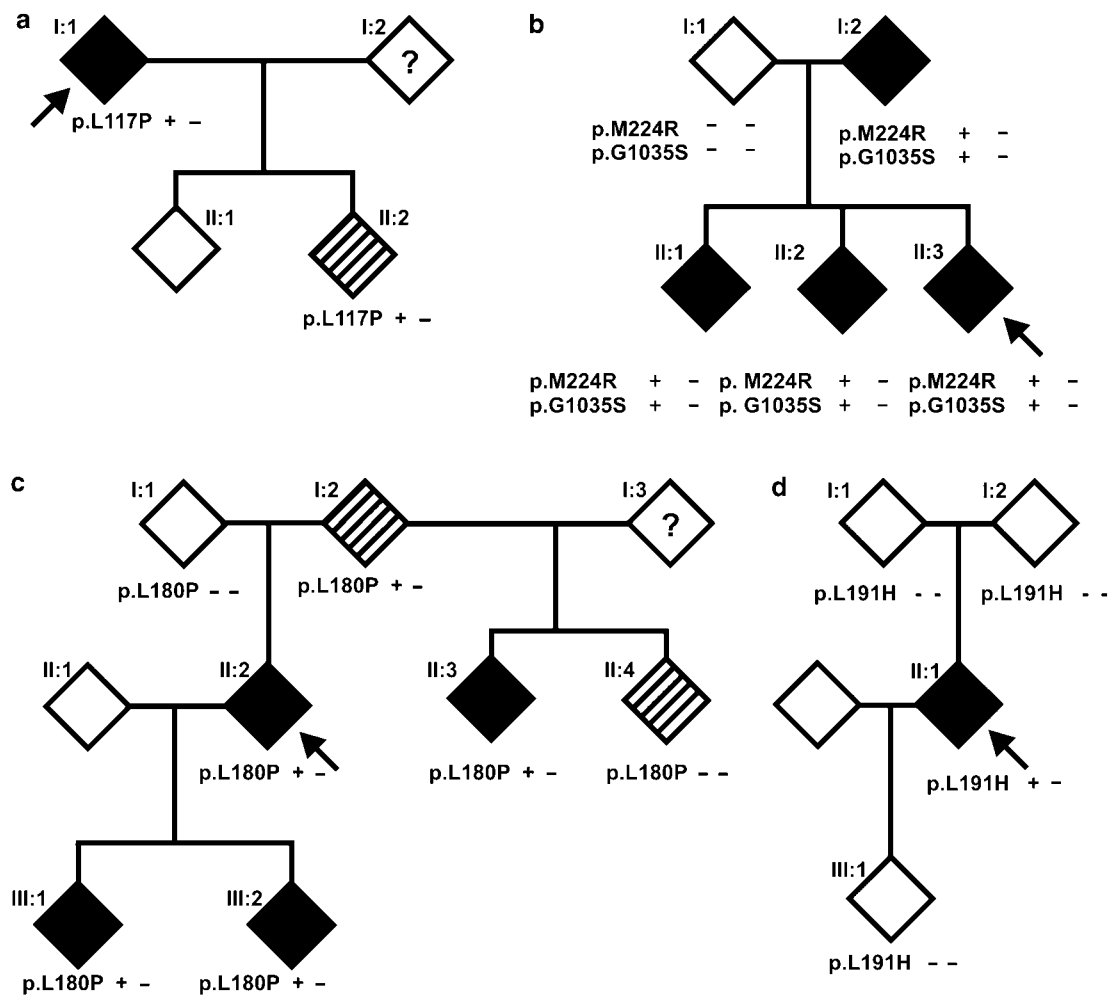

Figure 1 Pedigrees of the investigated families with TSC. Arrows indicate the index cases. Open symbols indicate no signs or symptoms of TSC; black symbols indicate individuals with definite TSC; hatched symbols indicate individuals with possible TSC. A question mark indicates individuals where no clinical data were available. Genotypes are indicated for the individuals where DNA was available for testing. (a) Family with TSC and the *TSC1* c.350T>C (p.L117P) variants. (b) Family with TSC and cosegregation of the *TSC1* c.671T>G (p.M224R) and c.3103G>A (p.G1035S) variants. (c) Family with cosegregation of TSC and the *TSC1* c.539T>C (p.L180P) variants. (d) Family with a *de novo TSC1* c.572T>A (p.L191H) mutation.

(II:2) had the c.350T>C change. Despite being somewhat hyperactive, this child developed normally until 4 years of age when epileptic seizures occurred and development stagnated. The child is now severely mentally retarded. No information was available about other signs of TSC. The eldest child (II:1), who could not yet be tested for the c.350T>C change, suffered severe anoxia at birth and has severe infantile encephalopathy with spastic tetraplegia and epilepsy.

The *TSC1* c.671T>G (p.M224R) and *TSC1* c.3103G>A (p.G1035S) changes were identified in two generations of a family with TSC[24] (Figure 1b). The index case (II:3) had definite TSC with multiple shagreen patches, hypomelanotic macules, ungual fibromas, dental pits, epilepsy and severe mental disability. One parent (I:2) and both siblings (II:1 and II:2) of the index case also fulfilled the diagnostic criteria for definite TSC. Individual I:2, who was seizure-free and of below-average intelligence (IQ 73), had skin lesions pathognomonic for TSC. Individual II:1, who was of normal intelligence (IQ 94), had seizures, cortical tubers and multiple TSC skin lesions. Individual II:2 had epilepsy, below-average intelligence (IQ 67) and multiple TSC skin lesions. All the affected individuals in this family were heterozygous for the c.671T>G and c.3103G>A changes. Three affected individuals (I:2, II:1 and II:2) were heterozygous for a polymorphism in the *TSC2* gene (*TSC2* c.1276-32C>G). The index case was homozygous for the wild-type *TSC2* 1276-32C allele, consistent with TSC segregating with a mutation at the *TSC1* locus in this family.

The *TSC1* c.539T>C (p.L180P) change was detected in three generations of a family with TSC (Figure 1c). Individual I:2 had an ungual fibroma as the only reported sign of TSC. Individual II:2 had epilepsy, no mental disability, skin signs typical for TSC and a subependymal giant cell astrocytoma as well as other brain lesions consistent with a definite diagnosis of TSC. Individual II:3, the half-sibling of II:2, had typical TSC-associated skin lesions and possible mild mental retardation. Individual II:4, the other half-sibling of II:2, had a history of seizures during puberty and some skin tags, not typical of TSC. Individual III:1, the child of II:2, had epilepsy, and typical TSC-associated skin and brain lesions. Individual III:2, the sibling of III:1, had multiple cardiac rhabdomyoma and Wolff–Parkinson–White syndrome. No mental disability was reported for either individual III:1 or III:2. TSC did not cosegregate with markers mapping close to the *TSC2* locus on chromosome 16p13.3, and no candidate *TSC2* mutation was identified in the index case.

The *TSC1* c.572T>A (p.L191H) change was identified in an individual who met the clinical criteria for definite TSC, including typical skin, heart and brain lesions. The individual had a history of seizures but no mental disability was reported. The c.572T>A change was absent in the individual's parents and child (Figure 1d). None of these individuals showed any signs of TSC.

Two TSC patients, one Finnish and one Dutch, were identified with the *TSC1* c.737G>A (p.R246K) change. No information was available on the parents of either of these two individuals. The Finnish individual had typical TSC-associated skin, brain and kidney lesions. No mental disability or history of seizures was reported. The Dutch individual was also reported to have definite TSC. The sibling of this individual did not have any signs of TSC and did not carry the c.737G>A change.

The *TSC1* c.1526G>A (p.R509Q) change was identified in a child of African origin, suspected of having TSC due to an echodensity that was detected prenatally in the septum of the heart. After birth, physical examination of the child did not reveal any signs of TSC but multiple congenital malformations that fitted with VACTERL (vertebral anomalies, atresia, cardiac malformations, tracheoesophageal fistula, renal anomalies and limb anomalies) association were identified. The same c.1526G>A change was identified in one of the parents. Neither parent reported any signs of TSC.

The *TSC1* c.3290G>A (p.R1097H) change was identified in a child with cardiac rhabdomyoma who subsequently developed epilepsy at the age of 3 months. An MRI scan of the brain showed multiple subependymal nodules, cortical tubers and white matter abnormalities. This individual fulfilled the diagnostic criteria for definite TSC, with angiomyolipoma and multiple skin lesions. The c.3290G>A change was also identified in one of the parents; neither parent showed any signs of TSC.

The *TSC1* c.379_381delTGT (p.128delV) change was detected in a child with epilepsy and a definite diagnosis of TSC (multiple skin signs, subependymal nodules and angiomyolipoma). No mental disability was reported and no information was available on the phenotypic or genetic status of the parents. The same change has been reported in another unrelated TSC patient.[25] The *TSC1* c.593_595delACT (p.N198F199delinsI), c.913G>A (p.G305R) and c.913G>T (p.G305W) missense changes have been reported earlier to cosegregate with TSC in three independent families.[15,26]

In all the above cases, no other putative pathogenic mutations were identified and comparison of the allele ratios of the index cases and parents (where possible) did not reveal any evidence for somatic mosaicism in the leukocyte DNA.

Comparative analysis of TSC1 amino-acid substitutions

During our initial mutation screening, the L117P change was the only putative pathogenic TSC1 amino-acid substitution identified. We compared the L117P variant with wild-type TSC1, an earlier characterised TSC1 in-frame deletion (N198F199delinsI)[27] and to a common TSC1 truncation mutation, R692X[3,10] (Figure 2). Wild-type TSC1 was detected predominantly in the post 10 000 *g*
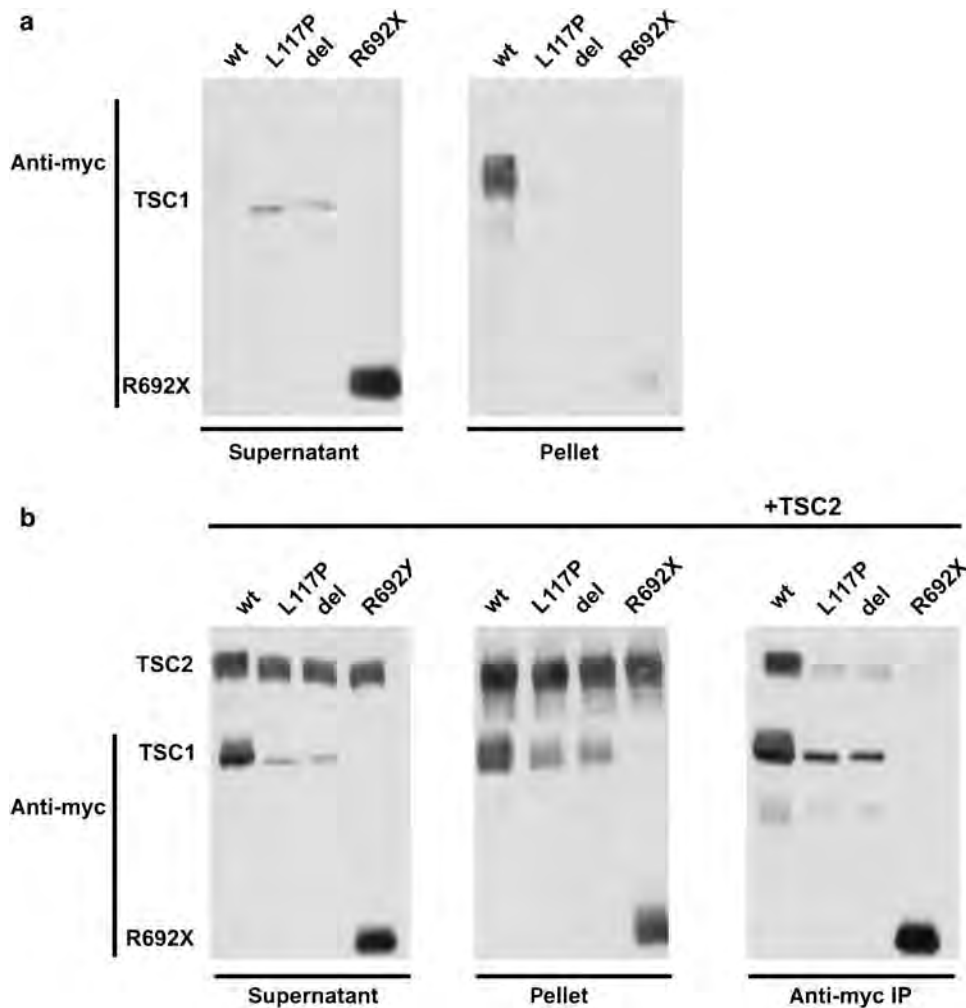
Figure 2 Analysis of the TSC1 L117P variant. Wild-type TSC1 (wt) or the L117P, N198F199delinsI (del) or R692X variants (all containing a C-terminal myc epitope tag) were overexpressed in HEK 293T cells alone (**a**) or in the presence of coexpressed TSC2 (**b**). Cell lysates were separated into post 10 000 *g* centrifugation pellet and supernatant fractions. The TSC1 variants were detected with a monoclonal mouse antibody against the myc epitope tag (9B11; Cell Signaling Technology). TSC1–TSC2 complexes were immunoprecipitated from the supernatant fractions using the same antibody. TSC2 was detected with a polyclonal rabbit antiserum.[8] (**a**) Expression of the TSC1 variants in the absence of TSC2. Wild-type TSC1 (wt) was detected predominantly in the pellet fraction. In contrast, the variants were detected predominantly in the supernatant fraction. The signals for the L117P and N198F199delinsI (del) variants are clearly less than wild-type TSC1 and the R692X variants (as detected with the 9B11 antibody). (**b**) Coexpression of TSC2 and the TSC1 variants. In the presence of TSC2, wild-type TSC1 and the variants were detected in both subcellular fractions. Coexpression of TSC2 resulted in a shift of wild-type TSC1 to the supernatant fraction and a shift of the variants to the pellet fraction. TSC1 and the TSC1 variants were immunoprecipitated with an antibody against the myc epitope tag. TSC2 was coimmunoprecipitated with all three variants. However, in each case, the TSC2 signal in the immunoprecipitate was clearly less than with the wild-type TSC1.

pellet fraction, whereas the three variants were detected in the supernatant fraction (Figure 2a). Upon coexpression of TSC2, the variants as well as wild-type TSC1 were detected in both subcellular fractions (Figure 2b). TSC2 was coimmunoprecipitated from the supernatant fraction with all three variants, although clearly less effectively than with wild-type TSC1.

Next, we investigated whether the variants could inhibit mTOR signalling. Expression of wild-type TSC1 alone is insufficient to inhibit mTOR activity.[28] Therefore, the variants were coexpressed with TSC2 and S6K in HEK

293T cells, and S6K T389 phosphorylation was analysed by immunoblotting (Figure 3a). To try and achieve comparable expression levels of the different variants, we used different quantities of the corresponding expression constructs. Coexpression of wild-type TSC1 and TSC2 resulted in a reduction in S6K T389 phosphorylation, even with low levels of the TSC1 expression construct. In contrast, coexpression of TSC2 with the variants did not reduce S6K T389 phosphorylation, indicating that they were unable to inhibit mTOR effectively. Compared with wild-type TSC1, the L117P
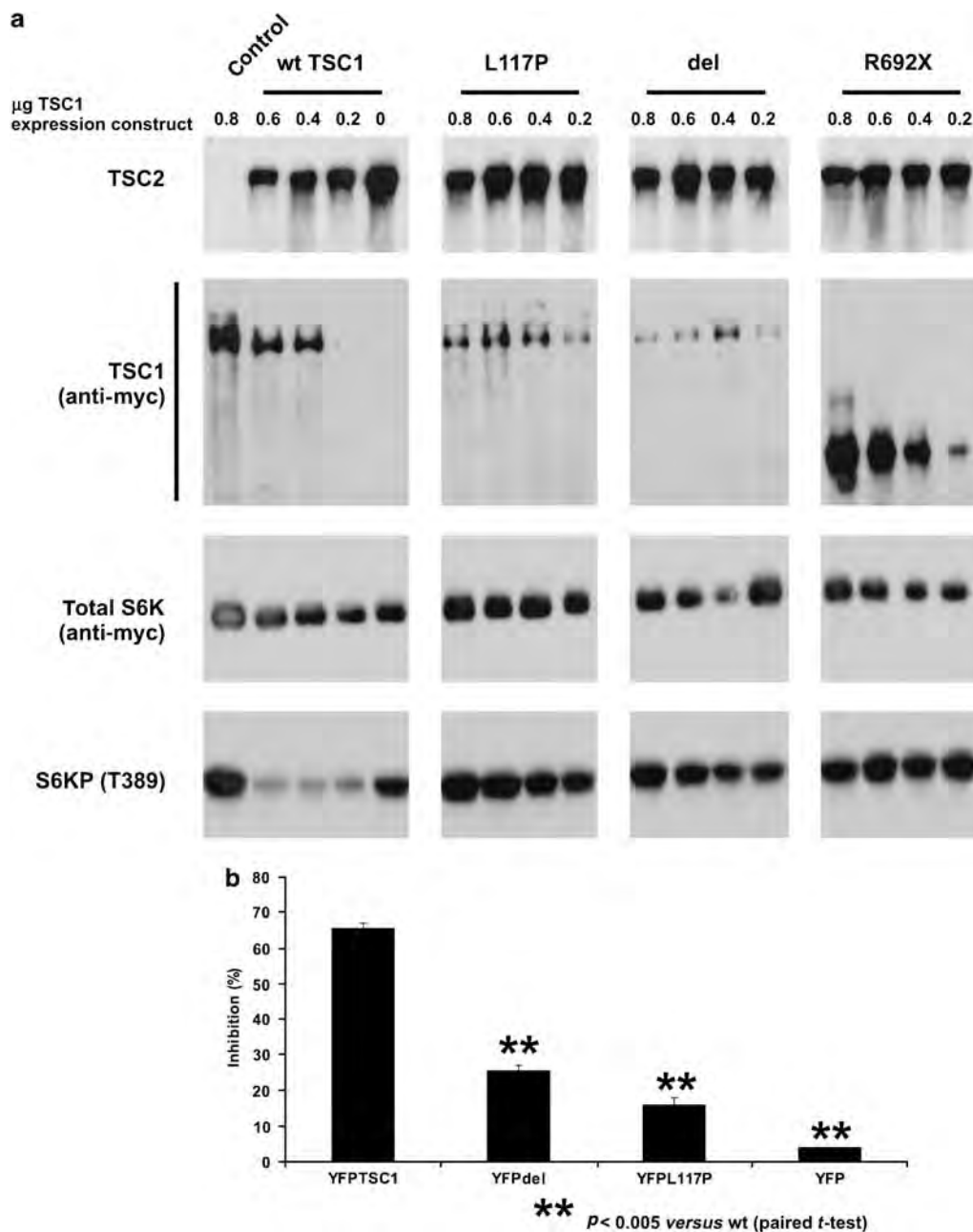
Figure 3 TSC1–TSC2-dependent inhibition of mTOR signalling by the TSC1 L117P variant. (**a**) T389 phosphorylation of S6K in HEK 293T cells coexpressing TSC2, myc-tagged S6K and myc-tagged wild-type TSC1 (wt) or the TSC1 L117P, N198F199delinsI (del) or R692X variants was determined by immunoblotting. Cells transfected with differing amounts of wild-type or variant expression constructs, as indicated, were analysed. The first lane on the left (control) corresponds to cells transfected with S6K and wild-type TSC1 expression constructs only (no TSC2 expression construct). The coexpression of only TSC2 and wild-type TSC1 inhibited S6K phosphorylation. (**b**) TSC1-dependent inhibition of S6 phosphorylation. YFP-tagged wild-type TSC1 (YFPTSC1) and the YFP-tagged N198F199delinsI (YFPdel) and L117P (YFPL117P) variants were expressed in $Tsc1-/-$ MEFs. S6 S235/236 phosphorylation in the YFP-positive cells was detected by immunofluorescent microscopy using an antibody specific for S235/236-phosphorylated S6 (Cell Signaling Technology). As a control, S6 phosphorylation in cells expressing YFP only was also determined. At least 50 cells were counted per variant per experiment. Mean percentage scores of three separate experiments are shown. Values significantly different from the wild type are indicated.

and N198F199delinsI variants were detected at low levels, even when the quantity of transfected expression construct DNA was increased.

To confirm that the L117P and N198F199delinsI variants were unable to inhibit mTOR, they were expressed in $Tsc1-/-$ MEFs. These cells exhibit constitutive S6 (S235/

236) phosphorylation.[7] As shown in Figure 3b, wild-type YFP-tagged TSC1 reduced S6 phosphorylation in >60% of the YFP-positive Tsc1−/− MEFs, consistent with earlier results.[8] In contrast, S6 phosphorylation was reduced in <30% of cells expressing the L117P or N198F199delinsI variants (paired t-test P<0.001). Nevertheless, a reduction in S6 phosphorylation was observed in a higher proportion of variant-expressing cells than in cells expressing YFP only (paired t-test P<0.02). Therefore, although both variants were clearly less effective than wild-type TSC, we could not exclude the possibility that the variants can antagonise mTOR activity.

As a result of on-going TSC1 and TSC2 mutation screening, we identified eight additional TSC1 single amino-acid changes: p.128delV, p.L180P, p.L191H, p.M224R, p.R246K, p.R509Q, p.G1035S and p.R1097H. The p.M224R and p.G1035S changes cosegregated with

TSC in a single family (Figure 1b). To investigate the effects of these two amino-acid substitutions on TSC1 function, the corresponding single and double variants were compared with wild-type TSC1 and the R692X truncation. As shown in Figure 4a, the M224R variant and the M224R/G1035S double variant were detected at lower levels than wild-type TSC1 and the G1035S variant. Furthermore, the expression of wild-type TSC1 or the G1035S variant reduced S6 phosphorylation in >50% of transfected Tsc1−/− MEFs whereas <20% of the MEFs expressing the M224R, M224R/G1035S or R692X variants showed a reduction in S6 phosphorylation (Figure 4b), indicating that the M224R substitution is the pathogenic mutation in this family and that the G1035S substitution is a cosegregating neutral variant.[24] We did not observe any differences between the M224R single mutant and the M224R/G1035S double mutant.
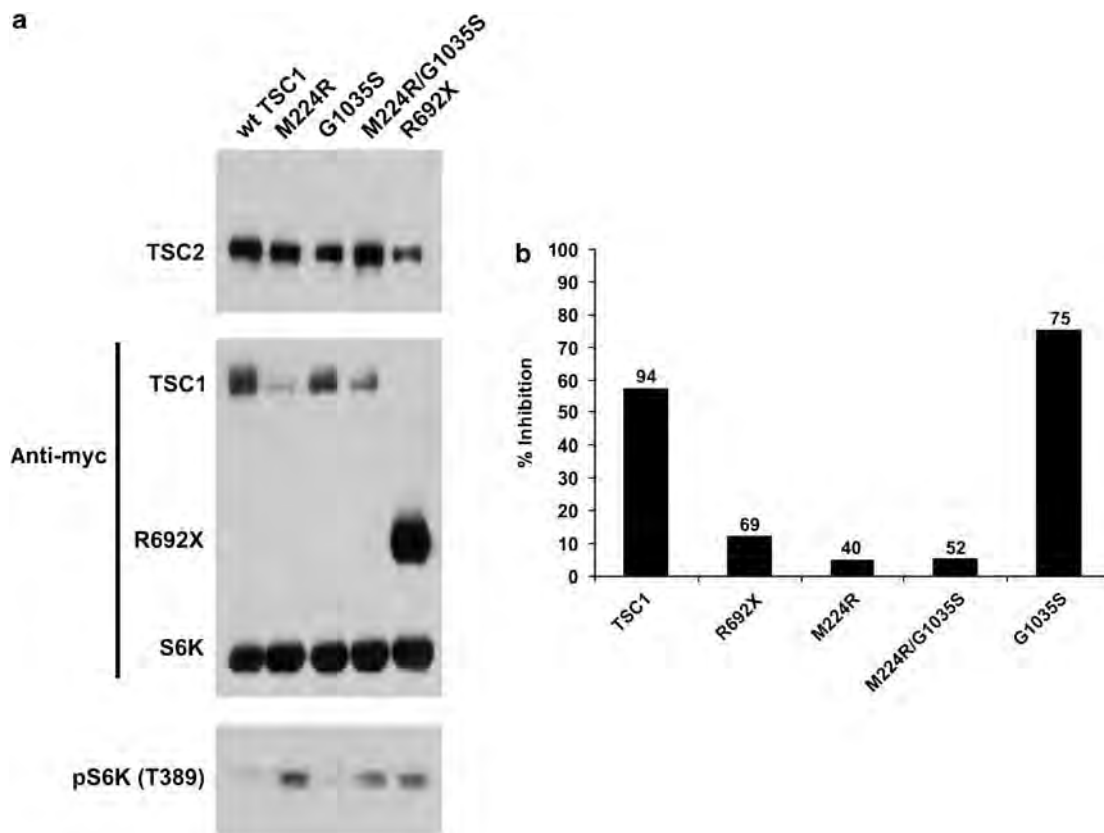

Figure 4 Results of the functional assays on the M224R, G1035S and M224R/G1035S variants. (**a**) TSC1–TSC2-dependent inhibition of S6K-T389 phosphorylation. TSC2, S6K and wild-type TSC1 (wt TSC1), or the TSC1 variants, were expressed in HEK 293T cells. T389 phosphorylation of S6K was determined by immunoblotting and was reduced in the presence of wild-type TSC1 and the G1035S variants only. S6K, wild-type TSC1 and the TSC1 variants were detected with an antibody against the myc epitope tag. The signal for the M224R and M224R/G1035S variants is reduced compared with wild-type TSC1 and the G1035S and R692X variants. A representative example of at least three separate experiments is shown. (**b**) Inhibition of S6 phosphorylation in Tsc1−/− MEFs. Wild-type myc-tagged TSC1 (TSC1) and the myc-tagged variants were expressed in Tsc1−/− MEFs. S6 S235/236 phosphorylation in the myc-positive cells was determined by double-label immunofluorescent microscopy using a rabbit polyclonal antibody specific for S235/236-phosphorylated S6 and a mouse monoclonal antibody specific for the myc tag. The percentage of Tsc1−/− MEFs expressing the TSC1 variants and showing a clear reduction in S6 phosphorylation is indicated. Because the signals for the M224R and M224R/G1035S variants were very low, it was difficult to unequivocally differentiate >50 expressing cells. Therefore, the total number of counted cells after two experiments is indicated above each bar.
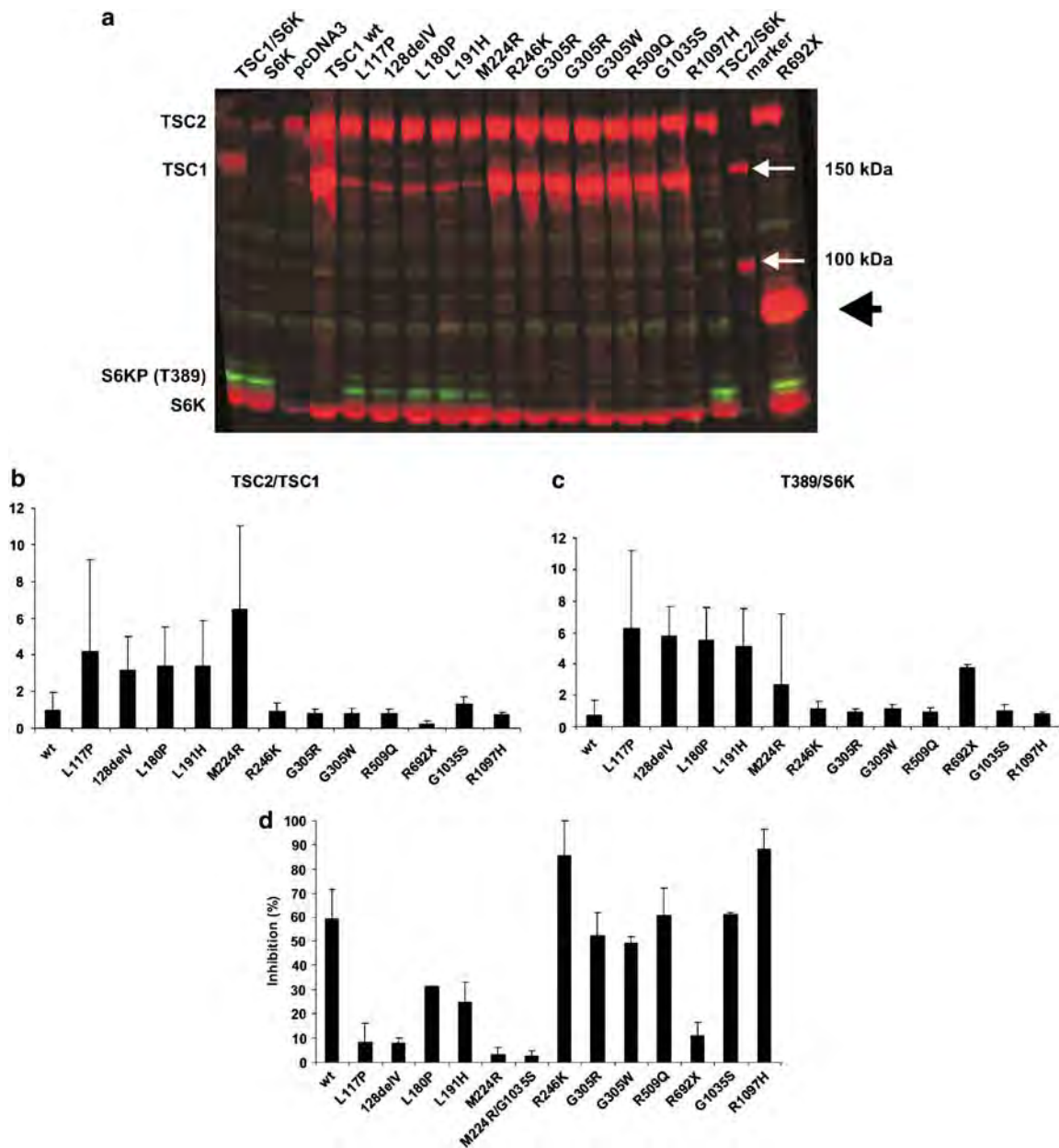
Figure 5 Analysis of the 128delV, L180P, L191H, R246K, G305R, G305W, R509Q and R1097H variants. (**a**) TSC1-dependent inhibition of S6K T389 phosphorylation. S6K T389 phosphorylation was determined by immunoblotting as before except that the blots were developed using Odyssey near infrared detection (Li-Cor Biosciences). Cells expressing S6K, TSC2 and wild-type TSC1 (wt) or the TSC1 variants were analysed. As controls, cells transfected with expression constructs for wild-type TSC1 and S6K only (TSC1/S6K), TSC2 and S6K only (TSC2/S6K), S6K only (S6K) or empty vector only (pcDNA3) were also analysed. S6K and the TSC1 variants were detected with an antibody specific for the myc epitope tag. The R692X truncation variant is indicated with a large arrowhead; molecular weight markers are indicated with small arrows. Expression of wild-type TSC1 or the R246K, G305R, G305W, R509Q, G1035S and R1097H variants clearly inhibited S6K phosphorylation. The signals for the L117P, 128delV, L180P, L191H and M224R variants were clearly reduced compared with wild-type TSC1 (see also panel b), and S6K T389 phosphorylation was increased (see also panel c). A representative example of three separate experiments is shown. (**b**) Relative expression of the TSC1 variants. The integrated intensities of the TSC1 and TSC2 signals for each variant were determined in three independent experiments using the Odyssey scanning software. The mean TSC2/TSC1 ratios, relative to the wild-type TSC1 (wt) (wild-type TSC1 TSC2/TSC1 ratio = 1), were determined. Standard deviations are indicated. (**c**) TSC1-dependent inhibition of S6K T389 phosphorylation. The ratio of the T389 S6K phosphorylation signal intensity to the total S6K signal intensity (T389/S6K) was measured in three independent experiments. The integrated intensity of each band was determined using the Odyssey scanning software and the mean T389/S6K ratios, relative to the wild-type TSC1 (wt) (wild-type TSC1 T389/S6K ratio = 1), were determined. Standard deviations are indicated. (**d**) Inhibition of S6 phosphorylation in *Tsc1*−/− MEFs. Wild-type myc-tagged TSC1 (wt) or the myc-tagged variants were expressed in *Tsc1*−/− MEFs. S6 S235/236 phosphorylation in the myc-positive cells was determined by immunofluorescent microscopy as before. At least 50 cells were counted per variant per experiment. Each variant was tested in at least two separate experiments. Mean percentages of *Tsc1*−/− MEFs expressing the TSC1 variants and showing reduced phosphorylation of S6 are shown. Standard deviations are indicated.

To determine whether the 128delV, L180P, L191H, R246K, R509Q and R1097H amino-acid changes were pathogenic, we compared these variants with the previously characterised L117P and R692X variants, and with two additional putative missense variants, G305R and G305W[15] (Figure 5). The R246K, G305R, G305W, R509Q and R1097H variants were detected at comparable levels with wild-type TSC1 (Figure 5a and b) and were just as effective at inhibiting S6K T389 phosphorylation (Figure 5a and c). In contrast, the 128delV, L180P and L191H variants were detected at low levels, similar to the L117P and M224R variants (Figure 5a and b). Furthermore, S6K T389 phosphorylation was not inhibited by the expression of these variants (Figure 5a and c). Consistent with the immunoblot data, the expression of the L117P, 128delV, L180P, L191H, M224R, M224R/G1035S and R692X variants in Tsc1−/− MEFs reduced S6 phosphorylation in <40% of cells, whereas wild-type TSC1 and the R246K, G305R, G305W, R509Q, G1035S and R1097H variants reduced S6 phosphorylation in >50% of the expressing cells (Figure 5d).

We concluded that the 128delV, L180P and L191H changes destabilise TSC1, resulting in increased mTOR activity. The R246K, G305R, G305W, R509Q, G1035S and R1097H amino-acid substitutions did not affect TSC1 function in our assays.

Splice-site prediction analysis
Splice-site prediction analysis of the identified variants was performed according to a standard protocol[13] using three independent splice-site prediction programs.[17–19] Effects were predicted for four of the variants: TSC1 c.379_381delTGT (p.128delV), c.737G>A (p.R246K) c.913G>A (p.G305R) and c.913G>T (p.G305W).

According to two of the prediction programs, the c.379_381delTGT mutation created a potential new acceptor site within exon 6. However, the values of the new site (0.48 and 0.33 in Fruitfly and NetGene2, respectively) were lower than the values of the wild-type acceptor site (0.98 and 0.97, respectively). It is therefore unlikely that this sequence change affects splicing.

The R246K, G305R and G305W amino-acid substitutions did not affect TSC1 function. However, the c.737G>A (p.R246K) nucleotide substitution altered the last nucleotide of exon 8 and all three programs indicated that this change disrupted the intron 8 splice donor site, leaving a new potential donor site 90 nucleotides downstream. Similarly, the c.913G>A (p.G305R) and c.913G>T (p.G305W) substitutions affect the last nucleotide of exon 9 and were predicted by all three programs to disrupt splicing to the intron 9 donor site. We concluded that these three variants are most likely pathogenic splice-site mutations, not missense mutations. Unfortunately, the effect of these sequence changes on TSC1 RNA splicing could not be confirmed experimentally because no new samples could be obtained.

An overview of the functional assays and splice-site analysis is presented in Supplementary Table 2.

Discussion
Mutation analysis of the TSC1 and TSC2 genes in individuals with TSC, and in those suspected of having the disease is important for diagnosis and genetic counselling. During our screening of a cohort of approximately 900 index cases with TSC, or possible TSC, we identified eight putative pathogenic TSC1 missense changes, c.350T>C (p.L117P), c.539T>C (p.L180P), c.572T>A (p.L191H), c.671T>G (p.M224R), c.737G>A (p.R246K), c.1526G>A (p.R509Q), c.3103G>A (p.G1035S) and c.3290G>A (p.R1097H), as well as a putative pathogenic in-frame deletion mutant, TSC1 c.379_381delTGT (p.128delV). We compared these variants with the earlier reported c.913G>A (p.G305R), c.913G>T (p.G305W), c.593_595delACT (p.N198F199delinsI) and c.2074C>T (p.R692X) mutants.[2,15,26]

The TSC1 L117P, 128delV, L180P, L191H, N198F199-delinsI and M224R changes resulted in reduced levels of TSC1 and a reduction in TSC1-dependent inhibition of mTOR activity, as detected by immunoblotting. In each case, the functional characterisation was consistent with the genetic and phenotypic findings and we concluded that the changes were pathogenic.

The R246K, G305R, G305W, R509Q, G1035S and R1097H amino-acid substitutions did not affect TSC1 function in our assays. However, we concluded that the TSC1 c.737G>A (p.R246K), c.913G>A (p.G305R) and c.913G>T (p.G305W) changes were most likely pathogenic splice-site mutations. The c.737G>A transition was predicted to destroy the splice donor site at the 3′ end of exon 8 and the c.913G>A and c.913G>T substitutions affect the last nucleotide of exon 9, also disrupting the normal splice donor site. The c.1526G>A (p.R509Q), c.3103G>A (p.G1035S) and c.3290G>A (p.R1097H) variants did not appear to affect either TSC1 RNA splicing or TSC1 function. The c.1526G>A change was identified in a foetus suspected of having TSC. However, after birth, the child showed multiple congenital malformations that fitted with VACTERL association, and a normal physical examination of the child did not reveal any signs of TSC. We concluded that this variant is unlikely to cause TSC. The c.3103G>A variant cosegregated with the pathogenic c.671T>G (p.M224R) variant and TSC in a single family.[24] We concluded that the p.G1035S substitution was a neutral variant, consistent with previous reports.[29,30] The c.3290G>A change was identified in a child with definite TSC and in one unaffected parent, and we concluded that it was also most likely a rare neutral variant.

Here we demonstrate that specific amino-acid substitutions close to the N-terminal of TSC1 (amino acids 117–

224) reduce the steady-state levels of TSC1. The location and the effects of these changes on TSC1 function are very similar to a small number of missense mutations described recently in some cases of bladder cancer,[31] suggesting that the pathogenetic mechanisms underlying TSC-associated lesions and tumours of the bladder may be related.

Several studies indicate that *TSC1* mutations are associated with a less severe clinical presentation in TSC patients.[9,12,13,15] The small number of patients that we identified with a *TSC1* missense mutation made it difficult to identify a specific phenotypic spectrum in this group. Nevertheless, the use of functional assays to differentiate between polymorphisms and pathogenic mutations, in TSC and other diseases, will not only facilitate the identification of pathogenic mutations but also help investigate possible genotype–phenotype correlations and provide insight into how specific amino-acid residues contribute to protein function.

Acknowledgements

References

1 Gomez M, Sampson J, Whittemore V eds: *The Tuberous Sclerosis Complex.* Oxford, UK: Oxford University Press, 1999.

2 Roach ES, DiMario FJ, Kandt RS *et al*: Tuberous sclerosis consensus conference: recommendations for diagnostic evaluation. National Tuberous Sclerosis Association. *J Child Neurol* 1999; **14**: 401–407.

3 van Slegtenhorst M, de Hoogt R, Hermans C *et al*: Identification of the tuberous sclerosis gene *TSC1* on chromosome 9q34. *Science* 1997; **277**: 805–808.

4 The European Chromosome 16 Tuberous Sclerosis Consortium: Identification and characterization of the tuberous sclerosis gene on chromosome 16. *Cell* 1993; **75**: 1305–1315.

5 Li Y, Corradetti MN, Inoki K *et al*: TSC2: filling the GAP in the mTOR signaling pathway. *Trends Biochem Sci* 2003; **28**: 573–576.

6 Zhang H, Cicchetti G, Onda H *et al*: Loss of *Tsc1/Tsc2* activates mTOR and disrupts PI3K-Akt signaling through downregulation of PDGFR. *J Clin Invest* 2003; **112**: 1223–1233.

7 Kwiatkowski DJ, Zhang H, Bandura JL *et al*: A mouse model of TSC1 reveals sex-dependent lethality from liver hemangiomas, and up-regulation of p70S6 kinase activity in *Tsc1* null cells. *Hum Mol Genet* 2001; **11**: 525–534.

8 Nellist M, Sancak O, Goedbloed MA *et al*: Distinct effects of single amino acid changes to tuberin on the function of the tuberin–hamartin complex. *Eur J Hum Genet* 2005; **13**: 59–68.

9 Jones AC, Shyamsundar MM, Thomas MW *et al*: Comprehensive mutation analysis of *TSC1* and *TSC2*, and phenotypic correlations in 150 families with tuberous sclerosis. *Am J Hum Genet* 1999; **64**: 1305–1315.

10 van Slegtenhorst M, Verhoef S, Tempelaars A *et al*: Mutational spectrum of the *TSC1* gene in a cohort of 225 tuberous sclerosis complex patients: no evidence for genotype–phenotype correlation. *J Med Genet* 1999; **36**: 285–289.

11 Au KS, Rodriguez JA, Finch JL *et al*: Germ-line mutational analysis of the *TSC2* gene in 90 tuberous sclerosis patients. *Am J Hum Genet* 1998; **62**: 286–294.

12 Dabora SL, Jozwiak S, Franz DN *et al*: Mutational analysis in a cohort of 224 tuberous sclerosis patients indicates increased severity of *TSC2*, compared with *TSC1*, disease in multiple organs. *Am J Hum Genet* 2001; **68**: 64–80.

13 Sancak O, Nellist M, Goedbloed M *et al*: Mutational analysis of the *TSC1* and *TSC2* genes in a diagnostic setting: genotype–phenotype correlations and comparison of diagnostic DNA techniques in tuberous sclerosis complex. *Eur J Hum Genet* 2005; **13**: 731–741.

14 Niida Y, Lawrence-Smith N, Banwell A *et al*: Analysis of both *TSC1* and *TSC2* for germline mutations in 126 unrelated patients with tuberous sclerosis. *Hum Mutat* 1999; **14**: 412–422.

15 Au K-S, Williams AT, Roach ES *et al*: Genotype/phenotype correlation in 325 individuals referred for a diagnosis of tuberous sclerosis complex in the United States. *Genet Med* 2007; **9**: 88–100.

16 Tuberous sclerosis database – Leiden Open Variation Database. [www.chromium.liacs.nl/lovd/index.php?select_db=TSC2].

17 NetGene2 Server. [www.cbs.dtu.dk/services/NetGene2].

18 SpliceSiteFinder. [www.genet.sickkids.on.ca/∼ali/splicesitefinder. html].

19 BDGP: Splice Site Prediction by Neural Network. [www.fruitfly. org/seq_tools/splice.html].

20 Nellist M, van Slegtenhorst MA, Goedbloed M *et al*: Characterization of the cytosolic tuberin–hamartin complex: tuberin is a cytosolic chaperone for hamartin. *J Biol Chem* 1999; **274**: 35647–35652.

21 van Slegtenhorst M, Nellist M, Nagelkerken B *et al*: Interaction between hamartin and tuberin, the *TSC1* and *TSC2* gene products. *Hum Mol Genet* 1998; **7**: 1053–1057.

22 Nellist M, Verhaaf B, Goedbloed MA *et al*: *TSC2* missense mutations inhibit tuberin phosphorylation and prevent formation of the tuberin-hamartin complex. *Hum Mol Genet* 2001; **10**: 2889–2898.

23 Jaeschke A, Hartkamp J, Saitoh M *et al*: Tuberous sclerosis complex tumor suppressor-mediated S6 kinase inhibition by phosphatidylinositide-3-OH kinase is mTOR independent. *J Cell Biol* 2002; **159**: 217–224.

24 Jansen FE, Braams O, Vincken KL *et al*: Overlapping neurologic and cognitive phenotypes in patients with *TSC1* or *TSC2* mutations. *Neurology* 2008; **70**: 908–915.

25 Lee-Jones L, Aligianis I, Davies PA *et al*: Sacrococcygeal chordomas in patients with tuberous sclerosis complex show somatic loss of *TSC1* or *TSC2*. *Genes Chromosomes Cancer* 2004; **41**: 80–85.

26 Goedbloed MA, Nellist M, Verhaaf B *et al*: Analysis of TSC2 stop codon variants found in tuberous sclerosis patients. *Eur J Hum Genet* 2001; **9**: 823–828.

27 Hodges AK, Li S, Maynard J *et al*: Pathological mutations in TSC1 and TSC2 disrupt the interaction between hamartin and tuberin. *Hum Mol Genet* 2001; **10**: 2899–2905.

28 Inoki K, Li Y, Zu T *et al*: TSC2 is phosphorylated and inhibited by Akt and suppresses mTOR signalling. *Nat Cell Biol* 2002; **4**: 648–657.

29 Young JM, Burley MW, Jeremiah SJ *et al*: A mutation screen of the TSC1 gene reveals 26 protein truncating and 1 splice site mutation in a panel of 79 tuberous sclerosis patients. *Ann Hum Genet* 1998; **62**: 203–213.

30 Dabora SL, Sigalas I, Hall F *et al*: Comprehensive mutation analysis of *TSC1* using two-dimensional electrophoresis with DGGE. *Ann Hum Genet* 1998; **62**: 491–504.

31 Pymar LS, Platt FM, Askham JM *et al*: Bladder tumour-derived somatic TSC1 missense mutations cause loss of function via distinct mechanisms. *Hum Mol Genet* 2008; **17**: 2006–2017.

Supplementary Information accompanies the paper on European Journal of Human Genetics website (http://www.nature.com/ejhg)

npg

ARTICLE

A reliable cell-based assay for testing unclassified *TSC2* gene variants

Ricardo Coevoets[1], Sermin Arican[1], Marianne Hoogeveen-Westerveld[1], Erik Simons[1], Ans van den Ouweland[1], Dicky Halley[1] and Mark Nellist*,[1]

[1]*Department of Clinical Genetics, Erasmus Medical Centre, Rotterdam, The Netherlands*

Tuberous sclerosis complex (TSC) is characterised by seizures, mental retardation and the development of hamartomas in a variety of organs and tissues. The disease is caused by mutations in either the *TSC1* gene or the *TSC2* gene. The *TSC1* and *TSC2* gene products, TSC1 and TSC2, form a protein complex that inhibits signal transduction to the downstream effectors of the mammalian target of rapamycin (mTOR). We have developed a straightforward, semiautomated in-cell western (ICW) assay to investigate the effects of amino acid changes on the TSC1–TSC2-dependent inhibition of mTOR activity. Using this assay, we have characterised 20 TSC2 variants identified in individuals with TSC or suspected of having the disease. In 12 cases, we concluded that the identified variant was pathogenic. The ICW is a rapid, reproducible assay, which can be applied to the characterisation of the effects of novel TSC2 variants on the activity of the TSC1–TSC2 complex.

Introduction

Tuberous sclerosis complex (TSC) is an autosomal dominant disorder characterised by seizures, mental retardation and the development of hamartomas in a variety of organs and tissues.[1] The disease is caused by mutations in either the *TSC1* gene on chromosome 9q34[2] or the *TSC2* gene on chromosome 16p13.3.[3] The *TSC1* and *TSC2* gene products, TSC1 and TSC2, form a protein complex that acts as a GTPase-activating protein (GAP) for the rheb GTPase, preventing the rheb-GTP-dependent stimulation of the mammalian target of rapamycin (mTOR).[4] In cells lacking either *TSC1* or *TSC2*, the downstream targets of mTOR, including p70 S6 kinase (S6K) and ribosomal protein S6, are constitutively phosphorylated.[5,6] The identification of the role of the TSC1–TSC2 complex in regulating mTOR has made it possible to compare the activity of different

TSC1 and TSC2 variants. The effects of amino acid changes on TSC1–TSC2 complex formation, on the activation of rheb GTPase activity, and on the phosphorylation status of the downstream effectors of mTOR, can be determined.[7]

Comprehensive screens for mutations at the *TSC1* and *TSC2* loci have been performed in large cohorts of TSC patients.[8–11] In most studies ∼20% of the identified mutations are either missense changes or small, in-frame insertions/deletions, predominantly in the *TSC2* gene. In some cases, when a missense change cosegregates with TSC, or when key relatives are not available for testing, it is difficult to establish whether the identified nucleotide change is a pathogenic mutation or a neutral variant. We identified a number of variants where it was not clear from the genetic data whether the identified variant was pathogenic or not.[10] To resolve some of these cases we tested the activity of the variant TSC1–TSC2 complexes using a variety of biochemical assays.[12]

To simplify and standardise the testing of TSC2 variants we have developed and tested an in-cell western (ICW) assay to determine whether specific *TSC2* sequence variants identified in individuals with, or suspected of having, TSC are disease

*Correspondence: Dr M Nellist, Department of Clinical Genetics, Erasmus Medical Centre, Dr Molewaterplein 50, 3015 GE Rotterdam, The Netherlands.
Tel: +31 10 7043357; Fax: +31 10 7049489;
E-mail: m.nellist@erasmusmc.nl*

causing. The ICW assay utilises secondary antibodies conjugated with near infrared fluorophores in combination with an infrared scanner enabling two distinct antibody signals to be detected simultaneously and quantified in fixed cells. The advantage of the ICW assay over immunoblot-based techniques is that no blotting step is required and the analysis and quantification can be performed directly in high-throughput multiwell plate formats. Therefore, the ICW assay streamlines both the experimental procedure and data analysis.

In-cell western assays to assess protein phosphorylation have been described previously.[13] However, in most reports, the effects of different pharmacological reagents have been monitored.[14] Here, we describe a transfection-based ICW assay to facilitate the characterisation of the effects of genetic changes in the *TSC2* gene on the activity of the TSC1–TSC2 complex and the mTOR signalling pathway. We have used this assay to characterise 20 TSC2 variants. Twelve variants (60%) did not inhibit mTOR activity in either the ICW assay or in a conventional immunoblot assay, and could therefore be classified as pathogenic mutations. Furthermore, we show that the ICW assay of TSC1–TSC2 function is amenable to the development of high-throughput, semiautomated protocols.

Materials and methods
Detection of TSC2 variants in TSC patients
Mutation analysis was performed as described previously[10] or by direct sequence analysis of all *TSC1* and *TSC2* coding exons and exon/intron boundaries. In addition, both genes were analysed using the multiplex ligation-dependent probe amplification assay (MRC Holland, Amsterdam, The Netherlands). Where possible, parental DNA was collected and tested for the presence of the identified variants and, in cases of *de novo* changes, paternity testing was performed. To investigate whether the identified sequence changes had an effect on splicing, three splice site prediction programs were used.[15–17]

Materials
Expression constructs encoding the 20 TSC2 variants (G62E, R98W, 275delN, Q373P, 580delASHATRVYEMLV-SHIQLHYKHSYTLP (hereafter referred to as 580del26), A607E, T1068I, T1075I, T1075T, V1199G, P1292A, S1410L, G1416D, D1512A, G1544V, 1553delTGLGR-LIELKDCQPDKVYL (hereafter referred to as 1553del19), H1617Y, V1623G, R1720Q and R1720W) were derived using the Stratagene QuikChange site-directed mutagenesis kit (Stratagene, La Jolla, CA, USA). Sequence changes were numbered according to the *TSC2* cDNA as originally published, as these corresponded to the cDNA used for the expression studies.[3] Nomenclature according to the *TSC2* mutation database[18] is given in Table 1.

All variants were verified by sequencing the complete *TSC2* cDNA open reading frame. All the other constructs used in this study have been described previously.[7,19,20] Polyclonal rabbit antisera specific for human TSC1 and TSC2 have been described previously.[19] Other antibodies were purchased from Cell Signaling Technology (Danvers, MA, USA) (1A5, anti-T389 phospho-S6K mouse monoclonal; 9B11, anti-myc tag mouse monoclonal; anti-myc tag

Table 1 Summary of the ICW-based functional characterisation of 20 TSC2 variants

Nucleotide change[a]	Amino acid change[a]	t-test vs wild-type[c]	t-test vs control[c]	Pathogenicity
203G>A (185G>A)	G62E	0.555398	**0.000106**	Unclassified
310C>T (292C>T)	R98W	**0.021536**	**0.013338**	Unclassified
842delACA (824delACA)	275delN	**0.001127**	0.475101	Pathogenic
1136A>C (1118A>C)	Q373P	0.278444	**0.000072**	Pathogenic[b]
1754del78 (1736del78)	580del26	**0.002041**	0.298704	Pathogenic
1838C>A (1820C>A)	A607E	**0.003675**	0.146591	Pathogenic
3221C>T (3203C>A)	T1068I	**0.000743**	0.622030	Pathogenic
3242C>T (3224C>T)	T1075I	0.658401	**0.000909**	Unclassified
3243C>T (3225C>T)	T1075T	0.184777	**0.000057**	Unclassified
3614T>G (3596T>G)	V1199G	**0.023734**	0.175070	Pathogenic
3892C>G (3943C>G)	P1292A (P1315A)	0.290908	**0.000063**	Unclassified
4247C>T (4298C>T)	S1410L (S1433L)	0.321151	**0.000192**	Unclassified
4265G>A (4316G>A)	G1416D (G1439D)	0.332362	**0.000246**	Unclassified
4553A>C (4604A>C)	D1512A (D1535A)	**0.000139**	0.811770	Pathogenic
4649C>T (4700C>T)	G1544V (G1567V)	**0.000316**	0.424123	Pathogenic
4675del57 (4726del57)	1553del19 (1576del19)	**0.032488**	0.641493	Pathogenic
4867C>T (4918C>T)	H1617Y (H1640Y)	**0.020428**	0.148090	Pathogenic
4886T>G (4937T>G)	V1623G (V1646G)	**0.039219**	0.347325	Pathogenic
5177G>A (5228G>A)	R1720Q (R1743Q)	**0.003169**	0.960154	Pathogenic
5176C>T (5227C>T)	R1720W (R1743W)	**0.017443**	0.521431	Pathogenic

[a]Nucleotide and amino acid numbering corresponding to reference.[3] Nucleotide and amino acid numbering corresponding to reference[18] are given in parentheses.
[b]Pathogenic *de novo* mutation, most likely causing aberrant splicing of the *TSC2* mRNA; the Q373P amino acid substitution did not affect TSC1–TSC2 complex function.
[c]P-values <0.05 are indicated in bold.

rabbit polyclonal), Zymed laboratories (San Francisco, CA, USA) (anti-TSC1 and anti-TSC2 mouse monoclonals) and Li-Cor Biosciences (Lincoln, NE, USA) (goat anti-rabbit 680 nm and goat anti-mouse 800 nm conjugates). Chemicals were from Merck (Darmstadt, Germany), unless specified otherwise.

Cell culture
Human embryonal kidney (HEK) 293T cells were grown in Dulbecco's modified Eagle's medium (DMEM) (Lonza, Verviers, Belgium) supplemented with 10% fetal bovine serum, 50 U/ml penicillin and 50 μg/ml streptomycin (DMEM +), in a 10% CO_2 humidified incubator.

Western blotting
Cells were seeded onto 24-well plates and transfected with 0.2 μg TSC2, 0.4 μg TSC1 and 0.1 μg S6Kmyc expression constructs using polyethyleneimine (PEI) (Polysciences Inc., Warrington, PA, USA). A 1:4 w/w mixture of plasmid DNA and PEI was incubated in 0.2 ml DMEM for 15 min at 20°C before adding to the cells. After 4 h, the DMEM/DNA/PEI was replaced with DMEM + . Twenty-four hours after transfection, the cells were transferred to ice, washed with phosphate-buffered saline (PBS) (4°C) and harvested in 50 μl lysis buffer (50 mM Tris-HCl pH 8.0, 150 mM NaCl, 50 mM NaF, 1% Triton X-100, protease inhibitor cocktail (Complete, Roche Molecular Biochemicals, Woerden, The Netherlands)). Cells were lysed for 10 min on ice before centrifugation (10 000 g for 10 min at 4°C). The supernatants were diluted in loading buffer, separated on 6% SDS-PAGE gels and transfered to nitrocellulose membranes, as described previously.[19] Membranes were blocked for 1 h at 20°C with 5% low-fat milk powder (Campina Melkunie, Eindhoven, The Netherlands) in PBS and incubated overnight at 4°C with the primary antibodies: 1/16 000 dilution of 1895 (rabbit polyclonal against TSC2[19]), 1/5000 dilution of 2197 (rabbit polyclonal against TSC1[19]), 1/5000 dilution of a rabbit polyclonal against the myc epitope tag and 1/2000 dilution of 1A5 (mouse monoclonal against p70 S6 kinase (S6K) phosphorylated at amino acid T389). Antibodies were diluted in blocking solution containing 0.1% Tween 20 (Sigma-Aldrich Fine Chemicals, Poole, UK). After washing 3 × for 5 min in PBS containing 0.1% Tween 20 (PBST), the membranes were incubated for 1 h at 20°C in the dark in PBST containing 1/5000 dilutions of goat anti-rabbit 680 nm and goat anti-mouse 800 nm secondary antibodies. After washing (3 × for 5 min in PBST, 1 × in PBS) the membranes were scanned using the Odyssey™ Infrared Imager (169 μm resolution, medium quality with 0 mm focus offset) (Li-Cor Biosciences, Lincoln, NE, USA). The integrated intensities of the protein bands were determined using the Odyssey™ software (default settings with background correction; 3 pixel width border average method).

ICW assays
Cells were seeded onto 96-well plates coated with 0.1 mg/ml poly-L-lysine (Sigma-Aldrich Fine Chemicals). Cells at 85–95% confluency were transfected with 0.1 μg TSC2, 0.2 μg TSC1 and 0.05 μg S6Kmyc expression constructs using PEI, as before. Each transfection mix was divided equally between three wells. After 4 h, the DMEM/DNA/PEI mixtures were replaced with DMEM + . ICW assays were performed 24 h after transfection. Cells were rinsed with PBS, fixed with freshly prepared 4% paraformaldehyde for 20 min at 20°C, washed 3 × for 5 min with PBS containing 0.1% Triton X-100 and incubated for 90 min in blocking solution before incubation overnight at 4°C with the primary antibodies. Three different primary antibody mixes were prepared: 1/200 dilution of mouse monoclonal anti-TSC2 antibody, 1/200 dilution of mouse monoclonal anti-TSC1 antibody and 1/200 dilution of 1A5 (S6K T389 phosphorylation-specific mouse monoclonal). The antibodies were diluted in blocking solution containing 0.1% Tween 20 and a 1/500 dilution of the rabbit polyclonal anti-myc antibody. Antibodies were diluted according to the manufacturer's recommendations and based on the results of calibration experiments (see Supplementary Figure 1).

After washing for 3 × for 5 min in PBST, the cells were incubated for 1 h at 20°C in the dark with a 1/500 dilution of goat anti-rabbit 680 nm and 1/500 dilution of goat anti-mouse 800 nm in PBST. After washing (4 × for 5 min in PBST) the plates were scanned using the Odyssey Infrared Imager (169 μm resolution, medium quality with 3 mm focus offset). The integrated intensities of the protein signals were determined using the Odyssey software (8.5 mm quantification grid with background correction; 3 pixel width border average method).

ICW assay automation
In-cell western assays were performed using a Tecan EVO200 liquid handling station (Tecan Benelux, Giessen, The Netherlands). Transfected cells were fixed as before, washed 3 × for 5 min with PBS containing 0.1% Triton X-100 and placed in the station for the subsequent incubation and wash steps. After aspiration of the wash buffer, the cells were incubated with blocking solution for 90 min followed by the primary antibody mixes for 8.5 h. After washing (3 × for 5 min with PBST), the cells were incubated for 5 h with the secondary antibodies and washed (3 × for 5 min with PBST; 1 × for 5 min with PBS). Finally the PBS was aspirated, and the plate removed for scanning on the Odyssey Infrared Imager, as before. All incubation steps were performed at 4°C in the dark.

Results
ICW assay for the analysis of TSC1-TSC2-mTOR signalling
To determine whether the ICW assay was suitable for the analysis of transfected HEK 293T cells, we compared S6K

T389 phosphorylation in cells expressing TSC1, S6K and either wild-type TSC2 or the TSC2 R611Q mutant. Control cells were transfected with the pcDNA3 expression vector alone (no *TSC2*, *TSC1* or *S6K* cDNA inserts) or were co-transfected with the TSC1 and S6K expression constructs only. A schematic of the 96-well plate is shown in Figure 1a, and the resulting scans are shown in Figure 1b. After subtraction of the background signals, the ratio of the TSC2, TSC1 or T389-phosphorylated S6K (T389) signal (green) to the total S6K signal (red) was determined (Figure 1c). S6K-T389 phosphorylation was reduced ∼2-fold in cells expressing wild-type TSC2, compared to either cells expressing the R611Q mutant or to cells without TSC2 expression. A similar reduction in S6K-T389 phosphorylation was observed when the protocol was modified for the Tecan EVO200 liquid handling station (Figure 1d).

ICW analysis of TSC2 variants
Next, we tested 20 TSC2 variants identified in our patient cohort, including three in-frame deletions (275delN, 580del26 and 1553del19), 17 missense changes (G62E, R98W, Q373P, A607E, T1068I, T1075I, V1199G, P1292A, S1410L, G1416D, D1512A, G1544V, H1617Y, V1623G, R1720Q and R1720W) and one silent change (T1075T). Two of the variants, R1720Q and R1720W, had previously been shown to be *de novo* changes occurring in sporadic TSC patients and, on this basis, were assumed to be pathogenic mutations.[10,18] In the other 18 cases, essential genetic and/or clinical data were unavailable and the identified variants could not be classified as either pathogenic or non-pathogenic. The positions of the variant amino acids are indicated in Figure 2.

All variants were analysed using the ICW assay in three independent experiments. The integrated intensities of the fluorescent signals were quantified using the Odyssey software and the signals for each TSC2 variant, and for TSC1 and T389-phosphorylated S6K in the presence of the different variants were determined relative to the total S6K signal in the same well. Subsequently, the degree of S6K-T389 phosphorylation in the presence of the different TSC2 variants, relative to wild-type TSC2, was determined.
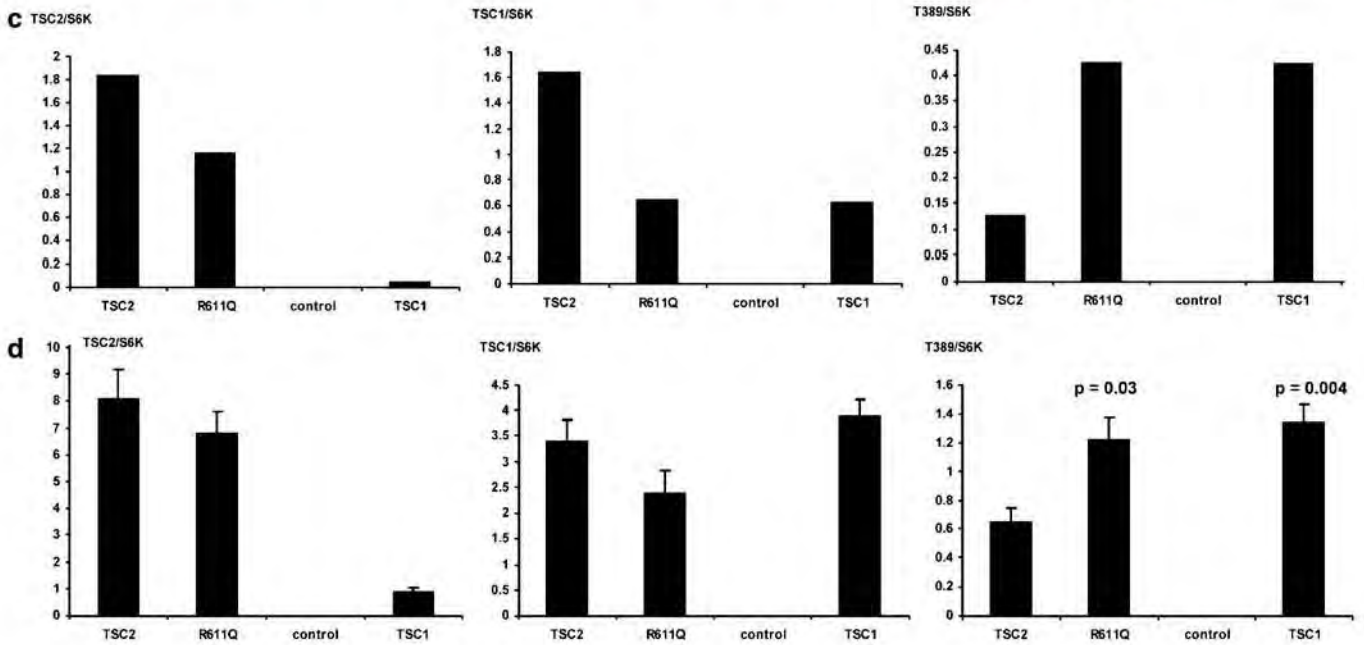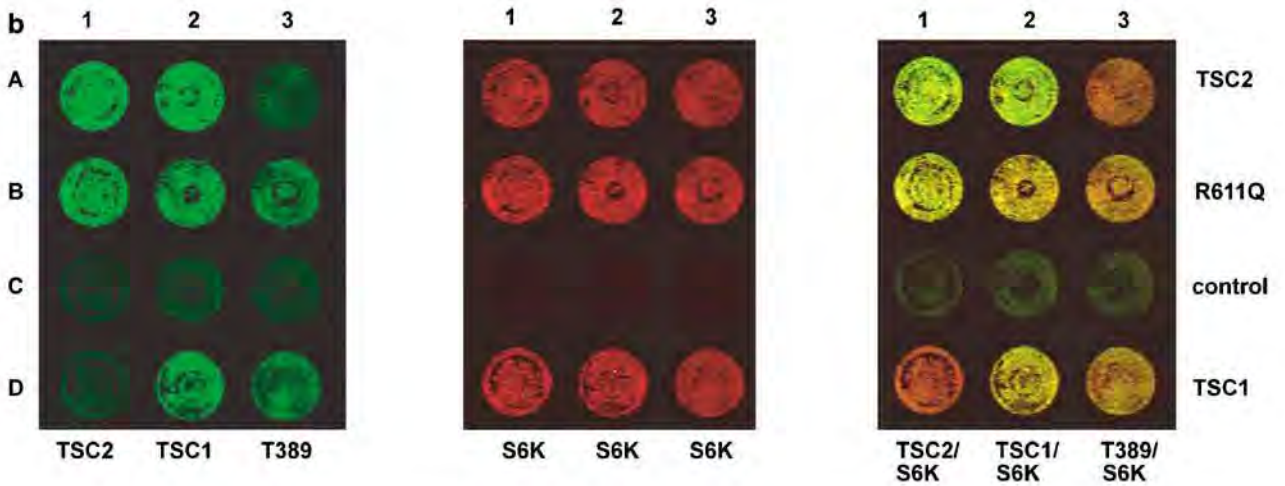
A representative scan is shown in Figure 3b. The total S6K signal was relatively constant across the different wells, indicating that inter-well differences in transfection efficiency and cell number were small. The signals for the different TSC2 variants were also relatively constant. None of the amino acid changes had a dramatic effect on the TSC2 signal, although a slight decrease was noted for the R611Q, 275delN, 580del26, A607E and V1623G variants. Similarly, the TSC1 signal was relatively constant, with only slight reductions in the presence of the TSC2 R611Q, 275delN, 580del26 and A607E variants. The T389 phosphorylation status of S6K was clearly dependent on the presence of the different TSC2 variants. TSC2-dependent inhibition of S6K-T389 phosphorylation was significantly reduced (ie, specific S6K T389 phosphorylation signal was increased compared to wild-type TSC2) in the presence of the R98W, 275delN, 580del26, A607E, T1068I, V1199G, D1512A, G1544V, 1553del19, H1617Y, V1623G, R1720Q and R1720W variants. As shown in Table 1, the T389/S6K ratio in the presence of these TSC2 variants was significantly different to the T389/S6K ratio in the presence of wild-type TSC2 (unpaired *t*-test $P<0.05$). Furthermore, in the presence of these variants, S6K T389 phosphorylation was comparable to T389 phosphorylation in the absence of TSC2 or in the presence of the TSC2 R611Q mutant (T389/S6K ratio was not significantly different from control: unpaired *t*-test $P>0.05$; Table 1). Only the R98W variant was significantly different from both the positive and negative controls (Figure 3 and Table 1). The G62E, Q373P, T1075I, T1075T, P1292A, S1410L and G1416D variants were as effective as wild-type TSC2 at inhibiting S6K T389 phosphorylation (T389/S6K ratio was not significantly different from wild-type TSC2: unpaired *t*-test $P>0.05$; T389/S6K ratio was significantly different from the T389/S6K ratio in the absence of TSC2: unpaired *t*-test $P<0.05$; Table 1).

Immunoblot analysis of the TSC2 variants
We analysed the effects of the TSC2 variants on mTOR activity by immunoblotting. In three independent experiments, the expression of TSC1 and the TSC2 variants, and the expression and T389 phosphorylation status of S6K

Figure 1 Optimisation of the ICW assay for analysis of TSC2 variants. (**a**) Schematic showing part of a 96-well cell culture plate. Cells in wells A1–A3 (row A) were transfected with expression constructs for wild-type TSC2, TSC1 and myc-tagged S6K (S6K); B1–B3 (row B) were transfected with expression constructs for the TSC2 R611Q variant, TSC1 and S6Kmyc; C1–C3 (row C) with vector only and D1–D3 (row D) with expression constructs for TSC1 and S6Kmyc only. A1–D1 (column 1) were probed with a monoclonal antibody specific for TSC2 (Zymed laboratories; green); A2–D2 (column 2) were probed with a monoclonal antibody specific for TSC1 (Zymed laboratories; green) and A3–D3 (column 3) were probed with a monoclonal antibody specific for T389-phosphorylated S6K (Cell Signaling Technology; green). All wells were probed with a polyclonal antibody specific for the S6K myc tag (Cell Signaling Technology; red). (**b**) Odyssey scans of the wells are shown in A, showing the 800 nm (green) channel (left), the 680 nm (red) channel (centre) and the merged image (right). The transfections in rows A, B and C are indicated on the right, the antibody signals revealed in columns 1, 2 and 3 are indicated below the scans. (**c**) Graphical representation of the scans is shown in B. The integrated intensities of the green and red fluorescent signals were determined using the Odyssey software. After subtraction of the background values (wells C1–C3; row C), the green:red ratio was calculated. (**d**) ICW assay using the Tecan EVO200 liquid handling station. Integrated intensities were determined and the green:red signal ratios calculated as in C for four separate transfection experiments. The mean TSC2/S6K, TSC1/S6K and T389/S6K ratios, and standard deviations are indicated. The mean T389/S6K ratio in the presence of wild-type TSC2 was significantly reduced compared to the TSC2 R611Q variant ($P=0.03$) and TSC1 only control ($P=0.004$).
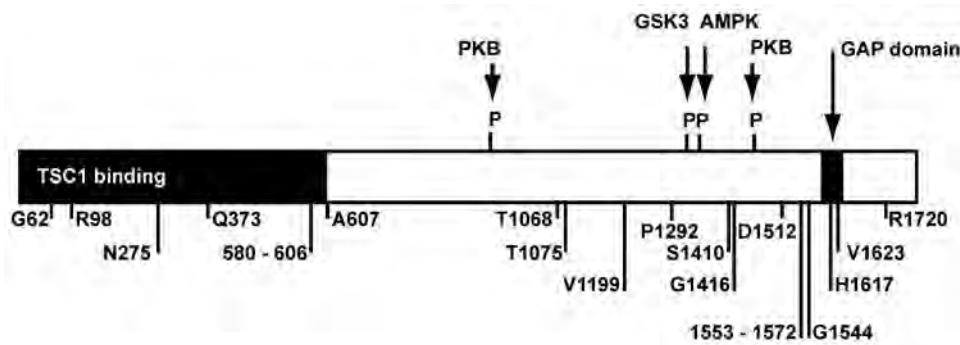
Figure 2 Schematic diagram of TSC2, showing the TSC1-binding and GAP domains, prominent sites of PKB, GSK3 and AMPK phosphorylation, and the positions of the variant amino acids tested in this study.

were determined (Figure 4). The results of the immunoblotting experiments were consistent with the ICW assays. Compared to wild-type TSC2 and the G62E, Q373P, T1075I, T1075T, P1292A, S1410L and G1416D variants, S6K T389 phosphorylation was increased in the presence of the R98W, 275delN, 580del26, A607E, T1068I, V1199G, D1512A, G1544V, 1553del19, H1617Y, V1623G, R1720Q and R1720W variants. The immunoblot data differed from the ICW data in that larger differences were detected in the signals of the different TSC2 variants, and in the TSC1 signal in the presence of the different TSC2 variants. The S6K signal was relatively constant, indicating that the observed differences were unlikely to be due to differences in cell number and transfection efficiency between the variants. Compared to wild-type TSC2, the signal for the R611Q variant was consistently reduced. In addition, the TSC1 signal was also reduced in the presence of the R611Q variant. Previous studies have demonstrated that the R611Q mutation disrupts the TSC1–TSC2 interaction, reducing the levels of TSC1 and TSC2 in cytosolic fractions.[20] A similar pattern was observed for the R98W, 275delN, 580del26 and A607E variants, indicating that these variants also have a reduced ability to interact with TSC1. The amino acids affected in these variants all map to regions of TSC2 that have previously been shown to be important for the TSC1–TSC2 interaction.[20–22]

Wild-type TSC2 was detected as a broad band on the immunoblots, consisting of 2–3 isoforms with slightly different migration characteristics. In contrast, some of the TSC2 variants appeared to migrate as a single band. This is most likely due to differences in the post-translational modification of the different variants.[7] We compared the phosphorylation status of the different variants using an antibody specific for TSC2 phosphorylated at the T1439 position. However, using this antibody, we did not observe any clear differences in TSC2-T1439 phosphorylation between wild-type TSC2 and the TSC2 variants (see Supplementary Figure 2).

Although the immunoblotting experiments supported the ICW data, the differences averaged over three inde-

pendent experiments were not always significant (unpaired t-test; Figure 4). Therefore, the ICW gave more consistent and reproducible data, and allowed us to classify the 20 variants as pathogenic or not in a relatively short period of time. The ICW required fewer manipulations than the immunoblot analysis and was always performed using the same 96-well grid. Variables such as the cell harvest and fractionation steps and the gel and buffer characteristics most likely resulted in more inter-experiment differences in the immunoblot assays. A comparison of the steps involved in the two techniques is shown in Figure 5.

The ICW assay indicated that the TSC2 275delN, 580del26, A607E, T1068I, V1199G, D1512A, G1544V, 1553del19, H1617Y, V1623G, R1720Q and R1720W variants were likely to be pathogenic, as they all disrupted the ability of the TSC1–TSC2 complex to inhibit mTOR activity. Immunoblot analysis confirmed that these 12 variants are inactive and therefore disease causing.

The G62E, Q373P, T1075I, T1075T, P1292A, S1410L and G1416D variants were indistinguishable from wild-type TSC2 in both the ICW and immunoblot assays. However, it was possible that the corresponding nucleotide changes could still be pathogenic through effects on TSC2 mRNA splicing. We analysed the nucleotide changes using three splice site prediction programs.[15–17] Only the 1136A>C (Q373P, TSC2 exon 10) substitution was predicted to affect splicing. Codon 373 is encoded by the last three nucleotides of TSC2 exon 10, and according to all three prediction programs, the 1136A>C substitution disrupts the exon 10 donor sequence, resulting in an aberrantly spliced TSC2 mRNA. We concluded that the 1136A>C (Q373P) variant was a pathogenic splice site mutation, and not a missense mutation. Subsequent genetic analysis of the parents of the TSC patient with the TSC2 1136A>C (Q373P) variant demonstrated that this was a de novo change. Paternity was also confirmed in this case (data not shown).

In contrast to the TSC2 variants discussed above, the R98W variant could not be classified as either pathogenic or non-pathogenic. This variant was able to inhibit S6K T389 phosphorylation in both the ICW and immunoblot
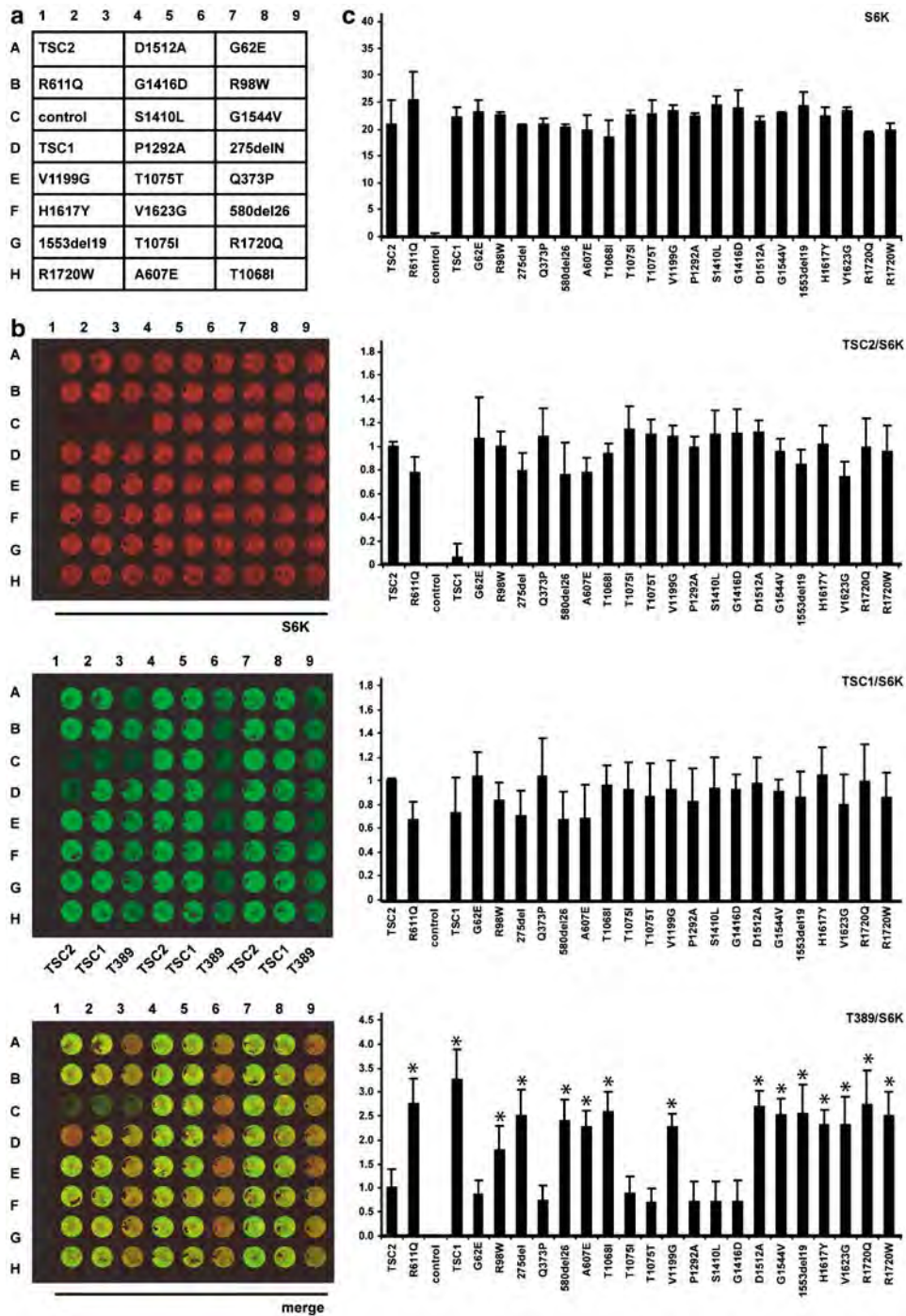
Figure 3 Characterisation of 20 TSC2 variants using the ICW assay. (**a**) Schematic showing part of a 96-well cell culture plate. Cells in wells A1–A3 (row A), B1–B3 (row B), C1–C3 (row C) and D1–D3 (row D) were transfected as before (see Figure 1). Cell in the remaining sets of three wells were transfected with expression constructs for the different TSC2 variants, TSC1 and S6Kmyc. All wells were probed with a polyclonal antibody specific for the S6K myc tag (red). Wells in columns 1, 4 and 7 were probed with a monoclonal antibody specific for TSC2 (green); wells in columns 2, 5 and 8 were probed with a monoclonal antibody specific for TSC1 (green) and wells in columns 3, 6 and 9 were probed with a monoclonal antibody specific for T389-phosphorylated S6K (green). (**b**) Odyssey scans of the wells are shown in (**a**). (**c**) Graphical representation of the results of three independent ICW assays. The integrated intensities of the green and red fluorescent signals were determined using the Odyssey software. In each case the background values, measured in wells C1–C3 (control), were subtracted from the integrated intensity. In the top graphic, the mean integrated intensity values for S6K are shown. In the three lower graphics, the expression of TSC2 and TSC1, and the T389 phosphorylation of S6K are indicated. To correct for inter-well differences in cell number and transfection efficiency, values are expressed relative to the total S6K signal. Standard deviations are indicated. TSC2 variants with a significantly different T389/S6K ratio than wild type ($P < 0.05$) are indicated with an asterisk.
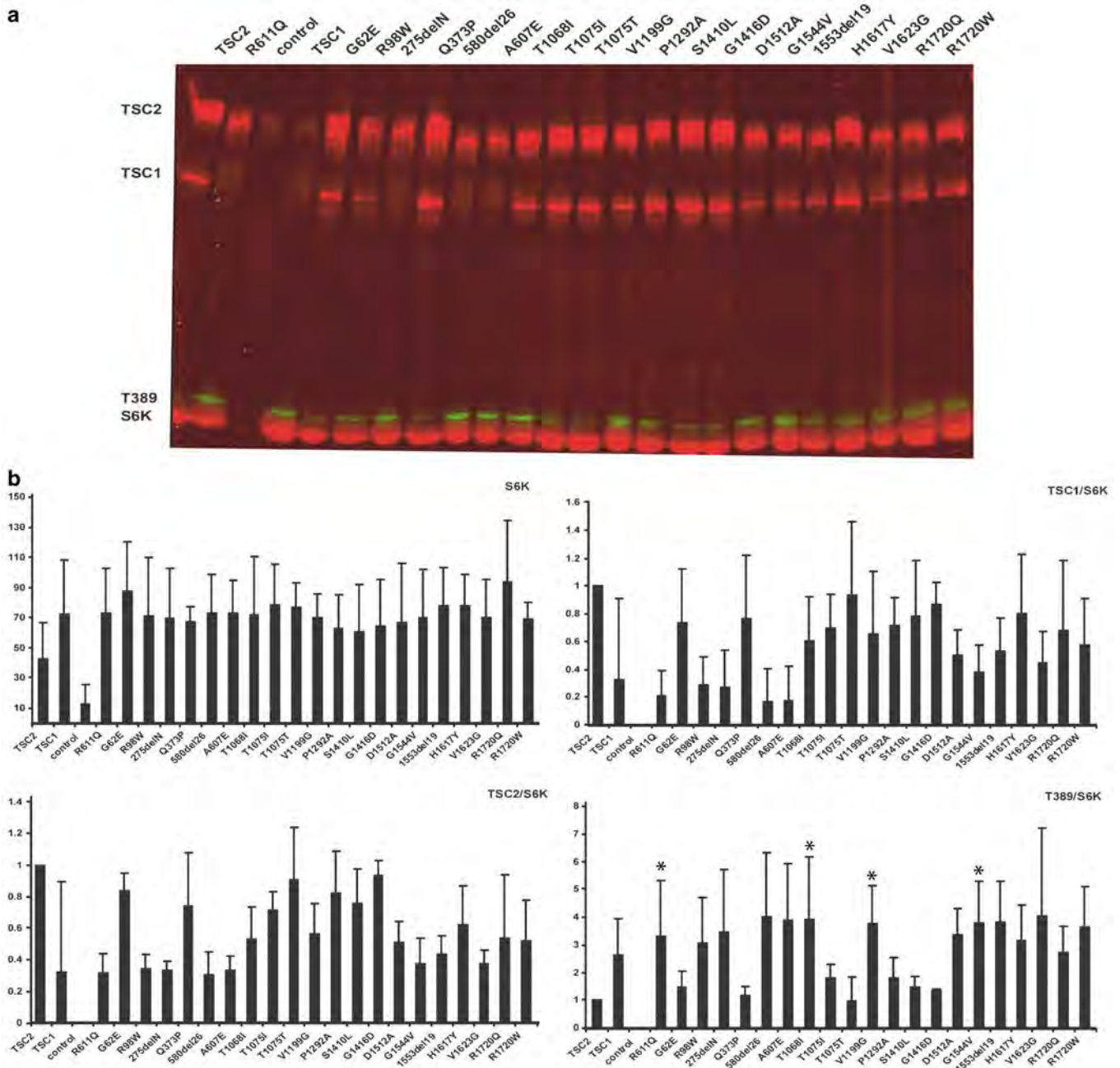
Figure 4 Characterisation of 20 TSC2 variants by immunoblot analysis. Cells co-transfected with expression constructs encoding TSC1, S6Kmyc and either wild-type TSC2 or one of the 20 TSC2 variants were harvested and cytosolic fractions separated on a 6% SDS-PAGE gel before transfer. Blots were probed with rabbit polyclonal antisera against TSC2, TSC1 and the myc epitope tag, and a mouse monoclonal against T389-phosphorylated S6K, followed by the Li-Cor goat anti-rabbit 800 and goat anti-mouse 680 secondary antibodies. (**a**) Representative scan of an immunoblot. Expression of the TSC2 variants, TSC1 and S6K (all red) and the T389 phosphorylation of S6K (green) are indicated. (**b**) Graphical representation of the results of three independent immunoblots. The integrated intensities of the green and red fluorescent signals were determined using the Odyssey software with background correction. In the top graphic, the mean values for S6K are shown. In the three lower graphics, the expression of TSC2 and TSC1, and the T389 phosphorylation of S6K are indicated. To correct for differences in cell number and transfection efficiency, values are expressed relative to the total S6K signal per lane. Standard deviations are indicated. TSC2 variants with a significantly different T389/S6K ratio than wild type ($P<0.05$) are indicated with an asterisk.
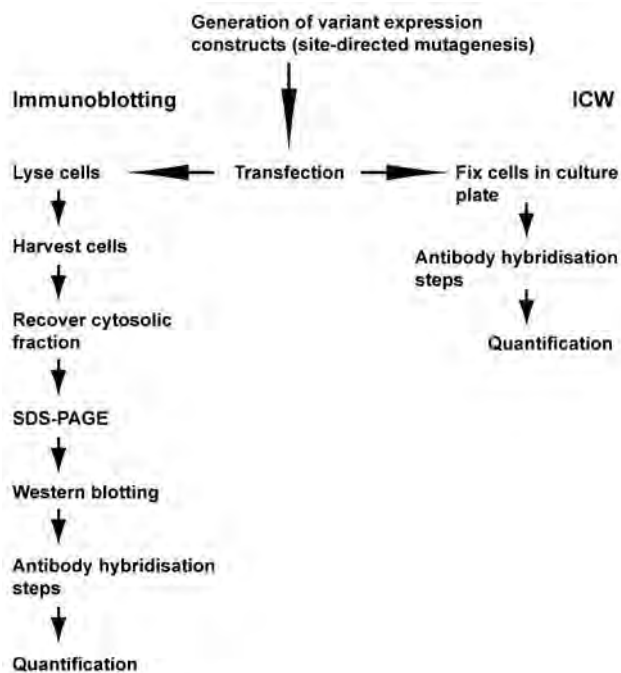
Figure 5 Flow diagram to show the steps involved in the ICW assay, compared to immunoblotting.
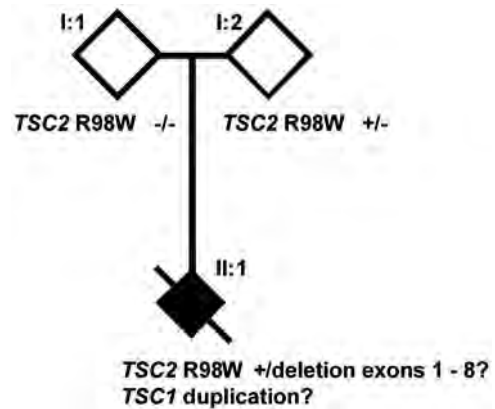

Figure 6 Pedigree showing inheritance of the TSC2 310 C>T (R98W) variant. Open symbols indicate no signs or symptoms of TSC; black symbol indicates definite TSC (diagnosed post-mortem). Genotypes, where known, are indicated.

assays, but was less effective than wild-type TSC2. On the immunoblots, the expression of the R98W variant was reduced compared to wild-type TSC2, and the expression of TSC1 was also consistently reduced in the presence of this variant. This suggests that the R98W substitution affects the TSC1–TSC2 interaction, and therefore reduces the ability of the complex to inhibit mTOR signalling.

As shown in Figure 6, the *TSC2* 310C>T (R98W) substitution was detected in a mother and a fetus. The fetus did not survive to term and was diagnosed with TSC post-mortem. No signs of TSC were reported in either parent. The mother was heterozygous for the *TSC2* 310C>T (R98W) variant, whereas the fetus appeared to be hemizygous for this variant as the wild-type allele was not detected and MLPA analysis of the fetal DNA indicated that there was a deletion of *TSC2* exons 1–8. MLPA analysis of the *TSC1* locus in the fetus suggested that there was also a duplication of the entire *TSC1* coding region. However, due to a lack of material, we were unable to confirm the MLPA data. Therefore, the clinical, genetic and functional data for this variant were all problematic and we were unable to determine for certain whether the R98W substitution disrupts the TSC1–TSC2 complex sufficiently to cause TSC. *TSC2* missense mutations with apparently mild phenotypic effects have been described previously,[23–25] and have been shown to affect TSC1–TSC2 function *in vitro*.[24,25] In the family shown in Figure 6, it seems most likely that the deletion of exons 1–8 at the *TSC2* locus

caused TSC in the fetus. We could not rule out the possibility that the TSC2 R98W substitution modifies the phenotype in this family.

Discussion

Mutation analysis of individuals with, or suspected of having, a genetic disease facilitates the diagnosis, treatment and genetic counselling of those individuals and their families. However, in some cases, it is not possible to determine from the genetic data whether an identified nucleotide change is disease causing. Functional analysis of the predicted protein variants provides an additional method for determining whether specific changes are pathogenic. Here, we show that the ICW assay is a robust and reproducible assay for the analysis of unclassified TSC2 variants and can complement standard DNA-based molecular diagnostics. We tested the activity of 20 different TSC2 variants and identified 12 pathogenic changes (275delN, 580del26, A607E, T1068I, V1199G, D1512A, G1544V, 1553del19, H1617Y, V1623G, R1720Q and R1720W), 7 neutral variants (G62E, Q373P, T1075I, T1075T, P1292A, S1410L and G1416D), and one variant (R98W) where the functional significance of the substitution was not clear.

Characterisation of the effects of different TSC2 amino acid changes on the TSC1–TSC2 complex will help provide insight into the structure and function of the complex. The N-terminal 769 amino acids of TSC2 are important for the TSC1–TSC2 interaction.[19,22] Four changes mapping to this domain (R98W, 275delN, 580del26 and A607E) reduced the levels of both TSC1 and TSC2 in cytosolic fractions. We did not observe any effect of either the G62E or Q373P substitutions, indicating that these residues are not critical for the TSC1–TSC2 interaction. We analysed seven TSC2

variants affecting amino acids close to the TSC2 GAP domain (amino acids 1593–1631)[3] (Figure 2). All of these changes prevented the TSC1–TSC2-dependent inhibition of mTOR signaling, indicating that residues within and flanking the reported GAP domain are essential for TSC2 activity.

The TSC is one of several diseases that are caused by mutations in genes involved in the mTOR signalling pathway.[26] The application of similar ICW assays to analyse unclassified variants in individuals with these diseases may also prove to be a useful adjunct to standard molecular genetic analysis.

References

1 Gomez M, Sampson J, Whittemore V (eds): *The Tuberous Sclerosis Complex*. Oxford, UK: Oxford University Press, 1999, pp 10–23.

2 van Slegtenhorst M, de Hoogt R, Hermans C *et al*: Identification of the tuberous sclerosis gene *TSC1* on chromosome 9q34. *Science* 1997; **277**: 805–808.

3 The European Chromosome 16 Tuberous Sclerosis Consortium: Identification and characterization of the tuberous sclerosis gene on chromosome 16. *Cell* 1993; **75**: 1305–1315.

4 Li Y, Corradetti MN, Inoki K, Guan K-L: TSC2: filling the GAP in the mTOR signaling pathway. *Trends Biochem Sci* 2004; **29**: 32–38.

5 Zhang H, Cicchetti G, Onda H *et al*: Loss of Tsc1/Tsc2 activates mTOR and disrupts PI3K-Akt signaling through downregulation of PDGFR. *J Clin Invest* 2003; **112**: 1223–1233.

6 Kwiatkowski DJ, Zhang H, Bandura JL *et al*: A mouse model of TSC1 reveals sex-dependent lethality from liver hemangiomas, and up-regulation of p70S6 kinase activity in *Tsc1* null cells. *Hum Mol Genet* 2001; **11**: 525–534.

7 Nellist M, Sancak O, Goedbloed MA *et al*: Distinct effects of single amino acid changes to tuberin on the function of the tuberin-hamartin complex. *Eur J Hum Genet* 2005; **13**: 59–68.

8 Jones AC, Shyamsundar MM, Thomas MW *et al*: Comprehensive mutation analysis of *TSC1* and *TSC2*, and phenotypic correlations in 150 families with tuberous sclerosis. *Am J Hum Genet* 1999; **64**: 1305–1315.

9 Dabora SL, Jozwiak S, Franz DN *et al*: Mutational analysis in a cohort of 224 tuberous sclerosis patients indicates increased severity of *TSC2*, compared with *TSC1*, disease in multiple organs. *Am J Hum Genet* 2001; **68**: 64–80.

10 Sancak O, Nellist M, Goedbloed M *et al*: Mutational analysis of the *TSC1* and *TSC2* genes in a diagnostic setting: genotype-phenotype correlations and comparison of diagnostic DNA techniques in tuberous sclerosis complex. *Eur J Hum Genet* 2005; **13**: 731–741.

11 Au K-S, Williams AT, Roach ES *et al*: Genotype/phenotype correlation in 325 individuals referred for a diagnosis of tuberous sclerosis complex in the United States. *Genet Med* 2007; **9**: 88–100.

12 Nellist M, Sancak O, Goedbloed M *et al*: Functional characterisation of the TSC1-TSC2 complex to assess multiple *TSC2* variants identified in single families affected by tuberous sclerosis complex. *BMC Med Genet* 2008; **9**: 10.

13 Wong SK: A 384-well cell-based phospho-ERK assay for dopamine D2 and D3 receptors. *Anal Biochem* 2004; **333**: 265–272.

14 Selkirk JV, Nottebaum LM, Ford IC *et al*: A novel cell-based assay for G-protein-coupled receptor-mediated cyclic adenosine monophosphate response element binding protein phosphorylation. *J Biomol Screen* 2006; **11**: 351–358.

15 NetGene2 Server. [www.cbs.dtu.dk/services/NetGene2].

16 SpliceSiteFinder. [www.genet.sickkids.on.ca/~ali/splicesitefinder.html].

17 BDGP. Splice Site Prediction by Neural Network [www.fruitfly.org/seq_tools/splice.html].

18 Tuberous sclerosis database—Leiden Open Variation Database. [www.chromium.liacs.nl/lovd/index.php?select_db = TSC2].

19 van Slegtenhorst M, Nellist M, Nagelkerken B *et al*: Interaction between hamartin and tuberin, the *TSC1* and *TSC2* gene products. *Hum Mol Genet* 1998; **7**: 1053–1057.

20 Nellist M, Verhaaf B, Goedbloed MA, Reuser AJJ, van den Ouweland AMW, Halley DJJ: *TSC2* missense mutations inhibit tuberin phosphorylation and prevent formation of the tuberin-hamartin complex. *Hum Mol Genet* 2001; **10**: 2889–2898.

21 Hodges A, Li S, Maynard J *et al*: Pathological mutations in TSC1 and TSC2 disrupt the interaction between hamartin and tuberin. *Hum Mol Genet* 2001; **10**: 2899–2905.

22 Li Y, Inoki K, Guan K-L: Biochemical and functional characterizations of small GTPase rheb and TSC2 GAP activity. *Mol Cell Biol* 2004; **24**: 7965–7975.

23 O'Conner SE, Kwiatkowski DJ, Roberts PS, Wollmann RL, Huttenlocher PR: A family with seizures and minor features of tuberous sclerosis and a novel TSC2 mutation. *Neurology* 2003; **61**: 409–412.

24 Mayer K, Goedbloed M, van Zijl K, Nellist M, Rott HD: Characterisation of a novel TSC2 missense mutation in the GAP related domain associated with minimal clinical manifestations of tuberous sclerosis. *J Med Genet* 2004; **41**: e64.

25 Jansen A, Sancak O, D'Agostino D *et al*: Mild form of tuberous sclerosis complex is associated with TSC2 R905Q mutation. *Ann Neurol* 2006; **60**: 528–539.

26 Inoki K, Corradetti MN, Guan K-L: Dysregulation of the TSC-mTOR pathway in human disease. *Nat Genet* 2005; **37**: 19–24.

Supplementary Information accompanies the paper on European Journal of Human Genetics website (http://www.nature.com/ejhg)

Title page:

Identification of a region required for TSC1 stability by functional analysis of *TSC1* missense mutations identified in individuals with tuberous sclerosis complex

Melika Mozaffari[1], Marianne Hoogeveen-Westerveld[1], David Kwiatkowski[2], Julian Sampson[3], Rosemary Ekong[4], Sue Povey[4], Ans van den Ouweland[1], Dicky Halley[1] and Mark Nellist[1,5]

[1] Department of Clinical Genetics, Erasmus Medical Centre, 3015 GE Rotterdam, The Netherlands.

[2] Division of Experimental Medicine and Medical Oncology, Brigham and Womens Hospital, Boston MA 02115, United States of America.

[3] Institute of Medical Genetics, University of Wales College of Medicine, Heath Park, Cardiff CF4 4XN, United Kingdom.

[4] MRC Human Biochemical Genetics Unit, University College London, London, United Kingdom.

[5] To whom correspondence should be addressed: Dr. Mark Nellist, Department of Clinical Genetics, Erasmus Medical Centre, Dr. Molewaterplein 50, 3015 GE Rotterdam, The Netherlands, Tel: +31 10 7043357; Fax: +31 10 7044736; email: m.nellist@erasmusmc.nl

Running title: Functional analysis of TSC1 variants

Abstract

Tuberous sclerosis complex (TSC) is an autosomal dominant disorder characterised by the development of hamartomas in a variety of organs and tissues. The disease is caused by mutations in either the *TSC1* gene on chromosome 9q34, or the *TSC2* gene on chromosome 16p13.3. The *TSC1* and *TSC2* gene products, TSC1 and TSC2, form a protein complex that inhibits signal transduction to the downstream effectors of the mammalian target of rapamycin (mTOR). Here we investigate the effects of *TSC1* missense mutations on TSC1 function and identify specific amino acid substitutions in the N-terminal region of TSC1 that result in proteosome-mediated degradation of TSC1, reducing steady state levels of the protein and leading to increased mTOR signalling. Our results suggest that the N-terminal region of TSC1 is important for either binding TSC2, or for the intracellular localisation of the TSC1-TSC2 complex.

Keywords: tuberous sclerosis complex, TSC1, TSC2

Introduction

Tuberous sclerosis complex (TSC) is an autosomal dominant disorder characterised by the development of hamartomas in a variety of organs and tissues, including the brain, skin and kidneys[1,2]. Mutations in either the *TSC1* gene on chromosome 9q34[3], or the *TSC2* gene on chromosome 16p13.3[4] cause TSC. In most studies, 75 - 85% of individuals with TSC have been shown to carry a germ-line *TSC1* or *TSC2* mutation[5-9]. In 5-10% of individuals with TSC, *TSC1* or *TSC2* variants are identified where it is not absolutely clear from the genetic data whether the change is disease-causing (a pathogenic variant), or not (a neutral variant). To determine whether these unclassified variants (UVs) are disease-causing, the effect of the changes on protein function can be investigated[10, 11,].

The *TSC1* and *TSC2* gene products, TSC1 and TSC2, interact to form a protein complex[12]. TSC2 contains a GTPase activating protein (GAP) domain and acts on the rheb GTPase to inhibit rheb-GTP-dependent stimulation of the mammalian target of rapamycin (mTOR)[13]. The exact role of TSC1 in the TSC1-TSC2 complex is less clear, but it appears to be required for maintaining the stability, activity and correct intracellular localisation of the complex[14]. Inactivation of the TSC1-TSC2 complex results in activation of mTOR and phosphorylation of the mTOR targets p70 S6 kinase (S6K) and 4E-BP1[15]. The effects of amino acid changes to TSC1 or TSC2 on TSC1-TSC2 complex formation, on the activation of rheb GTPase activity by the complex, and on the phosphorylation status of S6K and S6 can be determined[10, 11, 16]. Pathogenic missense changes towards the N-terminus of TSC2 prevent formation of the TSC1-TSC2 complex, while missense changes towards the C-terminus do not prevent TSC1-TSC2 binding but disrupt the rhebGAP activity of TSC2 directly[10]. Pathogenic TSC1

missense changes are rare[5-9]. However, recent studies of TSC1 missense variants identified in bladder cancers[17] and in patients with TSC[11] have shown that TSC1 amino acid substitutions can be pathogenic, reducing steady state levels of TSC1 and leading to increased mTOR activity.

Here, we test an additional 13 unclassified *TSC1* variants from the LOVD *TSC1* mutation database[18]. Our analysis confirms that *TSC1* missense mutations reduce steady state levels of TSC1, and result in increased mTOR signalling. Furthermore, we find that the intracellular localisation of pathogenic and neutral TSC1 variants is distinct. The variants we classified as pathogenic are clustered within the conserved, hydrophobic N-terminal region of TSC1, indicating that this region plays an important role in TSC1 function.

Materials and Methods

Comparative analysis of TSC1 amino acid substitutions

TSC1 variants identified in individuals with TSC, or suspected of having TSC, and submitted to the LOVD TSC mutation database[18] were chosen for analysis. To predict whether the variants were likely to be pathogenic, a multiple sequence alignment analysis was performed using SIFT software[19-20]. Hydrophobicity plots and secondary structure predictions were generated using DNAMAN (Lynnon BioSoft), SABLE[21] and PSIPRED[22] software. To determine whether the identified changes were likely to have an effect on splicing, 3 different splice-site prediction programs were used[23-25].

Generation of constructs and antisera

Expression constructs encoding myc-tagged TSC1 variants were derived using the QuikChange site-directed mutagenesis kit (Stratagene, La Jolla, CA, U.S.A.). In

each case the complete open reading frame of the mutated construct was verified by sequence analysis. Other constructs used in this study have been described previously[10, 11]. Antibodies were purchased from Cell Signaling Technology (Danvers, MA, U.S.A.), except for a mouse monoclonal antibody against TSC2 which was purchased from Zymed Laboratories (San Francisco, CA, U.S.A.).

Functional analysis of TSC1 variants

Immunoblot analysis of S6K T389 phosphorylation in cells over-expressing TSC1 variants. HEK 293T cells were transfected with a 4:2:1 mixture of the TSC1, TSC2 and S6K expression constructs. A total of 0.7 μg DNA was diluted in 50 μl Dulbecco's modified Eagle medium (DMEM) containing 2.1 μg polyethyleneimine (Polysciences, Warrington, PA, U.S.A.). Where necessary, an empty expression vector (pcDNA3; Invitrogen, Carlsbad, CA, U.S.A.) was added to make up the total amount of DNA. After 15 minutes at room temperature the DNA/polyethyleneimine complexes were added to 80% confluent cells in 24-well cell culture dishes. After 4 hours at 37°C the transfection mixture was replaced with DMEM containing 10% foetal calf serum. Twenty-four hours after transfection the cells were transferred to ice, the culture medium was removed and the cells were washed briefly with cold PBS. The washed cells were lysed by the addition of 75 μl lysis buffer containing 50 mM Tris-HCl pH 8.0, 150 mM NaCl, 50 mM NaF, 1% Triton X100 and a protease inhibitor cocktail (Complete, Roche Molecular Biochemicals, Woerden, The Netherlands). The lysates were cleared by centrifugation (10 000 g, 10 minutes, 4°C) and the supernatant and pellet fractions recovered for immunoblot analysis. The pellet fractions were resuspended in 100 μl sample buffer (62.5 mM Tris-HCl pH 6.8, 10% glycerol, 300 mM 2-mercaptoethanol, 2% SDS) and sonicated (8μm, 15 seconds, 4°C) prior to gel

electrophoresis. Samples were run on 4-12 % SDS-PAGE Criterion gradient gels (BioRad, Hercules, CA, U.S.A.) and blotted onto nitrocellulose. Blots were analysed using near infra-red fluorescent detection on an Odyssey[TM] Infrared Imager (169 μm resolution, medium quality with 0 mm focus offset) (Li-Cor Biosciences, Lincoln, NE, U.S.A.). The integrated intensities of the protein bands relative to the wild-type TSC1 values were determined in at least 3 separate experiments using the Odyssey[TM] software (default settings with background correction; 3 pixel width border average method). Signal intensities were compared as described previously[26].

Proteosome-mediated degradation of TSC1 variants. HEK 293T cells were transfected with expression constructs encoding TSC2, S6K and the different TSC1 variants. Twenty-four hours after transfection the culture medium was replaced with DMEM containing either 42 μM MG-132 (Sigma-Aldrich, St. Louis, MO, U.S.A.) or vehicle control. After 4 hours, insulin (200 nM; Sigma-Aldrich) or vehicle control was added to the culture medium and, after a further 30 minute incubation, the cells were harvested and analysed by immunoblotting, as before.

Immunofluorescent detection of TSC1 variants. HEK 293T cells were seeded onto glass coverslides coated with poly-L-lysine (Sigma-Aldrich). Twenty-four hours later the cells were transfected with expression constructs encoding TSC2 and/or the TSC1 variants. Twenty-four hours after transfection, the cells were processed for immunofluorescent microscopy as described previously[12]. Fixed, permeabilised cells were incubated with a rabbit polyclonal antibody specific for TSC2[12] and a mouse monoclonal antibody specific for the TSC1 C-terminal myc epitope tag (9B11, Cell Signaling Technology), followed by fluorescein isothiocyanate- and Cy3-coupled

secondary antibodies against mouse and rabbit immunoglobulins (DAKO, Carpinteria, CA, U.S.A.) respectively. Cells were studied using a Leica DM RXA microscope and Image Pro-Plus version 6 image analysis software.

Results

Comparative analysis of TSC1 amino acid substitutions

We searched the LOVD database[18] for unclassified *TSC1* missense variants and selected 13 amino acid substitutions that were either likely to be pathogenic changes, or could not be excluded as neutral variants (Table 1). In this group there was a single confirmed *de novo* change, *TSC1* c.182T>C (p.L61P), that was very likely to be pathogenic and a recurrent substitution, c.568C>T (p.R190C), that was very likely to be a neutral variant. This variant was of particular interest as a different substitution at the same codon c.569G>C (p.R190P) was reported as possibly pathogenic. In one individual with TSC, 2 *TSC1* missense changes, c.149T>C (p.L50P) and c.2420T>C (p.I807T), were reported. To establish whether either of these changes was responsible for TSC, or whether the combination of both changes was required to inactivate TSC1, we analysed a L50P-I807T double variant as well as the L50P and I807T single variants.

To predict whether the amino acid substitutions were likely to be pathogenic, we performed a SIFT analysis using a multiple sequence alignment of TSC1 derived from 14 different species (human, chimpanzee, macacca, cow, dog, horse, mouse, rat, chicken, pufferfish, honey bee, fruitfly, mosquito and fission yeast). The results of this analysis are shown in Figure 1 and Table 1. Overall, the N-terminal (amino acids 1 - 270) and C-terminal (amino acids 680 - 1164) regions of TSC1 were intolerant of amino acid substitutions while the central region (amino acids 270 - 680) was predicted to be

more tolerant. Of the 13 substitutions selected for this study, 7 were predicted to be tolerated and therefore unlikely to be pathogenic, while 6 were predicted not to be tolerated and therefore likely to be pathogenic (Table 1).

Splice site prediction analysis of the *TSC1* nucleotide changes was performed using 3 independent splice site prediction programs. Neither NetGene2[23] nor Human Splicing Finder[25] predicted any splicing defects for any of the 13 changes. In contrast, NNSPLICE 0.9[24] predicted that the *TSC1* c.1433A>G (p.E478G) change would result in a splice donor site 6 nucleotides downstream of the wild-type exon 14 donor site being preferred to the wild-type donor site. The wild-type site was no longer recognised as a splice donor site by the NNSPLICE site prediction program. Consequently, in addition to the E478G substitution, the creation of a new splice donor site by the *TSC1* c.1433A>G change resulted in the insertion of 2 extra codons (encoding amino acids GN) between TSC1 codons 479 and 480.

Functional analysis of TSC1 amino acid substitutions

We characterised the effects of the 13 TSC1 single missense variants and the 2 double missense variants on the activity of the TSC1-TSC2 complex. We compared the 15 variants to wild-type TSC1 and the TSC1-L117P pathogenic variant[11]. As shown in Figure 2, the L50P, L61P, L93R, V133F and R190P amino acid substitutions all resulted in reduced levels of TSC1 and increased mTOR activity, as estimated by the T389 phosphorylation status of S6K, the mTOR substrate. We did not observe any differences between the L50P variant and the L50P/I807T double variant. The L50P, L61P, L93R, V133F and R190P amino acid substitutions all had the same effect on TSC1 as the previously-characterised L117P variant. Furthermore, in each case the

T389/S6K ratio was significantly different to wild-type TSC1 (unpaired t-test $p <$ 0.05; see Table 1).

The E51D, R190C, S334L, E478G, Q550E, D658E, A659V and I807T variants were detected at comparable levels to wild-type TSC1 and S6K T389 phosphorylation was reduced to the same levels as in the presence of wild-type TSC1. In each case there was no significance difference in the T389/S6K ratio compared to wild-type TSC1 (unpaired t-test $p >$ 0.05; see Table 1).

TSC1 variants are degraded by the proteosome

We considered two possible reasons for why the TSC1 L50P, L61P, L93R, V133F and R190P variants were detected at low levels. One possibility was that the variants were insoluble and therefore not present in the cell lysate fraction analysed by immunoblotting. We analysed the insoluble post cell lysis pellet fractions, but did not detect any of the TSC1 variants in these fractions (data not shown).

The second possibility was that the L50P, L61P, L93R, V133F and R190P variants were subject to rapid turn-over and degradation. To investigate this possibility we treated cells expressing wild-type TSC1 or the L50P or L117P variants with the proteosome-inhibitor MG-132[27]. After 4 hours treatment we observed an increase in the levels of the L50P and L117P variants compared to wild-type TSC1, as shown in Figure 3. Next, we investigated whether the reduced turn-over of these variants caused by the inhibition of proteosome activity affected the TSC1-TSC2-dependent inhibition of mTOR signalling. We stimulated MG-132 treated cells with 200 nM insulin for 30 minutes and estimated mTOR activity by measuring the T389 phosphorylation status of S6K. As shown in Figure 3, treatment of the cells expressing the L50P and L117P variants with MG-132 resulted in increased S6K phosphorylation in both insulin-

stimulated and unstimulated cells. The same treatment did not affect S6K

phosphorylation in stimulated or unstimulated cells expressing wild-type TSC1 (Figure

3).

Intracellular localisation of the pathogenic variants

A shown in Figure 4, exogenous expression of the TSC1 E51D variant resulted

in the formation of large, cytoplasmic TSC1 protein aggregates, consistent with

previous results with wild-type TSC1[28]. Coexpression of TSC2 resulted in a reduction

in the number of aggregates, and both TSC2 and the TSC1 E51D variant were detected

throughout the cell cytoplasm. We compared the intracellular localisation of the TSC1

L50P, L61P, L93R, V133F and R190P variants to wild-type TSC1. As shown in Figure

4, the TSC1 L50P variant did not form large cytoplasmic aggregates, but was expressed

relatively uniformly throughout the cell cytoplasm. This localisation was unaffected by

coexpression of TSC2. The intracellular localisation patterns of the L61P, L93R, V133F

and R190P variants were indistinguishable from the L50P variant (data not shown).

We did not observe any differences in localisation between wild-type TSC1 and

the E51D, R190C, S334L, E478G, Q550E, D658E, A659V and I807T variants by

immunofluorescent microscopy.

Discussion

We investigated the effects of 13 putative pathogenic amino acid substitutions

on TSC1 function. Our findings are summarised in Table 1. The TSC1 L50P, L61P,

L93R, V133F and R190P changes resulted in reduced levels of TSC1, a reduction in the

TSC1-TSC2-dependent inhibition of mTOR activity and an altered intracellular

expression pattern compared to wild-type TSC1. In contrast, the E51D, R190C, S334L,

E478G, Q550E, D658E, A659V and I807T substitutions did not differ significantly from TSC1 in our assays. We concluded that the L50P, L61P, L93R, V133F and R190P changes were pathogenic and that the E51D, R190C, S334L, E478G, Q550E, D658E, A659V and I807T amino acid substitutions were most likely neutral TSC1 variants. Splice site prediction analysis did not reveal any evidence for aberrant splicing, except for the c.1433A>G (E478G) variant. Therefore, more work is required to determine whether this is a pathogenic splice site mutation and we are currently investigating whether the predicted splice product of this variant leads to expression of a functional TSC1 variant. We did not identify any predicted effects on *TSC1* splicing for any of the other nucleotide changes. Therefore we concluded that the c.149T>C (p.L50P), c.182T>C (p.L61P), c.278T>G (p.L93R), c.397G>T (p.V133F) and c.569G>C (p.R190P) substitutions are pathogenic missense mutations, and the c.153A>C (p.E51D), c.568C>T (p.R190C), c.1001C>T (p.S334L), c.1648C>G (p.Q550E), c.1974C>G (p.D658E), c.1976C>T (p.A659V) and c.2420T>C (p.I807T) substitutions are neutral variants. During subsequent, additional mutation screening in the Rotterdam cohort, TSC patients with the c.153A>C (p.E51D), c.568C>T (p.R190C) and c.1001C>T (p.S334L) substitutions were identified. In each case, a definite pathogenic *TSC2* mutation was identified (data not shown).

All of the amino acid substitutions that affected TSC1 function in our assays were in the N-terminal region of TSC1 shown by SIFT analysis to be relatively intolerant of amino acid changes. For each of these substitutions the results of the functional analysis were consistent with the SIFT prediction. According to the LOVD mutation database the L61P and L93R substitutions are probably pathogenic[18]. Our functional analysis supports this conclusion. The L50P, V133F and R190P substitutions are classified as unknown in the database. Our data indicates that these changes are also

probably pathogenic. Two amino acid substitutions from the substitution-intolerant N-terminal region, E51D and R190C, did not affect TSC1 function in our assays. Both aspartate (E) and glutamate (D) are acidic amino acids and the SIFT analysis predicted that the E51D substitution should be tolerated, which may be expected for a like-for-like substitution. In contrast, according to the SIFT analysis, the R190C substitution was not tolerated. However, this change has been identified in several individuals without TSC and is classified as having no known pathogenicity by the LOVD mutation database[18]. Furthermore, the R190C variant was indistinguishable from wild-type TSC1 in our assays, indicating that the SIFT prediction is inaccurate for this particular amino acid substitution. More generally, this result demonstrates that a conclusion with respect to pathogenicity should not be made based on *in silico* analysis only. Comparison of the TSC1 R190C and R190P variants reveals that different substitutions at the same amino acid codon can have distinct effects on protein function. In this case, either the basic charges of the arginine (R pKa = 12.48) or cysteine (C pKa = 8.35) residues are essential for TSC1 function, or the aliphatic proline (P) residue disrupts the native conformation of TSC1.

In addition to the E51D and R190C substitutions, 6 other TSC1 amino acid substitutions did not affect TSC1 function in our assays. Of these, 5 were within the substitution-tolerant central region of TSC1 (amino acids 270 - 680) defined by the SIFT analysis (Figure 1). The remaining change (I807T) was outside this region, but was also predicted to be tolerated. According to the LOVD mutation database the S334L, D658E and A659V substitutions are probably not pathogenic. Our data support this conclusion and, in addition, indicate that the Q550E and I807T substitutions are also unlikely to be pathogenic. Although the E478G substitution is unlikely to be pathogenic, splice site analysis indicated that the c.1433A>G nucleotide change may

influence splicing of the TSC1 gene and therefore may be a pathogenic splice site mutation. Unfortunately we did not have access to RNA from this particular individual, so were unable to investigate this possibility further.

To gain more insight into the effects of the pathogenic amino acid substitutions on TSC1 function we compared the predicted characteristics and secondary structure of wild-type and variant TSC1 isoforms with variants analysed as part of other studies[11, 18]. With one exception (R190P), all the pathogenic changes identified to date replaced a hydrophobic residue (L, V, M) with either a basic amino acid (R, H), proline (P) or phenylalanine (F), resulting in a reduction in hydrophobicity around the site of the substitution (Figure 5A). One possibility is that this domain mediates an important inter- or intramolecular interaction. Alternatively, it may play a role in the proposed membrane localisation of TSC1[29].

Although the pathogenic R190P change increases the hydrophobicity of the amino acid chain compared to wild-type TSC1, the neutral R190C change increases the hydrophobicity even more, indicating that at this residue, hydrophobicity is probably not the most critical characteristic of the protein chain. In contrast to the pathogenic amino acid substitutions, substitutions that did not affect TSC1 function did not have a consistent effect on the TSC1 hydrophobicity profile (Figure 5B).

The L50P, L61P, L93R, V133F and R190P variants were detected at lower levels compared to wild-type TSC1 and the E51D, R190C, S334L, Q550E, D658E, A659V and I807T variants. Inhibition of proteosome-mediated protein turnover using MG-132 resulted in increased expression of the L50P and L117P variants, indicating that the pathogenic TSC1 variants were rapidly degraded by the proteosome. Interestingly, increasing the levels of the TSC1 L50P and L93R variants by inhibiting proteosome activity resulted in an increase in mTOR activity, as measured by the extent

of S6K T389 phosphorylation. This suggests that the proteosome-mediated degradation of pathogenic TSC1 variants may be an important mechanism for preventing dominant negative effects of these mutant proteins on mTOR signalling.

Mutation analysis of the *TSC1* and *TSC2* genes in individuals with TSC, and in those suspected of having the disease is important for diagnosis and genetic counselling. However, in a significant minority of TSC patients, UVs are identified. For these individuals and their families considerable uncertainty can remain about, for example, the recurrence risk. Functional assays can help indicate whether these UVs are pathogenic or not. Here we have analysed 13 *TSC1* UVs predicted to cause missense changes to the TSC1 protein and identified 5 pathogenic changes. Several studies indicate that *TSC1* mutations are associated with a less severe clinical presentation in TSC patients[7-9] and it will be interesting to determine whether patients with a *TSC1* missense mutation have a distinct phenotypic spectrum from other TSC patients.

Here we show how the use of functional assays to differentiate between neutral and pathogenic variants facilitates the identification of pathogenic mutations in individuals with TSC and provides insight into how specific amino acid residues contribute to protein function.

Summary

Amino acid changes to the hydrophobic N-terminal region of TSC1 increase proteosome-mediated TSC1 degradation, reducing steady state levels of the protein and resulting in inceased signalling through mTOR.

Rapid degradation of the mutant TSC1 isoforms is necessary as increasing the levels of the mutant variants resulted in a dominant negative effect on the TSC1-TSC2 dependent inhibition of mTOR signalling.

Acknowledgments

References

1.	Gomez M, Sampson J, Whittemore V, eds. *The tuberous sclerosis complex*. Oxford University Press, Oxford, UK, 1999.

2.	Roach ES, DiMario FJ, Kandt RS *et al:* Tuberous sclerosis consensus conference: recommendations for diagnostic evaluation. National Tuberous Sclerosis Association. *J Child Neurol* 1999; **14**: 401-407.

3.	van Slegtenhorst M, de Hoogt R, Hermans C *et al*. Identification of the tuberous sclerosis gene *TSC1* on chromosome 9q34. *Science* 1997; **277**: 805-808.

4.	The European Chromosome 16 Tuberous Sclerosis Consortium. Identification and characterization of the tuberous sclerosis gene on chromosome 16. *Cell* 1993; **75**:1305-1315.

5.	Jones AC, Shyamsundar MM, Thomas MW *et al:* Comprehensive mutation analysis of *TSC1* and *TSC2*, and phenotypic correlations in 150 families with tuberous sclerosis. *Am J Hum Genet* 1999; **64**: 1305-1315.

6.	Dabora SL, Jozwiak S, Franz DN *et al:* Mutational analysis in a cohort of 224 tuberous sclerosis patients indicates increased severity of *TSC2*, compared with *TSC1*, disease in multiple organs. *Am J Hum Genet* 2001; **68**: 64-80.

7.   Sancak O, Nellist M, Goedbloed M *et al:* Mutational analysis of the *TSC1* and *TSC2* genes in a diagnostic setting: genotype-phenotype correlations and comparison of diagnostic DNA techniques in tuberous sclerosis complex. *Eur J Hum Genet* 2005; **13**: 731-741.

8.   Niida Y, Lawrence-Smith N, Banwell A *et al:* Analysis of both *TSC1* and *TSC2* for germline mutations in 126 unrelated patients with tuberous sclerosis. *Hum Mutat* 1999; **14**: 412-422.

9.   Au K-S, Williams AT, Roach ES *et al:* Genotype/phenotype correlation in 325 individuals referred for a diagnosis of tuberous sclerosis complex in the United States. *Genet Med* 2007; **9**: 88-100.

10.   Nellist M, Sancak O, Goedbloed MA *et al*: Distinct effects of single amino acid changes to tuberin on the function of the tuberin-hamartin complex. *Eur J Hum Genet* 2005; **13**: 59-68.

11.   Nellist M, van den Heuvel D, Schluep D *et al*.: Missense mutations to the *TSC1* gene cause tuberous sclerosis complex. *Eur. J. Hum. Genet.* (2008) epub ahead of print.

12.   van Slegtenhorst M, Nellist M, Nagelkerken B *et al:* Interaction between hamartin and tuberin, the *TSC1* and *TSC2* gene products. *Hum Mol Genet* 1998; **7**: 1053-1057.

13.   Li Y, Corradetti MN, Inoki K *et al*: TSC2: filling the GAP in the mTOR signaling pathway. *Trends Biochem Sci* 2003; **28**:573-576.

14.   Rosner M, Hanneder M, Siegel N *et al*: The tuberous sclerosis gene products hamartin and tuberin are multifunctional proteins with a wide spectrum of interacting partners. *Mut Res* 2008; **658**: 234-246.

15.   Huang J and Manning BD: The TSC1-TSC2 complex: a molecular switchboard controlling cell growth. *Biochem J.* 2008; **412**:179-90.

16.   Nellist M, Sancak O, Goedbloed MA *et al*: Functional characterisation of the TSC1-TSC2 complex to assess multiple TSC2 variants identified in single families affected by tuberous sclerosis complex. *BMC Med Genet*. 2008; **9**:10.

17.   Pymar LS, Platt FM, Askham JM *et al*: Bladder tumour-derived somatic TSC1 missense mutations cause loss of function via distinct mechanisms. *Hum Mol Gene*. 2008; **17**: 2006-2017.

18.   Tuberous sclerosis database - Leiden Open Variation Database [www.chromium.liacs.nl/lovd/index.php?select_db=TSC1].

19.   Ng PC and Henikoff S: Predicting the effects of amino acid substitutions on protein function. *Annu. Rev. Genomics Hum. Genet*. 2006; **7**: 61-80.

20.   Ng PC and Henikoff S: Accounting for human polymorphisms predicted to affect protein function. *Genome Res*. 2002; **12**: 436-446.

21.   Adamczak R, Porollo A and Meller J: Accurate Prediction of Solvent Accessibility Using Neural Networks Based Regression. *Proteins: Structure, Function and Bioinformatics*. 2004; **56**:753-767.

22.   Jones DT: Protein secondary structure prediction based on position-specific scoring matrices. *J. Mol. Biol*. 1999; **292**: 195-202.

23.   NetGene2 Server [www.cbs.dtu.dk/services/NetGene2].

24.   BDGP: Splice Site Prediction by Neural Network [www.fruitfly.org/seq_tools/splice.html].

25.   Human Splicing Finder [www.umd.be/HSF/HSF.html].

26.   Coevoets R, Arican S, Hoogeveen-Westerveld M *et al*: A reliable cell-based assay for testing unclassified *TSC2* gene variants. *Eur. J. Hum. Genet*. (2008) epub ahead of print.

27.   Lee DH and Goldberg AL: Proteasome inhibitors: valuable new tools for cell biologists. *Trends Cell Biol.* 1998; **8**: 397-403.

28.   Nellist M, van Slegtenhorst MA, Goedbloed M *et al*: Characterization of the cytosolic tuberin-hamartin complex: tuberin is a cytosolic chaperone for hamartin. *J Biol Chem* 1999; **274**: 35647-35652.

29.   Cai SL, Tee AR, Short D *et al*.: Activity of TSC2 is inhibited by AKT-mediated phosphorylation and membrane partitioning. *J Cell Biol*. 2006; **173**: 279-89.

Table 1.

Nucleotide change	Exon	Amino acid substitution	SIFT	LOVD	Effect on TSC1 function? (t-test)
c.149T>C	4	p.L50P	not tolerated	unknown	yes (p = 0.03)
c.153A>C	4	p.E51D	tolerated	probably not pathogenic	no (p = 0.3)
c.182T>C	4	p.L61P	not tolerated	confirmed pathogenic	yes (p = 0.002)
c.278T>G	5	p.L93R	not tolerated	probably pathogenic	yes (p = 0.03)
c.397G>T	6	p.V133F	not tolerated	unknown	yes (p = 0.005)
c.569G>C	7	p.R190P	not tolerated	unknown	yes (p = 0.004)
c.568C>T	7	p.R190C	not tolerated	no known pathogenicity	no (p = 0.19)
c.1001C>T	10	p.S334L	tolerated	probably no pathogenicity	no (p = 0.19)
c.1433A>G	14	p.E478G	tolerated	unknown	no (p = 0.6)
c.1648C>G	15	p.Q550E	tolerated	unknown	no (p = 0.9)
c.1974C>G	15	p.D658E	tolerated	probably no pathogenicity	no (p = 0.13)

c.1976C>T	15	p.A659V	tolerated	probably no pathogenicity	no (p = 0.1)
c.2420T>C	19	p.I807T	tolerated	unknown	no (p = 0.18)

Titles and legends to figures

Figure 1: Results of the SIFT prediction analysis.

(A) Graphical representation of the SIFT analysis results for TSC1. Each amino acid is represented by a box. Solid green boxes represent positions that are completely tolerant (all amino acid changes are possible); open green boxes represent positions where one or two amino acid substitutions are not tolerated. Solid red boxes represent completely intolerant positions (no amino acid changes are tolerated); open red boxes represent positions where only three or fewer amino acid changes are tolerated. The positions of the amino acid variants tested as part of this study are indicated in orange.

Figure 2: Inhibition of S6K-T389 phosphorylation by the TSC1 variants.

(A) Cells expressing S6K, TSC2 and wild-type TSC1 (wt) or the TSC1 variants were analysed by immunoblotting. Levels of TSC1, TSC2, total S6K and T389-phosphorylated S6K were determined using Odyssey^{TM} near infra-red detection (Li-Cor Biosciences) and quantification software. As controls, cells transfected with expression constructs for wild-type TSC1 and S6K only (TSC1/S6K), TSC2 and S6K only (TSC2/S6K), S6K only (S6K) or empty vector only (control) were also analysed. S6K and the TSC1 variants were detected with an antibody specific for the myc epitope tag. The signals for the L117P, L50P, L61P, L93R, V133F and R190P single variants and L50P/I807T double variant were clearly reduced compared to wild-type TSC1 (see also B). Furthermore, S6K T389 phosphorylation was increased in the presence of the L117P, L50P, L61P, L93R, V133F, R190P and L50P/I807T variants compared to the E51D, R190C, S334L, E478G, Q550E, D658E, A659V and I807T variants. (see also D). A representative example of 3 separate experiments is shown.

(B) Expression of the TSC1 variants. The integrated intensities of the TSC1 signals for each variant were determined in 3 independent experiments. The TSC1 signals, relative to wild-type TSC1 (TSC1 wt) were determined. Standard deviations are indicated. The signals for the L117P, L50P, L61P, L93R, V133F and R190P single variants and L50P/I807T double variant were clearly reduced compared to wild-type TSC1 and the E51D, R190C, S334L, E478G, Q550E, D658E, A659V and I807T variants.

(C) Expression of TSC2 in the presence of the TSC1 variants. The integrated intensity of the TSC2 signal in the presence of each of the different TSC1 variants was determined in 3 independent experiments. The TSC2 signals, relative to the signal in the presence of wild-type TSC1 (TSC1 wt), were determined. Standard deviations are indicated. The TSC2 signals in the presence of the different TSC1 variants were not significantly different to the TSC2 signal in the presence of wild-type TSC1 (unpaired t-test, p value >0.05).

(D) Inhibition of S6K T389 phosphorylation in the presence of different TSC1 variants. The ratio of the T389 S6K phosphorylation signal intensity to the total S6K signal intensity (T389/S6K) was measured in 3 independent experiments. The integrated intensity of each band was determined using the Odyssey scanning software and the mean T389/S6K ratios, relative to the wild-type TSC1 (wt) (wild-type TSC1 T389/S6K ratio = 1) were determined. Standard deviations are indicated. The S6K-T389 phosphorylation: total S6K ratio in the presence of the L117P, L50P, L61P, L93R, V133F and R190P single variants and L50P/I807T double variant was significantly increased compared to wild-type TSC1 (unpaired t-test p< 0.05; see Table 1.). In contrast the values for the E51D, R190C, S334L, E478G, Q550E, D658E, A659V and

I807T variants were not significantly different from wild-type TSC1 (unpaired t-test p > 0.05; see Table 1.).

(E) Expression of S6K in the presence of the TSC1 variants. The integrated intensity of the total S6K signal in the presence of each of the different TSC1 variants was determined in 3 independent experiments using the Odyssey scanning software. The S6K signals, relative to the signal in the presence of wild-type TSC1 (TSC1 wt), were determined. Standard deviations are indicated. The total S6K signals in the presence of the different TSC1 variants were not significantly different to the S6K signal in the presence of wild-type TSC1 (unpaired t-test, p value >0.05), indicating that the transfection efficiency and gel-loading was relatively constant.

Figure 3. Proteosome-mediated degradation of pathogenic TSC1 missense variants.

(A) Immunoblot showing levels of TSC2, TSC1 variants (L50P, L117P and wild-type (TSC1)), S6K and T389-phosphorylated S6K (T389) in transfected HEK 293T cells treated with 42 µM MG-132 and 200 nM insulin (+insulin/MG-132), 42 µM MG-132 only (+MG-132), 200 nM insulin only (+ insulin), or left untreated (basal).

(B) Graphical representation of the immunoblot experiments showing MG-132-dependent inhibition of proteosome-mediated degradation of the TSC1 L50P and L117P variants. The integrated intensities of the signals for the TSC1 variants were compared to the wild-type signals. Inhibition of proteosome-mediated degradation with MG-132 resulted in a relative increase in the signals for the pathogenic variants compared to wild-type TSC1 in both insulin stimulated (+ insulin) and unstimulated (basal) cells.

(C) Graphical representation of the immunoblot experiments showing increased mTOR activity after treating cells with the proteosome inhibitor MG-132. To estimate mTOR activity, the T389/S6K ratio in the presence of MG-132, insulin and the TSC1 L50P and

L117P variants was determined. Inhibition of the proteosome-mediated degradation of the L50P and L117P variants (+ MG-132) resulted in increased mTOR activity, compared to untreated cells.

(D) Graphical representation of the immunoblot experiments. The mean T389/S6K ratio is shown for wild-type TSC1 (TSC1) and the L50P and L117P variants, after treatment with MG-132 only (MG-132), insulin only (insulin), both reagents (MG-132/insulin) or untreated (basal). The T389/S6K ratio was significantly increased by addition of MG-132 for the TSC1 variants (paired t-test, $p < 0.05$), but not for wild-type TSC1 (paired t-test, $p > 0.05$).

Figure 4: Intracellular localisation of TSC1 detected by immunofluorescence microscopy.

(A - C) Immunofluorescence microscopy was performed on HEK 293T cells coexpressing TSC2 and the TSC1 E51D variant. (A) DAPI nuclear stain; (B) Diffuse cytoplasmic localisation of the E51D variant in the presence of TSC2 (C) Diffuse cytoplasmic localisation of TSC2.

(D - F) Immunofluorescence microscopy was performed on HEK 293T cells coexpressing TSC2 and the TSC1 L50P variant. (D) DAPI nuclear stain; (E) Diffuse cytoplasmic localisation of the L50P variant in the presence of TSC2 (F) Diffuse cytoplasmic localisation of TSC2.

(G - H) Immunofluorescence microscopy was performed on HEK 293T cells expressing the TSC1 E51D variant. (G) DAPI nuclear stain; (H) Punctate cytoplasmic localisation of the E51D variant.

(I - J) Immunofluorescence microscopy was performed on HEK 293T cells expressing the TSC1 L50P variant. (G) DAPI nuclear stain; (H) Diffuse cytoplasmic localisation of the L50P variant.

Figure 5: Comparative hydrophobicity profiles of TSC1 and TSC1 variants. Hydrophobicity values for each amino acid residue of wild-type and variant TSC1 isoforms were calculated using DNAMAN software (default parameters). The differences in the predicted hydrophobicity per amino acid residue between the wild-type and variant isoforms were plotted. Values > 0 indicate an increase in hydrophobicity of the variant relative to the wild-type sequence; values < 0 indicate a decrease.

(A) Predicted comparative hydrophobicity of pathogenic TSC1 variants. Pathogenic variants analysed as part of this and as part of a previous study[17] are indicated.

(B) Predicted comparative hydrophobicity of neutral TSC1 variants. Non-pathogenic variants from the LOVD mutation database[18] were compared to wild-type TSC1. The R190C, S334L, E478G, A659V and I807T variants are indicated. The E51D, Q550E and D658E substitutions did not affect the TSC1 hydrophobicity profile. The relative positions of these substitutions are indicated with arrows.
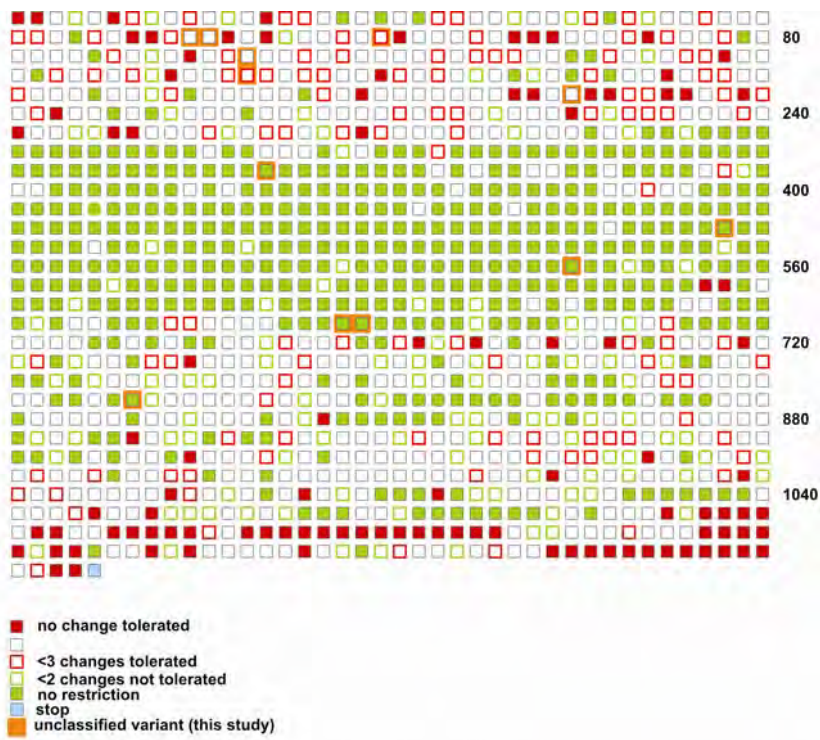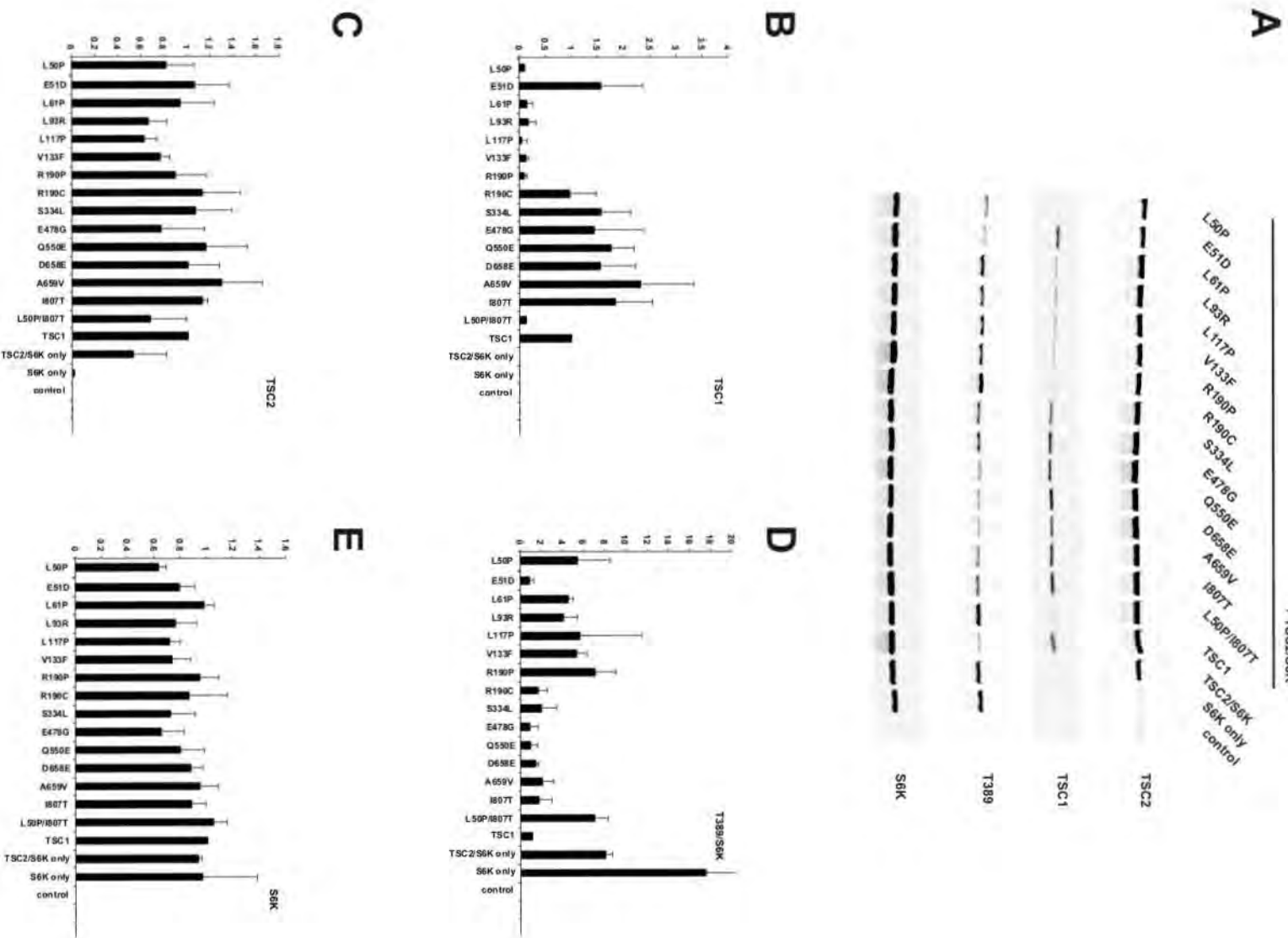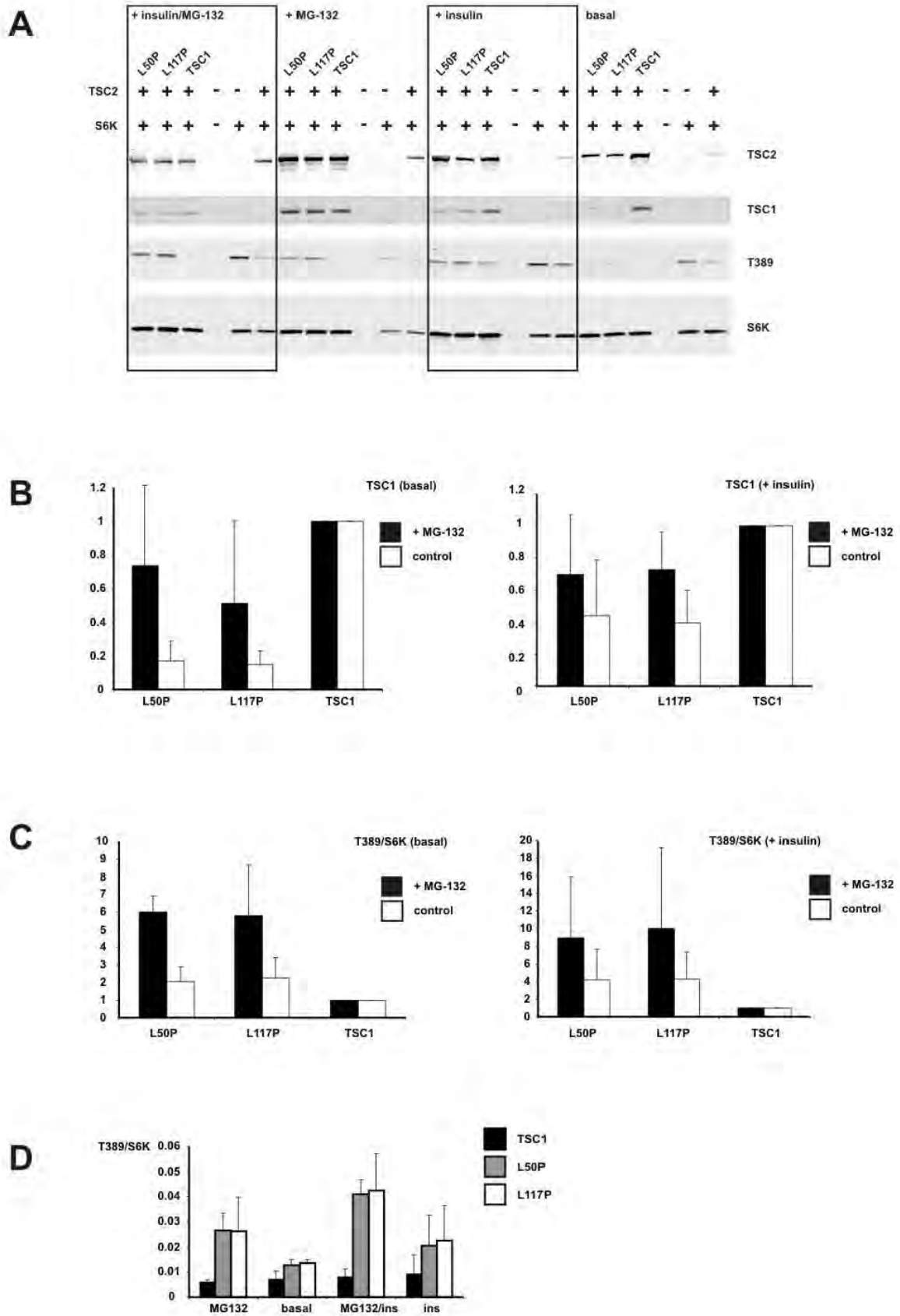
Figure 1.

Figure 2.

manuscript in preparation

Figure 3.

Figure 4.

Figure 5.